IDENTIFICATION AND CHARACTERIZATION OF VOLTAGE-GATED POTASSIUM CHANNELS AS THE CELL SURFACE TARGET THAT MEDIATES THE ANTI-PROLIFERATIVE ACTIVITY OF SNAKE VENOM MYOTOXINS

A Dissertation

by

CHUNHUI YIN

Submitted to the Office of Graduate and Professional Studies of
Texas A&M University
in partial fulfillment of the requirements for the degree of

DOCTOR OF PHILOSOPHY

Chair of Committee,	Peter Davies
Co-Chair of Committee,	Clifford Stephan
Committee Members,	Yubin Zhou
	Margie Moczygemba
	Elda E. Sánchez
Head of Department,	Warren Zimmer

August 2019

Major Subject: Medical Sciences

ABSTRACT

Background: Myotoxins are a family of small protein toxins present in the venom of multiple species of pit vipers that have selective toxic effects on different types of tissues. Method: In order to better protect people from these toxins and to potentially develop these proteins as the basis for new therapeutics, we investigated the mechanism of the cytotoxicity of a specific myotoxin, helleried crotamine (HR-crotamine). Results: The results we have obtained demonstrate the specific and selective binding of HR-crotamine to selected voltage gated potassium (Kv) channels (Kv1.1, Kv1.2, Kv1.3). The expression level of these channel proteins correlates positively with the effect of HR-crotamine on the inhibition of proliferation in multiple cancer cell lines. The binding of HR-crotamine to Kv1.3 in Jurkat cells is associated with the inhibition of intracellular calcium influx as reflected by the inhibition of NFAT translocation and the inhibition of IL-2 secretion. Discussion: These results indicate a direct connection between the binding of HR-crotamine to cell surface Kv1.3 channel and the inhibition of cell proliferation mediated by the suppression of intracellular Ca^{2+} signaling. Conclusion: We have characterized the cell surface-binding target for HR-crotamine that mediates its effects on intracellular signaling. In future studies, the mechanistic model we have developed can be used to develop single-chain antibody molecules (scFv proteins) that can be used both as molecular probes and HR-crotamine anti-toxins. These antibodies may be used to decrease the myotoxin toxicity, which is an important component in the pathophysiology of rattlesnake snakebite.

ACKNOWLEDGEMENTS

I would like to acknowledge Peter Davies, Ph.D., Clifford Stephen, Ph.D., Yubin Zhou, Ph.D., Margie Moczygemba, Ph.D., Lei Guo, Ph.D. and Walter Cromer. Ph.D. from the Texas A&M University-Health Science Center for providing valuable opinions and critical experimental resources used in the study. I am also grateful to Lian He, Ph.D, Yifan Zhang, Ph.D, Sevinj Isgandarova and Guolin Ma, Ph.D for technical help and support in the conduct of these studies. I also wish to express my thanks to other personnel in CTCR lab: Nghi "Ivy" Nguyen, Goeun Bae, Mary Sobieski and Yong Sung Park.

I wish to grateful for the work finished by the personnel in National Natural Toxins Research Center (NNTRC) and further support from Elda E. Sanchez, Ph.D., Montamas Suntravat, Ph.D and Jacob A. Galan, Ph.D.

I also wish to thank Rongfu Wang, Ph.D., Helen Wang, Mingjun Wang. PhD, Bingnan Yin and Motao Zhu. Ph.D. for the training and support in the first year of my Ph.D program .

I also want to express special thanks for the support I have received from Denelle Orellana, Cynthia Lewis and Michael Weldon. I also want to thank my friends: Lewis Lu, Qian Zhang, Xiao Yu, Xiao Liang, Xiao Wang, Yusheng Liu, Yanan Wang, Chen Peng, Lingyi Tang, Yue Dong, Esteban Cantu, William Allen, Sharon Tan, Ping Wang and Wen Zheng for the great support they have provided me during my graduate studies, they have made my life as a student much easier.

The thesis is also dedicated to the memory of my grandfather: Fang Yin, who had passed away during my study. Finally, I wish to convey my deepest gratitude to my family: Yuanjing Li, Boqing Yin and my dear love Misi Chen for all the love and support they have shown me during my graduate studies.

CONTRIBUTORS AND FUNDING SOURCES

Contributors

This work was supervised by a dissertation committee consisting of Peter Davies, M.D., Ph.D., Clifford Stephan, Ph.D. and Yubin Zhou, Ph.D. from the Center for Translational Cancer Research, Texas A&M Institute of Biosciences and Technology (IBT), Dr. Margie Moczygemba, Ph.D. from the Center for Infectious and Inflammatory Disease, IBT and Elda Sánchez. Ph.D. from the National Natural Toxins Research Center (NNTRC), Texas A&M University-Kingsville (TAMU-K).

The flow cytometry system used in the cell analysis studies was provided by Dr. Moczygemba. The crude venoms and purified myotoxins used in the study were provided by scientists from the NNTRC.

All other experiments and associated work conducted for this thesis were carried out by myself.

Funding Sources

Graduate study and all research expenses were supported by discretionary funds available to Dr. Davies from Texas A&M Institute of Biosciences and Technology and the Margaret B. Alkek Foundation.

NOMENCLATURE

HR-crotamine	Helleried crotamine
FACS	flow cytometry
PCR	polymerase chain reaction
ELISA	enzyme-linked immunosorbent assay
IL-2	Interleukin-2
PI	propidium iodide
HPLC	high-performance liquid chromatography
PFA	paraformaldehyde
TBST	tris-buffered saline and Polysorbate-20
IC_{50}	half maximal inhibitory concentration
EC_{50}	half maximal effect concentration
BC_{50}	half maximal binding concentration
FITC	fluorescein isothiocyanate
GAPDH	glyceraldehyde 3-phosphate dehydrogenase

TABLE OF CONTENTS

Page

LIST OF FIGURES

Page

LIST OF TABLES

Page

CHAPTER I

INTRODUCTION OF THE CYTOTOXICITY OF HELLERIED MYOTOXIN

Introduction and literature review

The biologic basis for the cytotoxic activity of snake venoms

Biologic basis

Snake venom is highly modified saliva("Adult nonfiction: Pure sciences,")("Adult nonfiction: Pure sciences,") containing zootoxins that facilitate the immobilization of the snake's prey and its pre-digestion. Snake venoms are also an important defense mechanism discouraging future predation by the snake's natural predators (Greenbaum, Galeva, & Jorgensen, 2003). During a snake bite, venom is injected into the prey's tissues by specialized fangs, although some species of snake are also capable of projecting venom as a defensive measure via a spitting mechanism. Most snake venoms contain 20 or more different kinds of proteins and polypeptides (Jackson et al., 2013). These bioactive proteins and peptides (Greenbaum et al., 2003) either immobilize or directly kill the snake's prey (Weisman, Lizarralde, & Thompson, 1996). In addition, enzymatic components of the venom play an essential role in the pre-digestion of prey facilitating its disintegration once it is ingested by the snake. Snake venoms also contain a number of other bioactive proteins and peptides that have biological activities that contribute in one way or another to the success of the specific species of the snake as a predator (Bottrall, Madaras, Biven, Venning, & Mirtschin, 2010). The protein constituents in snake venoms impact multiple key biological functions in the snake's prey including blood coagulation, blood pressure regulation,

skeletal muscular contractility, the propagation of electrical activity within both the central and peripheral nervous systems and the skeletal muscular system. Because of their diverse bioactive components and generous volumes, snake venoms have frequently served as the starting point for the development of new classes of drugs and diagnostic procedures (Luna-Ramirez et al., 2013).

Medical applications of drugs derived from snake venom toxins

Multiple components of snake venoms from multiple species of snakes have served as the starting point for the development of new classes of therapeutics. Small molecule therapeutics based on the activity of snake venom toxins have been used for the development of treatments for hypertension, thrombotic disease including stroke and myocardial infarction, and the treatment of neurological disease including brain injuries.

Snake venom hemotoxins have been used to develop drugs to prevent heart attack and treat blood coagulopathies. The ACE Inhibitors, a class of pharmacologic agents, used extensively for the treatment of high blood pressure and other angiotensin-related diseases, were developed based on the activity of specific snake venom toxins (Goodman, Gilman, Brunton, Lazo, & Parker, 2006). Both eptifibatide and tirofiban, anti-platelet drugs developed from toxins in rattlesnake and African saw-scaled viper venoms, are used to treat pre-infection angina and minor heart attacks. Both of these drugs block platelet aggregation and accelerate the dissolution of the blood clots. New treatments for stroke patients, based on the activity of a toxin in Malayan pit viper venom are being developed and tested (Shahidi Bonjar, 2014).

Snake venom neurotoxins are being used to develop new drugs for the treatment brain and neuronal diseases such as Alzheimer's diseases, Parkinson's diseases, and various pain disorders. In addition, drugs derived from snake venom toxins are being developed for the treatment of cancer. Some of these toxins interfere with the blood supply to tumors tissue often by inhibiting tumor angiogenesis or by disrupting the function of tumor-associated endothelial cells (Bridges & Harris, 2015). Other snake venom toxins have direct cytotoxicity activity to the tumor cells often by triggering lethal signaling pathways. On a completely different track, some components of venom have been found to have the significant anti-bacterial and or anti-fungal (Yount et al., 2009). These toxins are being explored as leads for the development of new classes of small molecule antibiotics and antifungal agents.

Molecular basis for the cytotoxic activity of pit viper venoms

Metalloproteinase, phospholipases

Recent comprehensive analysis of the transcriptomes presents in snake venom gland cDNA libraries have provided a much fuller and unbiased picture of the range of toxin molecules that constitute an individual venom. For instance in an analysis of a cDNA library derived from *Crotalus adamanteus* venom glands (Rokyta, Lemmon, Margres, & Aronow, 2012), the authors were able to cluster the transcripts into 78 groups with less than 1% nucleotide divergence. In this particular snake venom gland library, Phospholipase A2-based toxins (PLA2) were among the most functionally diverse classes of toxins identified in the venom. Secreted Phospholipase A2 is an

essential component of many snake and insect venoms, mammalian digestive fluids and inflammatory exudates where it leads to degradation of membranes and emulsified lipids (Heffernan et al., 2006). Snake venom PLA2's is a complex family of isoenzymes that have been assigned to at least nine sub-groups. These toxins function at membrane interfaces cleaving the SN-2 acyl chains from phospholipids and releasing arachidonic acid and other biologically active fatty acids. Snake venom PLA2 toxins are have biological effects ranging from neurotoxicity to myotoxicity and cardiotoxicity.

Metalloproteinases with multiple metalloproteinases and metalloproteinase-like proteins are also major components of pit viper venoms. Some of these snake venom enzymes are comprised of the metalloproteinase domain only, while others have additional disintegrin-like and high cysteine domains. In some snake venom metalloproteinases, an additional lectin-like subunit or other subdomains may contribute to specific functional activities. All of the venom metalloproteinases with zinc-dependent enzymes domain have highly similar zinc binding environments.

Some snake venom metalloproteinases have direct hemorrhagic activity by directly impacting capillary blood vessels, cleaving in a highly selective fashion, key peptide bonds of basement membrane components, thereby affecting the interaction between the basement membrane and endothelial cells (Rucavado, Escalante, & Gutierrez, 2004; Takeda, Takeya, & Iwanaga, 2012). In addition to their hemorrhagic activity, venom metalloproteinases also induce myonecrosis and ischemia. Micro vessel disruption by metalloproteinases also impairs skeletal muscle regeneration, contributing to fibrosis and permanent tissue loss after snakebites (Gutierrez & Rucavado, 2000;

Moura-da-Silva et al., 2008). Venom metalloproteinases contribute to the widespread degradation of extracellular matrix components and subsequent prominent local inflammatory response that leads to edema and the activation of endogenous matrix metalloproteinases and pro-inflammatory cytokines following snakebite (Fernandes, Pereira Teixeira Cde, Leite, Gutierrez, & Rocha, 2007; Markland & Swenson, 2013; Rucavado, Borkow, Ovadia, & Gutierrez, 1995).

Myotoxins

There is some confusion in the field because the term "myotoxin" has been applied to two very different types of venom proteins, large homodimeric PLA2- like molecules (many that actually lack enzymatic activity) and small, basic peptides related to crotamine, a myotoxin isolated from the venom of *Crotalus durissus terrificus*, a tropical South American rattlesnake. Crotamine was the first myotoxin to have been isolated and identified and is the mostly intensively studied of the low molecular weight myotoxins but several different species of rattlesnakes have been shown to secrete crotamine-like myotxins in their venoms. Myotoxins are important components of snake venoms because they use non-enzymatic mechanisms to induce muscle paralysis and necrosis. Because of the very rapid onset of their activity, myotoxins can cause immediate paralysis that prevents the snake's prey from escaping and leads to its eventual death due to diaphragmatic paralysis (Griffin & Aird, 1990; Samejima, Aoki, & Mebs, 1991). Most myotoxins appear to act without affecting the integrity of the muscle cell membranes, rather they have been observed to cause cell swelling, mitochondrial

alterations and dilation of sarcoplasmic reticulum (Mamede et al., 2013). Most recent studies of crotamine-like myotoxins fall into 7 major categories: gene cloning, protein structure analysis, DNA binding mechanism, cell penetration mechanism, cell-specific activity, such as anti-tumor, antibacterial and anti-fungal activities and interactions with ion channels (Chen, Hayashi, Oliveira, & Karpel, 2012; Cui et al., 2012; Hayashi, Oliveira, Kerkis, & Karpel, 2012).

The crotamine-like myotoxins have generally conserved structures: the total length of the peptide is approximately 42 amino acids with three disulfate bonds to stabilize the molecular structure. The low molecular weight myotoxin family includes, in addition to crotamine (isolated from *Crotalus durissus terrificus*), myotoxin A isolated from the *Crotalus viridis viridis* and the hellerid myotoxins (from *Crotalus oreganus helleri*) that are the subject of this dissertation (Radis-Baptista & Kerkis, 2011; Saviola et al., 2015). Crotamine is encoded by the Crt-pl gene that gives rise to a 1.8kb crotamine mRNA. Structural studies have shown that the 3D structure of crotamine is very similar to that of human beta-defensins (Sanchez et al., 2018). While the molecular targets of the crotamine-like myotoxins has not been definitively established, these toxins have been reported to affect the electrical activity on multiple types of cells pointing to a likely activity against selected ion channels. In addition, a suggested analgesic activity of crotamine is reversed by nalozxone, suggesting possible interactions with opioid receptors. In addition, crotamine has been demonstrated to penetrate into dividing cells and to localizes to the nucleus (Goodman et al., 2006).

What makes crotamine-like myotoxins particularly interesting

Medically significant activities of crotamine

The evolutionary and structural links between the myotoxins and the beta-defensins has led to their evaluation as anti-microbial agents. Exposure to crotamine kills *Escherichia coli* (Yount et al., 2009) with a very rapid onset (1-2 hr) of activity. This anti-microbial activity can be abolished by 12.5 mM NaCl. Interestingly, crotamine's intramolecular disulfide bonds do not appear to be critical for this activity (Nicastro et al., 2003) since reduced crotamine works as well as the native protein. The anti-bacterial activity of crotamine is quite strain specific, with varying sensitivities the myotoxin was also found to have pronounced antifungal activity against several stains *Candida spp. albicans* (Oguiura, Boni-Mitake, Affonso, & Zhang, 2011).

Crotamine has been of medical interest because of its selective anti-tumor activity. Much of this interest has related to its selectivity for proliferating cells and its ability both to penetrate cells deliver cargo such as plasmid DNA into the cancer cells (Chen et al., 2012; Hayashi et al., 2012; Nascimento et al., 2007). Others have characterized the cytotoxic activity of crotamine against tumor cells both *in vitro* and *in vivo*. These studies reported that crotamine, at 5 μg/ml (about 1 μM), was lethal to several melanoma cell lines but had no activity against normal cells (Pereira et al., 2011). Twenty-one days of continuous treatment of tumor-bearing mice with crotamine (1 g/day) significantly inhibited tumor implantation increasing survival rate and decreasing weight loss (Pereira et al., 2011). Studies that compared tumor cell lines with non-tumor cells consistently demonstrated the selectivity of crotamine's cytotoxic

activity for active proliferating tumor cells (Zhang et al., 2006). Crotamine's intracellular localization properties, also showed it to be a potential marker of centrioles in actively proliferating cells (A. Kerkis et al., 2004; Oguiura, Boni-Mitake, & Radis-Baptista, 2005).

In addition to its anti-tumor activity, crotamine has also been studied for potential activity in neurological disease. Low concentrations of crotamine have been shown to improve neurotransmission in isolated neuromuscular preparations from myasthenic rats by modulating sodium channels. *In vivo*, in the same animal model, single dose treatment with crotamine for 2 weeks resulted in significant improvements in exercise tolerance and decreases in the number of fatigue episodes. This study demonstrated that low doses of crotamine are highly efficient in enhancing muscular performance in myasthenic rats, possibly by improving the safety factor for neuromuscular transmission (Hernandez-Oliveira e Silva et al., 2013).

Structural information

The structure of crotamine has been demonstrated to be closely related to the structure of human β-defensin 2 (hBD-2) (Volk, Schwartz, Li, Rosenberg, & Simons, 1999) (Dalla Valle, Benato, Maistro, Quinzani, & Alibardi, 2012; Whittington et al., 2008). Beta-defensins, a family of mammalian defensins, have antimicrobial peptides that contribute to the resistance of epithelial surfaces to microbial colonization. Their mass ranges from 2-6 kDa, they are all highly cationic and show activity against many Gram-negative and Gram-positive bacteria, fungi, and enveloped viruses (White,

Wimley, & Selsted, 1995). The beta-defensins typically have three intramolecular disulfide bonds that stabilize their structure. On the basis of their size and pattern of disulfide bonding, mammalian defensins are mainly classified into alpha, beta and theta categories. In human, rabbit and guinea pig, the β-defensins induce the activation and degranulation of mast cells, resulting in the release of histamine and prostaglandin D2. Similar to other defensins, β-defensins are cationic and, therefore, can interact with the negatively charged membrane of invading microbes. Based on its electric charge, beta-defensin peptides can insert directly into the bacterial membrane (van Dijk, Veldhuizen, & Haagsman, 2008) and establishing pore complexes that cause membrane depolarization and cell lysis (van Dijk et al., 2008). Based upon its similarity with the structure of beta-defensins, crotamine has been projected to have similar binding behavior to microbial membranes. There are however significant differences in the properties of the two classes of molecules (Dalla Valle et al., 2012; Yount et al., 2009) based on the fact that hBD-2 does not penetrate normal mammalian cell membranes whereas crotamine does.

Proposed mechanisms of action

To better understand the properties of crotamine, we have collected information from a wide variety of published studies. Current research on crotamine and crotamine-like myotoxins have been focused on the following areas: 1) *In vitro* studies of crotamine's cell-specific cell penetration activity (Nascimento et al., 2007; Sieber, Bosch, Hanke, & Fernandes de Lima, 2014); 2) the selective cytotoxicity activity of

crotamine and the induction of apoptosis (Pereira et al., 2011); 3) crotamine's effects on ion channel conductance through interference of Kv channel activity; 4) the selective accumulation of administered crotamine in cancer tissue, *in vivo*; and 5) transient effects of crotamine on intracellular calcium kinetics.

Cell-penetrating and DNA binding activity

Several groups have investigated the cell penetrating activity of crotamine and similar myotoxin, however, the conclusions of these studies are controversial. The most commonly held theory is that crotamine interacts with heparan sulfate proteoglycans on the surface of susceptible cells. Normal endocytic processes the deliver the crotamine into the interior of the cell leading to accumulation of the cationic peptide within the acidic endosomal vesicles. In a final step, the contents of the vesicles leaks to the cell cytosol due to the permeabilization of endosomal membranes (Ownby, Gutierrez, Colberg, & Odell, 1982). In addition to crotamine, snake venom myotoxin I and myotoxin II have been evaluated for the effect of altering membrane lipid content on their cytotoxic in C2C12 myoblast cells. These studies demonstrated that the cytolytic activity of both myotoxin I & II was increased in cholesterol-depleted membranes whereas the cytolytic activity of myotoxin II was decreased in direct proportion to a lowering of the temperature, implicating membrane fluidity in the process (I. Kerkis, Silva Fde, Pereira, Kerkis, & Radis-Baptista, 2010). Similar results were obtained by Santos N.C. who demonstrated that crotamine can cross lipid bilayer membranes even in the absence of a receptor (Rodrigues et al., 2012). These observations are very similar to

reports from other labs that crotamine can interact with lipid bilayers and can potentially penetrate cells via a variety of entry mechanisms (Hayashi et al., 2008; Nascimento et al., 2007).

Crotamine also has DNA binding activity and has been explored as a nanoparticle delivery system capable of delivering dsDNA, ssDNA and siRNA into the cell both *in vivo* and *in vitro* condition (Hayashi et al., 2012). When crotamine binds to DNA, the peptide occupies a span of about two and a half nucleotide pairs, so that about four crotamine molecules bind within a 10bp turn of a B-DNA helix. Salt sensitivity studies indicate a maximum of three ionic interactions between the protein and DNA (Mandal et al., 2012). These constraints assign the DNA binding activity of crotamine to the positive charges on the C-terminus of crotamine molecule. Detailed analysis of the 3-D structure of the C-terminus, suggest that five residues in positions 31 to 35, Arg-Trp-Arg-Trp-Lys are the putative DNA-binding site. The actual delivery of DNA into cells depends on the aggregation and precipitation of crotamine-DNA complexes at low ionic strength and their subsequent cellular uptake. This mechanism explains the preference for long chain over short chain DNA molecules for crotamine-mediated cellular delivery (Chen et al., 2012).

Ion channel activity

Voltage-dependent ion channels are members of the voltage-dependent cation channel family, which includes the voltage-dependent K^+, Na^+, and Ca^{2+} channels (Favre, Moczydlowski, & Schild, 1996). It has been suggested that crotamine can inhibit

Kv channel activity and thereby change resting membrane potentials. The Kv channels are found in both eukaryotic and prokaryotic cells. The intact Kv channel is comprised of four identical protein subunits that associate to form a four-fold symmetric complex arranged around a central ion-conducting pore (Orlova, Papakosta, Booy, van Heel, & Dolly, 2003). The TM, T1 and β domains (from extracellular to intercellular) in each subunit defines the basic structural organization of the channel protein. Critical components of all K^+ channels include the conserved structures that serve as the K^+ selectivity filter on the extracellular side of the pore; the inner pore varies in its confirmations among different members of the family (Doyle et al., 1998). The β-domain plays a vital role in the regulation of channel activity. The intact channel includes four beta subunits, auxiliary proteins that associate with alpha subunits in a one-to-one stoichiometry (α4β4) (Pongs et al., 1999).

Voltage-gated Kv1 channel plays a critical role in regulating resting membrane potential, action potential duration and neurotransmitter release in mammalian neurons. The activity of Kv1.3 channel has been most extensively investigated in the function of T-lymphocytes (Ouadid-Ahidouch & Ahidouch, 2008; Ouadid-Ahidouch, Roudbaraki, Ahidouch, Delcourt, & Prevarskaya, 2004; Pardo, 2004; Wonderlin & Strobl, 1996) where its activity has been linked to progression through the G1 phase of the cell cycle. Studies in multiple cell lines, have demonstrated that the expression of Kv1.3 channels appear to be cell cycle-dependent and seems to contribute activity in both S and G1 phase of the cell (Chittajallu et al., 2002). Kv1.3 inhibitors have been considered to have potential applications as immunosuppressant therapies. There has also been interest in

the potential role of Kv channels as targets for the development of new anti-tumor therapies. The Kv1.5 channel, and to a lesser extent the Kv1.3 channel are aberrantly expressed in a number of human cancers (Bielanska et al., 2012; Bielanska et al., 2009; Ouadid-Ahidouch et al., 2000; Zhou, Unlap, Li, & Ma, 2002).

There is evidence that a number of snake venom toxins target Kv channel activity. Dendrotoxins, components of Mamba venoms, are potent Kv1.1 channel inhibitor, that have been used extensively to profile the structural determinants of Kv channel activity. Myotoxins have also been implicated as Kv channel modulators. Patch clamp studies with crotamine have shown selective inhibition of some but not all Kv channels (Kv1.1, Kv1.2, Kv1.3 but not Kv 1.5) (Mouhat, Andreotti, Jouirou, & Sabatier, 2008; Mouhat, Jouirou, Mosbah, De Waard, & Sabatier, 2004).

In addition to its effects on Kv channels, myotoxins such as crotamine have also been reported to modify the activity of voltage-sensitive Na^+ channels in both muscle and mast cells (Toyama et al., 2000). Crotamine increases the Na^+ conductance of skeletal muscle membranes, an effect that can be blocked by tetrodotoxin. Crotamine induced depolarization of myocytes was investigated using an improved loose patch-clamp technique; and a dose-dependent curve with an EC_{50} of 0.15 μg/ml was observed (Matavel, Ferreira-Alves, Beirao, & Cruz, 1998). These studies suggest either that crotamine is increasing the number of functioning Na^+ channels or increasing the number of channels that are in the "open" state during membrane depolarization. (Matavel et al., 1998).

Heparan sulfate proteoglycans (HSPG) binding

Many snake venom toxins have an affinity for HSPGs, a property that presumable enhances their association with cell membranes and facilitates their interactions with specific membrane receptors. Myotoxins in particular bind due HSPG's because, as strongly cationic peptides they have a high affinity for the negatively-charged HS-side chains of the HSPG's (A. Kerkis et al., 2004). In the case of crotamine, the direct binding to HSPG's appears to facilitate the cell-penetrating activity of the peptide. There is a direct correlation between the level of the HSPG's expressed on the surface of different types of cells and their vulnerability to penetration by crotamine.

The goal of this project

Hypothesis

The goal of our study is to identify the cellular and molecular basis for the selective inhibitory effect of snake venom myotoxins, on the proliferative activity of certain types of cancer cells. Although we consider a full range of possibilities for the molecular basis of this activity, based on evidence drawn from the literature, we tested the hypothesis that crotamine binds specifically to certain Kv channels expressed on the surface of cancer cells and that the binding of the toxin to this target results in molecular events that result in the suppression of cellular proliferation.

Goals – identify the cell surface binding target for crotamine and understand the intracellular mechanism of its effect.

To achieve the goal of our study, we have divided our research into the following steps:

1) To investigate whether Kv channels on cancer cells are the target for the anti-proliferative activity of crotamine. This involve: a) investigation of the specific binding of crotamine to Kv channels expressed on the surface of crotamine sensitive cells; b) determination of the effect of the binding of crotamine to specific Kv channels on the surface of susceptible cells results in an inhibition of cellular proliferation.

2) To establish the molecular mechanism for the target dependent effect of crotamine on the proliferative activity of sensitive cells. This involve: a) characterization of the cellular mechanisms involved in the anti-proliferative activity of crotamine; b) characterization the intracellular mediator of the anti-proliferative activity of crotamine.

Materials and Methods

Sequence analysis

The sequences of helleried crotamine (HR-crotamine) isolated from *Crotalus oreganus helleri* and crotamine (isolated from *Crotalus durissus terrificus*) [Fig. 1] were aligned and investigated for the similarity. There are seven of the full-length amino acid sequences, identified with the codenames 5J11, 3M19, 6O01, 5C09, 1l06, 1N24, 5i03. The studies included in this thesis used molecule designated with the codename 6O01.

Source of cell lines – validation

Cancer cell lines (REN, HeLa, HeLa NFAT 1-460, HEK293T, CCRF CEM) were obtained from Center of Translational Cancer Research, Texas A&M Institute of Biotechnology (IBT). The B16-F10 cell line was provided by Dr. DeKai Zhang lab in IBT, the Mia PaCa-2 cell and Jurkat cell lines were obtained through collaborative labs in University of Texas MD Anderson Cancer Center, and the C2C12 cell line was obtained from Baylor College of Medicine (BCM). The SK-Mel-28 cell was obtained from Dr. Bartholomeusz's, (MD Anderson Cancer Center) and the Molt-3 cell line was obtained from Dr. Lacorazza, in Texas Children Hospital. All cell lines were cultured under the condition listed in Table 1.

Source of myotoxins – characterization

The myotoxin used in these studies was isolated from the venom of *Crotalus oreganus helleri* by High-Performance Liquid Chromatography (HPLC). [Fig. 2] The diluted venom was injected into the ion exchange column, and the expected fraction of the 6^{th} elution peak was collected and lyophilized for stock. After a desalting step, the sample was resuspended in PBS. The FITC labelling was accomplished by direct conjugation to HR-crotamine using the DyLight 488 antibody labeling kit (Thermo Scientific, MA).

Fig.1.

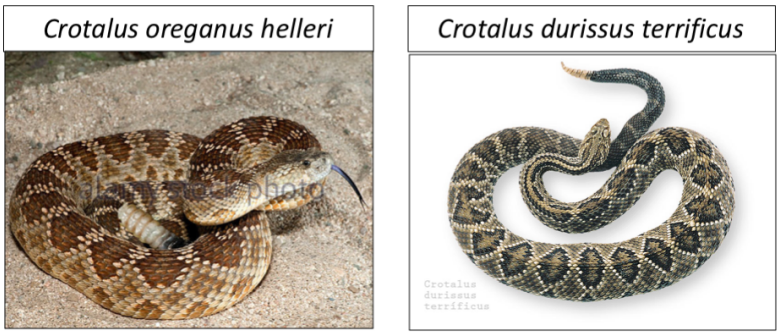

Fig. 1. The HR-crotamine used in our study is isolated from the venom of Crotalus oreganus helleri
Crotamine is isolated from the venom of *Crotalus durissus terrificus.*

Table 1. Cell Culture Conditions for the Cell Lines Used in Our Study.

Cell line	Source tissue	Medium	Condition
REN	Human mesothelioma cell line	RPMI-1640, 10%FBS, 1%100xGluMax	37°C, 5% CO_2
HeLa NFAT 1-460	Human cervical adenocarcinoma cell line engineered to contain and an NFAT reported system	DEME, 10%FBS, 1%100xGluMax,1%HEPES, 1%Sodium Pyruvate	37°C, 5% CO_2
HeLa	Human cervical adenocarcinoma cell line	DEME, 10%FBS, 1%100xGluMax,1%HEPES, 1%Sodium Pyruvate	37°C, 5% CO_2
C2C12	Mouse myoblast cell line	DEME, 10%FBS, 1%100xGluMax,1%HEPES, 1%Sodium Pyruvate	37°C, 5% CO_2
Jurkat	Human T cell leukemia cell line	RPMI-1640, 10%FBS, 1%100xGluMax	37°C, 5% CO_2
HEK293T	Human Embryonic Kidney cell line 293	DEME, 10%FBS, 1%100xGluMax,1%HEPES, 1%Sodium Pyruvate	37°C, 5% CO_2
B16-F10	Mouse melanoma cell line	DEME, 10%FBS, 1%100xGluMax,1%HEPES, 1%Sodium Pyruvate	37°C, 5% CO_2
SK-mel-28	Human melanoma cell line	DEME, 10%FBS, 1%100xGluMax,1%HEPES, 1%Sodium Pyruvate	37°C, 5% CO_2
Mia PaCa-2	Human pancreatic adenocarcinoma cell line	DEME, 10%FBS, 1%100xGluMax,1%HEPES, 1%Sodium Pyruvate	37°C, 5% CO_2
Molt-3	Human T cell leukemia cell line	RPMI-1640, 10%FBS, 1%100xGluMax	37°C, 5% CO_2
CCRF CEM	Human T cell leukemia cell line	RPMI-1640, 10%FBS, 1%100xGluMax	37°C, 5% CO_2

Fig.2

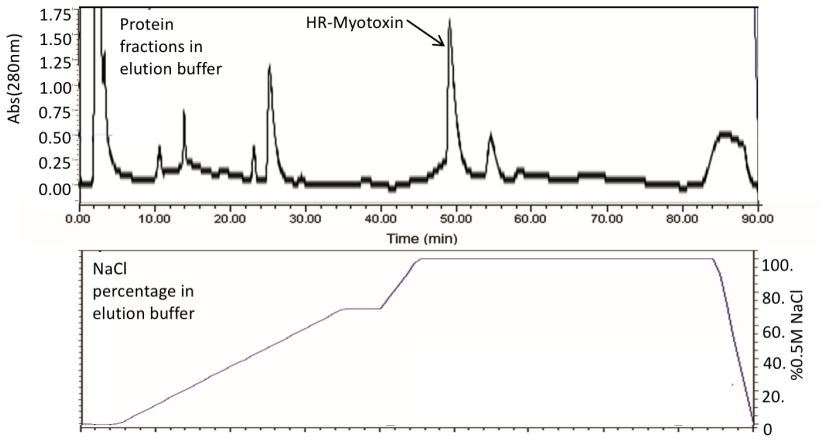

Fig. 2. HPLC Cation Exchange Fractionation of Southern Pacific Rattlesnake (Crotalus oreganus helleri) venom
Crude venom (10 mg) from Southern Pacific Rattlesnake (*Crotalus oreganus helleri*) was first bound to the HPLC column in an equilibrating buffer (0.02 M Tris-HCl, *p*H=8.0) and eluted with a gradient of increasing 0.5 M NaCl. HR-crotamine was eluted when the elution buffer reaches 100%. The total running time is 90 min.

Cell viability assays

At time 0, individual cell lines were seeded into 384-well plates at a density at 1000 cells/well using a Multidrop dispenser with low spray speed to ensure the even distribution of the cells. All cell growth determinations were performed in quadruplicate. After the dispensing of the cells, the plates were shaken for 10 min to avoid an uneven distribution of the cell in the wells. After overnight incubation, the HR-crotamine or other test substances were added to the cells in half-fold gradient concentration from 0-10 μM. After 72 hr, cultured T cells were fixed with 4% PFA for 15min and followed

washing with PBS twice. The cells were permeabilized by the addition of 0.5% Triton-X100, for 10 min and then treated with 1 μg/mL DAPI for 10 min for visualization. The test plates were imaged in an InCell 6000 high-throughput confocal fluorescent microscope with DAPI filter at 4X power. The images from individual wells were analyzed based on nuclear segmentation and counting using InCell Developer. An IC_{50} was calculated for each of the test substances added to the wells and for each of the cell lines tested.

For CellTiter-Glo determinations (measure of total ATP content), cells were seeded into 384-well plates at an appropriate cell density. Each determination was performed in a quadruplicate to ensure the reliability and accuracy of the values obtained. The seeded cells were cultured with the presence of HR-crotamine, PBS (negative control) and Etoposide (positive control) for 72 hr. The HR-crotamine and Etoposide were added in a half fold linear dilution gradient with the highest concentration at 800 nM and 100 μM, respectively. At the end of the experiment, the test plate was centrifuged and the volume of media was reduced to 15 μl. The CellTiter-Glo reagent was added at 1:1 ratio with the residual volume. After 45 min of incubation, luminescence intensity was determined using a plate reader. The values obtained were analyzed for growth inhibition, compared to the negative control. In the metabolism rate test, cells were seeded in gradient density and then incubated with HR-crotamine for 72 hr, and each well were tested with CellTiter-Glo.

Cytotoxicity kinetics test

C2C12, HEK293T, HeLa, SK-Mel-28 cells and Jurkat cells were seeded in a 384 well plates. The test substances (0.02% SDS or HR-crotamine in 8-half fold dilutions from 1 μM) were added for 0.5, 2, 24 and 72 hr and cell viability and the number of dead cells was determined using Hoechst 33342 and DRAQ7 staining (Thermo Fisher Scientific and Biostatus, respectively). PBS served as the negative control. DRAQ7 staining was observed through the Texas Red channel with a 4X objective. The images were processed and compared using the InCell Developer.

Transcript and protein profiling studies

Gene-specific PCR assay and Real-time PCR analysis

Total mRNA was extracted from cells with the Qiagen RNeasy Mini Kit and according to instructions provided by the manufacturer. Briefly, adherent cells in 10 cm dishes (approx. 2.5-10 x 10^6 cells per dish) were lysed directly in the culture dish after a PBS wash. Cells growing in suspension were pelleted by centrifugation for 5min at 500 x g and washed once with PBS prior to lysis. An appropriate volume of RLT buffer is added, cells are resuspended by vortexing and then lysed by passage through a 20-gauge needle fitted to an RNase-free syringe for 5-10 times. The same volume of 70% ethanol is added to the lysate and mixed by pipetting. Seven hundred microliters of the samples are then transferred to an RNeasy spin column placed in a 2 ml collection tube and centrifuged for 30s at 8,000 x g. After discarding the flow-through and 700 μl of buffer, RW1 is added to the RNeasy spin column followed by a second centrifugation for 30s, at

8,000 x g. RPE buffer (500 µl) is added to the RNeasy spin column and the column is centrifuged for 30s at 8,000 x g. The flow-through is also discarded. This step is repeated once with an additional 2 min of centrifugation time added to the repeat. The RNeasy spin column is placed in a new 1.5 ml collection tube and the total RNA is eluted by 30-50 µl RNase-free water or elution buffer by centrifugation for 1 min, at 10,000 x g.

Reverse transcript synthesis was accomplished with the SuperScript III first-strand synthesis system. Total mRNA from a specific cell sample is combined with primer and buffer that includes Oligo(dt)20 1 µl, dNTP 1 µl, RNA solution 5 µl, and molecular grade water 3 µl for a final volume of 10 µl. The samples are heated to 65^{o}C for 5 min in Bio-rid thermal cycler followed by cooling down on the ice for 1 min. Then, 10 µl of cDNA synthesis Mix (10x RT buffer 2 µl, MgCl2 4 µl, 0.1 M DTT 2 µl, RNaseOUT 1 µl and SuperScript III RT 1 µl) was added to the chilled samples. The samples are then heated to 50^{o}C for 50min and 85^{o}C for 5 min. 1 µl of RNase H was added to the sample and incubated at 37^{o}C for 20 min. The samples were then ready for the PCR analysis and were stored at -20^{o}C.

Gene-specific PCR was used to confirm the expression of the Kv1.1, Kv1.2, Kv1.3 and Kv1.5 transcripts as well as the specificity of the gene-specific primers for real-time PCR analysis. The sequences of primers used in this study are listed in the Table 2. The PCR mix was made in a 20 µl reaction system, which includes 10x PCR buffer 2 µl, $MgCl_2$ 1 µl, forward primer 1 µl, reverse primer 1 µl, dNTP 1 µl, Template DNA 1 µl, HotTaq enzyme 0.5 µl and water 12.5 µl. The PCR is run under the following

protocol: the initial denaturation is at 95ºC for 5 min, followed by 40 cycles of amplification. Each cycle includes 95ºCfor 30sec; different annealing temperatures were tested (55ºC, 50ºC and 47ºC for 30sec.) and then 72ºC for 30sec. The final extension was performed at 72ºC for 3min followed by a cool-down step to room temperature. The PCR product was analyzed on a 2% agarose gel, and DNA was visualized by UV illumination. [Fig. 3]

Table 2. The table lists the primer designed for the gene specific qPCR

Gene Specific primer for the regular PCR test and real time PCR

Gene's name	Forward primer	Reverse primer
Kv1.1	5-GAATCAGAAGGGCGAGCA-3	5-GGAGTGGCGGGAGAGTTT-3
Kv1.2	5-GAGATGTTTCGGGAGGATGA-3	5-TTCCAGACAGAAGCTGACGA-3
Kv1.3	5-CTCATCTCCATTGTCATCTTCTGA-3	5-TTGAAGTTGGAAACAATCAC-3
Kv1.5	5-GGATCACTCCATCACCAG-3	5-GGCTTCCTCCTCCTTCCTTG-3

Fig.3

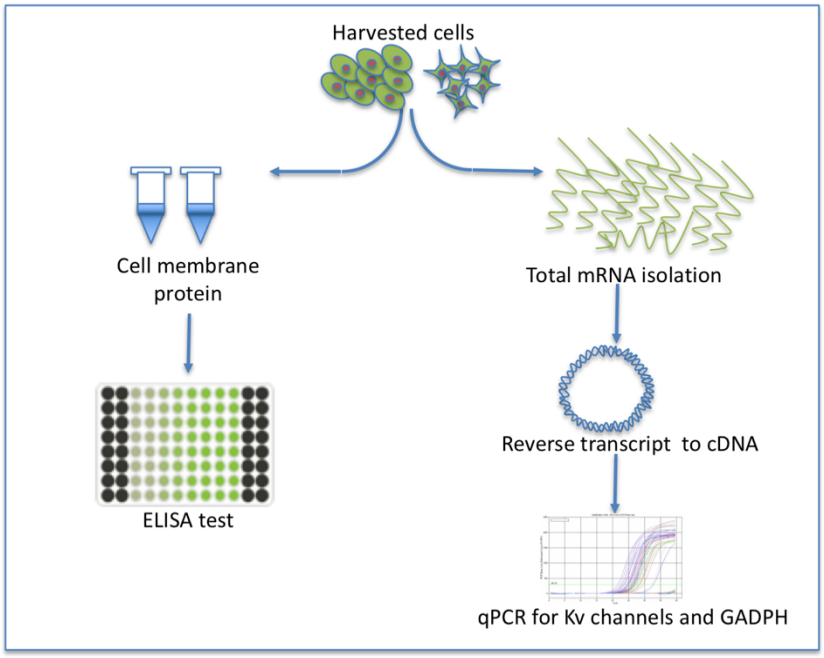

Fig. 3. The processes of sample preparation for both real time qPCR and the ELISA analysis of cell membrane proteins

i. SDS-PAGE and Western blot

For cell membrane protein preparation, cells were washed with PBS and then lysed with a digitonin lysis cocktail with protease inhibitor. The lysate was centrifuged at 500 x g to remove the DNA and another cellular debris released in the supernatant. The pellets were digested in 0.5% Triton-X100 lysis buffer with the protease inhibitor (shaken on ice for 30 min) and the pellets were removed by centrifugation at 10,000 x g for 5 min. The protein concentration of the supernatant was measured using the Bradford assay. Briefly, samples were diluted 10-20 fold and mixed with Bradford assay buffer (Coomassie blue G-250) and the absorbance at 600 nm was read and used to calculate protein concentration. Sixty micrograms of each protein sample were diluted to 20 µl

and mixed with 5 µl of 5x SDS-PAGE sample loading buffer. The samples were heated to 95ºC for 5 min and loaded onto the SDS-PAGE gels. Electrophoresis was at 150 volts for 50 min. Proteins on the gel were transfer to a PVDF membrane with a Bio-Rad mini trans system. The membrane was blocked with 5% non-fat milk for 2 hr. The Kv1.3 protein was detected by rabbit anti-Kv1.3 antibody (1:200) for 1 hr and HRP-conjugated anti-rabbit secondary antibody (1:500) for 1hr. After washing the membranes with TBST buffer (Tris buffer, 0.5% Tween-20) 3 times, 15 min each time, protein was visualized by Immobilon Western Chemiluminescent HRP Substrate.

The cell surface staining and cell imaging of Kv1.3 channel expression

Experiments were performed in glass bottom 96-well plates with 500 cells per well seeded at Day 0. After overnight incubation, the media was removed and the cells were fixed with 4% PFA after washing twice with PBS. Non-fat milk 5% in TBST buffer was added into the wells for 2 hr after washing removed the PFA; and proteins was detected with rabbit anti-Kv1.3 channel antibody (1:200) or FITC direct conjugated rabbit anti-Kv1.3 antibody for 2 hr. If the unconjugated antibody was applied, then an extra secondary antibody incubation step with donkey anti-rabbit antibody was needed. After washing 3 times with TBST buffer, fluorescent antibody staining was visualized result using a Delta Vision fluorescent microscope system with a 60x oil immersion lens.

Transfection studies

Kv channel clone and recombinant expression

The Kv1.1 channel, Kv1.2 channel, Kv1.3(truncated and full sequence) channel and the Kv1.5 channel was cloned into a eukaryotic expression vector with an mCherry fusion protein at the C-terminal of fusion protein. [Fig.4] The specific primer with an adapter sequence was designed for each gene. [Table 3]

Fig. 4.

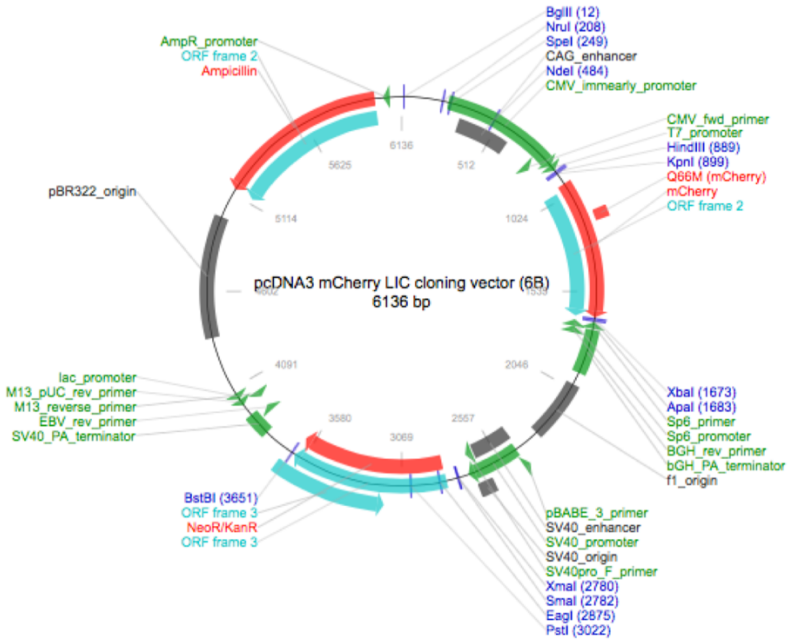

Fig. 4. The vector map for the pcDNA3 expression vector
The pcDNA3 mCherry LIC cloning vector (6B) was utilized for the overexpression of the Kv channels in cells. With a CMV promoter, a mCherry florescent tag can be fused with the recombinant protein at C-terminus.

Table 3. The vector compatible gene specific cloning primers are listed in the table The Kv1.3 truncated primer can be used to amplify the truncated Kv1.3 gene, in which first 52 residues are deleted from the full-length molecule

Kv channel clone primer

Gene's name		Clone primer sequence for pcDNA3 mCherry LIC cloning vector (6B)
Kv1.1	F	5-TACTTCCAATCCAATGCCACC ATGACGGTGATGTCTGGGGAGAA-3
	R	5- CTCCCACTACCAATGCC AAC ATC GGT CAG TAG CTT GC-3
Kv1.2	F	5-TACTTCCAATCCAATGCCACC ATGACAGTGGCCACCGGAGA-3
	R	5- CTCCCACTACCAATGCC ATA CAT CCT GTG CAA TGT AGT TAC AGC TGG -3
Kv1.3 full	F	5-TACTTCCAATCCAATGCCACC ATGGACGAGCGCCT-3
	R	5- CTCCCACTACCAATGCC AAC ATC GGT GAA TAT CTT TTT GAT G-3
Kv1.3 truncate	F	5-TACTTCCAATCCAATGCCACC ATGACCGTGGTGCCC-3
Kv1.5	F	5-TACTTCCAATCCAATGCCACC ATGGAGATCGCCCTGGTGCC-3
	R	5-CTCCCACTACCAATGCC CAA ATC TGT TTC CCG GCT GG-3

The gene specific sequences for the Kv1.1 channel, Kv1.2 channel, truncated Kv1.3 channel cDNA's were cloned from other non-expression vectors and the Kv1.3 full-length channel and Kv1.5 channel cDNA's were cloned from a cDNA pool made from the reverse transcription of Jurkat cell total mRNA. The total mRNA extraction procedure was the same as the protocol described above and the primers used are also listed in the Fig. 3. The PCR reaction was designed with longer extension time to ensure the quality of the PCR product. After confirmation of the cloning with 1.5% agarose gel electrophoresis, the PCR product was purified by QIAquick Gel Extraction kit (Qiagen, Mo). The restriction enzyme digested PCR product was re-purified by the gel electrophoresis. The ligation was transferred into competent *E.coli* (BL21) using a transfection protocol based on heat shock for 40 seconds followed by cooling on the ice for 30 min.

Transfected *E.coli* were cultured at 37^{o}C for overnight on an orbital shaker, 225 rpm. The *E.coli* were harvested by centrifugation at 10,000 x g and the plasmid was extracted using a QIAGEN Plasmid Mega Kit. The detailed steps followed the protocol

provided by vendor. After the final steps, the plasmids concentration was determined using the NanoDrop™ Lite Spectrophotometer to ensure a final concentration that is above 200 ng/µl. The cloning results were confirmed by both PCR-gel electrophoresis and sequencing; the insert was amplified by gene-specific primers, and the length was confirmed by gel electrophoresis. The CMV and mCherry primers were used to sequence the insertions.

The transfection protocol was optimized to identify the best combination of conditions for the highest efficiency of transfection. HeLa cells were seeded into 384 well plates before the experiment. A gradient concentration of lipofectamine 2000, (from 2 times to 1/8 times of recommended dosage), was tested to determine the level giving 70-90% fusion. Different doses of input DNA was also tested. The detailed protocol used was the one recommended by the vendor. Briefly, 100-800 ng of plasmid DNA was mixed with 5 µl Optimal DMEM media and the 0.0125-0.125 µl of lipofectamine 3000 was also dissolved into 5 µl of Optimal DMEM media. After mixing the lipofectamine 3000 and plasmid DNA for 30 min, the mixture was added to the well and the transfected cells were cultured for 48 hr to allow for the accumulation of the expressed protein. At the end of the incubation, cells were fixed and permeabilized with 4% PFA and 0.5% TritonX-100. After staining with DAPI, images were collected using an InCell 6000 microscope and the images were analyzed by InCell Developer software.

Surface and intracellular staining of cells with FITC conjugated HR-crotamine

Forty-eight hours after the transfection, HEK293T or Jurkat cells (on poly-D-lysine coverslip or 6 wells-plate) were fixed and washed twice with PBS. To test intracellular staining, cells were permeabilized with 0.5%v/v of Triton-X100 buffer for 15 min. The cells were then blocked with 5% low-fat milk (or 5% BSA) for 2 hours at room temperature. FITC labeled HR-crotamine (300 nM-10 μM) was added to the blocking buffer and applied to the cells for 1 hr at room temperature followed by washing with TBST buffer 3 times. Coverslips were then used for fluorescent imaging and the cells in the 6 wells plates were scraped and suspended for flow cytometry analysis.

Enzyme digestion studies

Enzyme digestion studies were based on the Heparinase III (New England labs Inc., MA) digestion of the HSPG on the surface of cultured cell lines. Different cell lines were treated following a published protocol (Welch, Svensson, Kucharzewska, & Belting, 2011). Specifically, cells were cultured in 12 well plates or coverslip at 70-80% confluence. Cells were then washed with PBS and treated with the enzymes. The Heparinase III digestion buffer contains 20 mM Tris-HCl, 100 mM NaCl, 1.5 mM $CaCl_2$, *pH* 7 and 2% FBS. The concentration of the Heparinase III was 10 units/ml. The reaction condition involved incubating cells in 37^{o}C cell incubator for 3 hr followed by washing of the cells with PBS to remove the enzyme and digested HSPG side chain.

Trypsin (Sigma-Aldrich, MO) was used as positive control; and the digested cell were stained for FACS or microscopy studies.

Results

Specificity - Comparison of myotoxins

Crotamine versus helleried crotamine

The amino acid sequences of crotamine and helleried crotamine (HR-crotamine) have been aligned and compared. The alignment demonstrated about 90% of the residues are identical. A few sites of heterogeneity were also identified. In these aligned sequences, both proteins include a 22 amino acids signal peptide at the N-terminus. Overall amino acid sequences are highly with at least 36 of the 42 amino acids residues shared between the two proteins. Both sequences contain 11 basic amino acids, 9 lysins, and 2 arginines, and 6 cysteines. The cysteines generate 3 intramolecular disulfide-bonds that help maintain its 3-D structure of the protein. The 3-D structure of both myotoxins is very similar to that of human beta-defensins, important components in the mammalian innate immunity system. Based on the deduced amino acids sequences of both proteins, we have a calculated molecular weight of 4905.96 Da and p*I* point of 9.51. The molecule is highly positive charged cationic peptide, which contains $7e^+$ positive change in at physiological p*H*. The amino acids sequence of our HR-crotamine was obtained and confirmed with mass spectrometry and the peptide was observed to have an actual molecular weight at 4858.575 Da. [Fig.5 A] Counting from the first amino acid of the mature protein, several differences in the amino acid sequence were recognized,

including Arg^{3} vs Gln^{3}, Leu^{19} vs Ile^{19}, Arg^{33} vs Lys^{33}, and Glu^{42} Lys^{43} vs Val^{42} Asn^{43}. Some of the isoforms of HR-crotamine have variations at the 15^{th} and 16^{th} residue (Glu^{15} Lys^{16} vs Thr^{15} Val^{16}) and a C-terminal extension that is several residues longer than the published crotamine sequence. The corresponding cDNA sequences for those amino acid differences were also compared. Only one base pair switch is required to explain the differences between Arg^{3} vs Gln^{3}, Leu^{20} vs Ile^{20}. In contrast, some other isoforms, such as the $Glu^{15}Lys^{16}$ vs $Thr^{15}Val^{16}$ and the C-terminal extension requires significant differences in the encoded gene sequences. Based on the molecular weight determinations, HR-crotamine (6O01) was believed to have a 7 amino acids truncation at C-terminal end of the molecule. The major differences in sequences were considered as reflecting evolutionary changes rather than simple point mutation in the individual genes. Since there is strong homology between crotamine and HR-crotamine and there are only minor differences in their amino acid sequences, we have felt comfortable using HR-crotamine as a probe to investigate the molecular properties of snake venom myotoxins. We have based our studies of HR-crotamine on the results obtained by others in the previous investigation of the activity crotamine isolated from *C. durrisus terrificus* [Fig.5 B, C]

Fig.5.

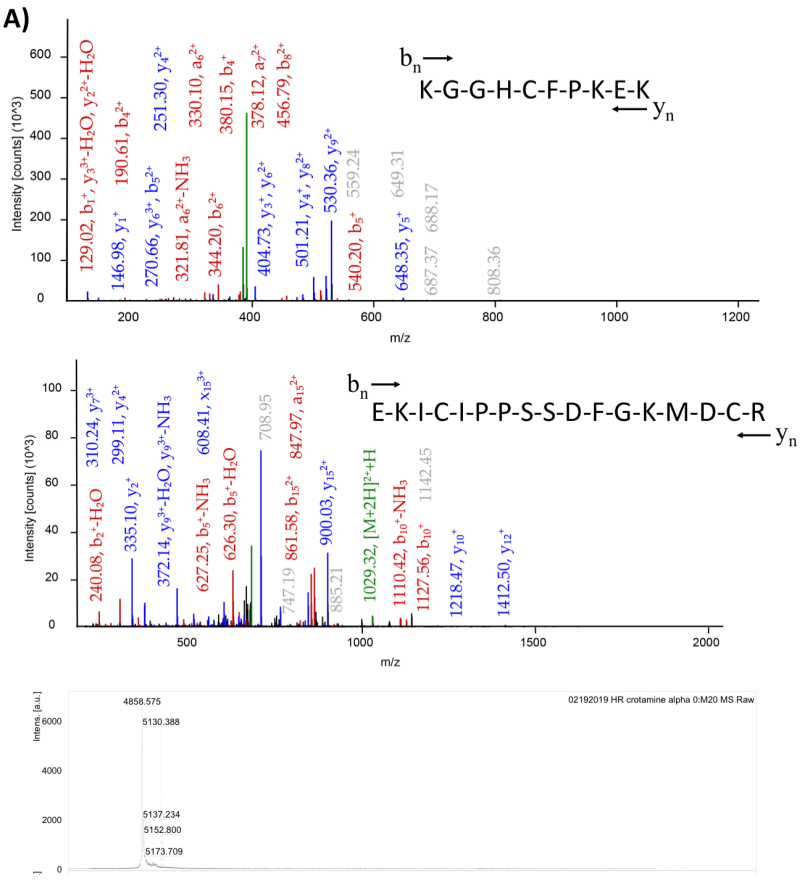

Fig. 5. The protein sequence and structure of helleried crotamine

A) *CID spectra of HR-crotamine.* The CID spectrum of peptides KGGHCFPKEK (m/z 1187.590), EKICIPPSSDFGKMDCR (m/z 2056.930). The characteristic peptide bond fragment ions, type b and type y, are labeled. In the lower panel, the chart indicating an accurate mass measurement of the HR-crotamine peptide using CytC as a calibrant in linear mode. The result is included here: mz=4858.575 Da.

(Fig. 5 Continued)

B)

	1	2	3	4	5	6	7	8	9	10	11	12	13	14	15	16	17	18	19	20	21	22	1	2	3	4	5	6	7	8	9	10	11	12	13	14	15	16	17	18	19	20
Crotamine(AAF34911.1)																							Y	K	Q	C	H	K	K	G	G	H	C	F	P	K	E	K	I	C	L	P
HR-crotamine(6001)	M	K	I	L	Y	L	L	F	A	F	L	F	L	A	F	L	S	E	P	G	N	A	Y	K	R	C	H	K	K	G	G	H	C	F	P	K	E	K	I	C	I	P
3M19	M	K	I	L	Y	L	L	F	A	F	L	F	L	A	F	L	S	E	P	G	N	A	Y	K	Q	C	H	K	K	G	G	H	C	F	P	K	E	K	I	C	I	P
5C09	M	K	I	L	Y	L	L	F	A	F	L	F	L	A	F	L	S	E	P	G	N	A	Y	K	R	C	H	K	K	G	G	H	C	F	P	K	E	K	I	C	I	P
5I03	M	K	I	L	Y	L	L	F	A	F	L	F	L	A	F	L	S	E	P	G	N	A	Y	K	R	C	H	K	K	G	G	H	C	F	P	K	E	K	I	C	I	P
5J11	M	K	I	L	Y	L	L	F	A	F	L	F	L	A	F	L	S	E	P	G	N	A	Y	K	R	C	H	K	K	G	G	H	C	F	P	K	T	V	I	C	L	P
1I06	M	K	I	L	Y	L	L	F	A	F	L	F	L	A	F	L	S	E	P	G	N	A	Y	K	R	C	L	K	K	G	G	H	C	F	P	K	T	V	I	C	L	P
1N24	M	K	I	L	Y	L	L	F	A	F	L	F	L	A	F	L	S	E	P	G	N	A	Y	K	R	C	H	K	K	G	G	H	C	F	P	K	T	V	I	C	L	P

(Continue)	21	22	23	24	25	26	27	28	29	30	31	32	33	34	35	36	37	38	39	40	41	42	43	44	45	46	47	48	49	50	51	52	53	54	55	56	57	58	59	60	61
Crotamine(AAF34911.1)	P	S	S	D	F	G	K	M	D	C	R	W	R	W	K	C	C	K	K	G	S	G	K																		
HR-crotamine(6001)	P	S	S	D	F	G	K	M	D	C	R	W	K	W	K	C	C	K	K	G	S	V	N	N	A	I	S	I													
3M19	P	S	S	D	F	G	K	M	D	C	R	W	K	W	K	C	C	K	K	G	S	G	K																			
5C09	P	S	S	D	F	G	K	M	D	C	R	W	K	W	K	C	C	K	K	G	K	W	K	I	M	P	S	P	S	R	T	M	D	I	F	K	I	W	P	R	T
5I03	P	S	S	D	F	G	K	M	D	C	R	W	K	W	K	C	C	K	K	G	S	G	K																			
5J11	P	S	S	D	F	G	K	M	D	C	R	W	K	W	K	C	C	K	K	G	S	G	K																			
1I06	P	S	S	D	F	G	K	M	D	C	R	W	K	W	K	C	C	K	K	G	S	V	N	N	A	I	S	I													
1N24	P	S	S	D	F	G	K	M	D	C	R	W	K	W	K	C	C	K	K	G	S	V	N	N	A	I	S	I													

C)

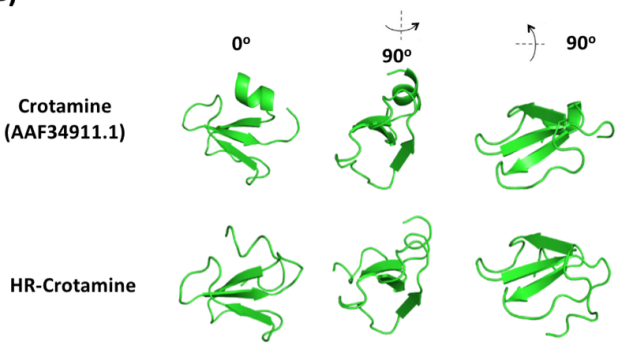

B) *The alignment presenting the comparison of the amino acids sequences between the HR-crotamine from Crotalus oreganus helleri and the published crotamine sequence (from Crotalus durissus terrificus)*. A 22 amino-acids signal sequence at N-terminus is marked out in black box and the HR-crotamine's residue that heterogeneous to crotamine's are labeled in red and green. A tail sequence (in blue) at C-terminus can be recognized on HR-Crotamine and other 3 similar HR-crotamine molecules. A 7 amino acids truncation at C-terminal of the 6O01molecule is marked in blue box. C) *The 3-D structural model for both crotamine and HR-crotamine were calculated and predicted according to the amino acid sequences* The helical ribbons: α-helices and β-strands the direction of the chain are marked; and each structure are compared in front, side and bottom view (related by180-degree rotation through the x and y axis). The high similarity for the structure of these two molecules are recognized.

Dose-dependent effect of crotamine / HR-crotamine on cell proliferation and cell viability – IC_{50} Table

Previous patch clamp studies with crotamine have indicated that crotamine inhibits the activity of Kv1.1, Kv1.2, Kv1.3 channels. To test the biological activity of

HR-crotamine, we applied HR-crotamine to a panel of different cancer cell lines including REN, HeLa, HEK293, B16-F10, MIA PaCa-2, SK-Mel-28, Jurkat, Molt-3, CCRF CEM cells and mouse myoblast cell, C2C12. Information on these cell lines are listed in Table.1. HR-crotamine in a half fold dilution gradient was applied to each of the cell lines and the cell viability was investigated with DAPI staining. The test, which was conducted in quadruplicate (n=4), was conducted using the high throughput liquid dispensing robot. The standardized results obtained are summarized in a dose -dependent chart of growth inhibitory activity for each of the cell lines tested. [Fig.6 A] The results are expressed as growth inhibition, or cell death percentage compared with the number of cells at the starting point of the experiment and the growth of the negative control population during the course of the experiment (72 hr in our tests). The differences in the sensitivity of different cell lines to the growth inhibitory effects of HR-crotamine suggests that cells with higher sensitivity to the myotoxin may have higher levels of a receptor that mediates HR-crotamine's activity on cell proliferation.

The results of this experiment indicated that Jurkat cells are the most sensitive and HeLa cells are the least sensitive of the cell lines tested to the growth inhibitory effects of HR-crotamine. The significant differences between these two cell lines in effective concentration of HR-crotamine required to produce growth inhibition reflects the notable cell-specific selectivity for HR-crotamine's toxicity and suggests that there may be a specific receptor, or target, in Jurkat cell that mediates the effects of HR-crotamine. However, because of HR-crotamine's potential cell penetrating activity, this cell viability experiment, on its own, cannot prove whether there is a specific HR-

crotamine receptor located at the cell surface. An alternative explanation is that the mechanisms for HR-crotamine's activity on Jurkat versus HeLa cells may be different and that this explains the large differences in the EC_{50}'s. HR-crotamine could have multiple receptors at the cell surface or/and intracellular sites.

Fig.6

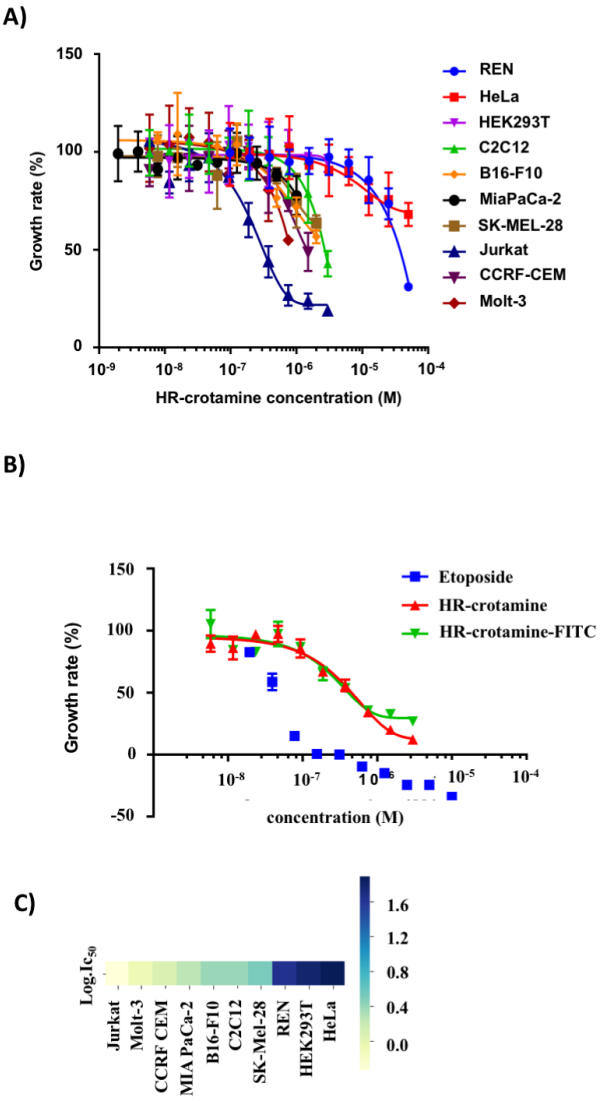

Fig. 6. The effects of HR-crotamine's on cell proliferation
A) *The anti-proliferative effect of HR-crotamine on multiple cancer cell lines* Each experiment was performed in 4-6 replications with means and curve fitting trend line presented. The concentration of HR-crotamine (horizontal axis) is in logarithmic scale.

(Fig. 6. Continued)
REN, HeLa, C2C12, HEK293T, B16-F10, SK-Mel-28, MIA PaCa-2, CCRF-CEM, Molt-3 and Jurkat cells were incubated with graded concentrations of HR-crotamine for 72 hours. Cell numbers were measured by DAPI image segmentation and were expressed as percent (%) for growth/death of control. B) *The cell growth inhibitory effect of FITC labeled HR-crotamine* The chart indicates the cell proliferation was inhibited while the graded concentration of HR-crotamine was present. The PBS was used as the negative control. The positive control is cells treated with Etoposide. Each data point is the mean+/-standard deviation, calculated from 4 replicated determination. The curve was fitted based on each data point with least square method. C) *The heatmap for the IC_{50} of HR-crotamine on multiple cell lines* After the application of the growth inhibition test in multiple cell lines, the growth curve for HR-crotamine with graded concentrations was obtained. The IC_{50} for each cell line was obtained from the curve fitting procedure. Due to the significant range of IC_{50}'s, the logarithmic IC_{50} was use to generate the heat map.

We compared the activity of HR-crotamine and FITC conjugated HR-crotamine to confirm that they have similar activity. Using the cell viability assay described above, FITC conjugated HR-crotamine was also applied to Jurkat cell to determinate its anti-proliferative activity. The overlapping curves obtained from multiple experiments with conjugated and unconjugated HR-crotamine confirms the reproducibility of the assay and the very similar behavior of the unconjugated and conjugated HR-crotamine up to 1 μM concentration. Based on this result, we are confident that FITC conjugated HR-crotamine can be used to study the effects of HR-crotamine on the cells. [Fig.6 B]

In each cell line, ten concentrations of HR-crotamine were tested and the cells death/growth inhibition index was calculated. The curve fitting was then used to generate an IC_{50} value for each cell line. To compare the IC_{50}'s from multiple cell lines we generated the heat map based on a logarithm scale. [Fig.6 C] After comparison of each cell line, we concluded that Jurkat cells demonstrated the highest sensitivity to HR-crotamine with an IC_{50} of 650 nM; while HeLa cells were less sensitivity exhibiting

partial growth inhibition with an IC_{50} of greater than 25 μM. Mouse myoblast C2C12 cells were less sensitive than Jurkat cells, (IC_{50} at 2.8 μM), while the human mesothelioma cells, REN cells, exhibited limited sensitivity (IC_{50} at 44 μM). Two human melanoma cell lines were relatively insensitive, the B16-F10 cell line exhibited slight growth inhibition with concentrations of the HR-crotamine >500 nM while the SK-Mel-28 exhibited no significant growth inhibition. The pancreatic cancer cell line MIA PaCa-2 demonstrated similar sensitivity to C2C12 cells with a calculated IC_{50} of 1.79 μM. In conclusion IC_{50} concentrations for HR-crotamine between different cell lines varied greatly reflecting the notable selectivity of HR-crotamine's growth inhibitory activity.

Our results demonstrating the cell-selective activity in the cytotoxicity of HR-crotamine parallels a report in the literature (Pereira et al., 2011) that also noted the very selective effects of *C. durissus terrficus* crotamine, on cancer cell cytotoxicity. The cell selective effects of myotoxins on cell proliferation argue against that this activity reflects a non-specific interaction of the positively charged toxin with the negatively charged cell membrane. Also, some cells with a very small surface-to-volume ratio, such as non-adherent Jurkat cells are very sensitive whereas adherent cells, such as HeLa cell, HEK293T cell and REN cell, with much larger plasma membrane surface areas were relatively insensitive.

There is a published report that attributes the selective cytotoxic effects of crotamine on cancer cells to their underlying proliferative rate (Nascimento et al., 2012). However, the results we have obtained in our screen of multiple cancer cell lines does

not support this hypothesis. The melanoma cell lines we tested have a doubling time of between 24 hr (B16-F10) and 35 hr (SK-Mel-28). In contrast, HEK293T cell has a doubling time of 20 hr. Jurkat cells have an 18 hr and C2C12 double every 20 hr. There is no correlation between the doubling times of the cells we have used in our screen and their relative sensitivity to the anti-proliferative activity of HR-crotamine. We interpreted the results we have obtained as being compatible with our hypothesis that a specific target (or receptor) expressed on the surface of certain cancer cells, but not others, accounts for the selective effects of HR-crotamine on the proliferative activity of cancer cells.

Time course of the cytotoxic effect of HR-crotamine on selected cancer cell lines

We used some of the same cell lines tested in cell viability study to evaluate the time course for the cytotoxic activity of HR-crotamine. Specifically, we wanted to determine if the anti-proliferative activity observed in the cell viability study (as measured at 72 hr) reflected a very acute effect of the toxin (which might be compatible with an acute biophysical effect on membrane permeability, or whether it reflected a sustained effect on cellular function. To address this question the effect of HR-crotamine on cell growth was evaluated 24, 48 and 72 hr after the addition of the toxin to the cells. [Fig.7 A] The results we obtained demonstrated that differences in cell number in Jurkat cells was detectable at 24 hr and increased progressively thereafter, indicating a sustained anti-proliferative effect. Comparison of results obtained with Jurkat, REN and HeLa cells indicated that the anti-proliferative effect of HR-crotamine reflected

sustained anti-proliferative activity and not an acute effect. [Fig.7 B, C] To confirm this observation, we used a CellTiter-Blue® assay to measure the effect of HR-crotamine on the viability of multiple cell lines under multiple conditions. [Fig.7 D] The results obtained demonstrate that Jurkat cells were much more susceptible to the cytotoxic activity of HR-crotamine at both 24 hr and 72 hr than the other cell lines tested.

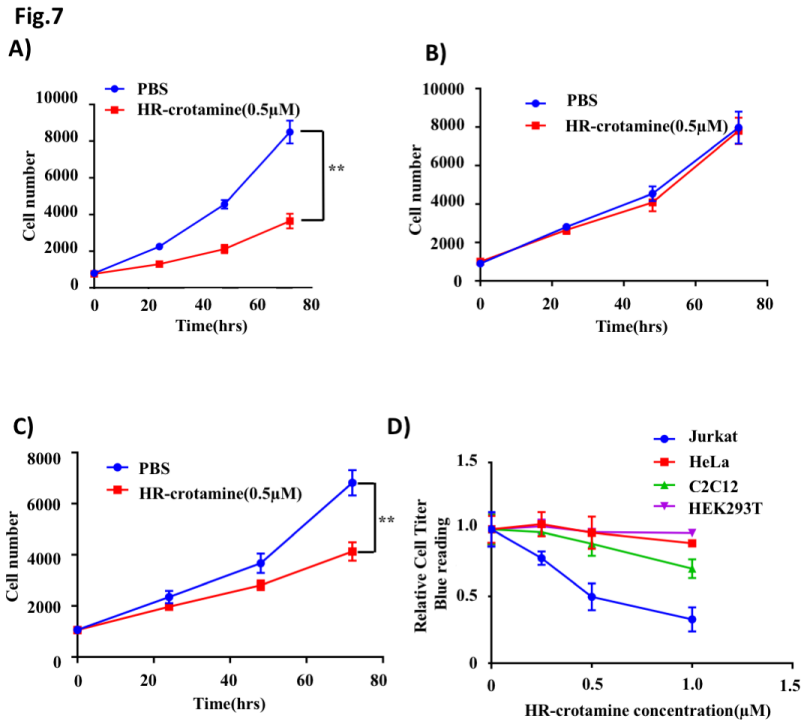

Fig. 7. The growth inhibitory effect of HR-crotamine on Jurkat cell
A) *The time course for the effect of HR-crotamine (0.5 μM) on Jurkat cell proliferation.* PBS serves as the negative control. The results shown are the mean+/-standard deviation for 4 replicates of cell number determinations at the times indicated. (** significance, P<0.05) B) *The time course for the effect of HR-crotamine (0.5 μM) on HeLa cell proliferation* Conditions the same as for Panel A C) *The time course for the effect of HR-crotamine(0.5 μM) on REN cell proliferation* The conditions same as for Panel A . D) *CellTiter-Blue assay for the effect of HR-crotamine on cancer cell proliferation* Cells were treated by HR-crotamine with graded concentration (up to 1 μM) was cultured for 72hr. CellTiter-Blue (CTB) activity was measured by 560/590 absorbance was monitored and the data normalized to the 0 hr values. The results shown are the mean+/-standard deviation for 4 replicates of CTB activity determinations at the times indicated.

Measurement of apoptosis vs necrosis

To further characterize the effects of HR-crotamine on cell viability, we measured whether HR-crotamine induced apoptosis or necrosis in cancer cell lines. Apoptosis was detected using the CellEvent™ Caspase-3/7 assay using both fluorescent cell imaging and flow cytometry. The results obtained showed that there was no evidence for the induction of apoptosis as measured by Caspase-3/7 signal compared with Etoposide, the positive control, in both Jurkat and HeLa cells HR-crotamine does not induce measurable apoptosis in all of the test concentration, up to 1 µM [Fig. 8].

Fig. 8

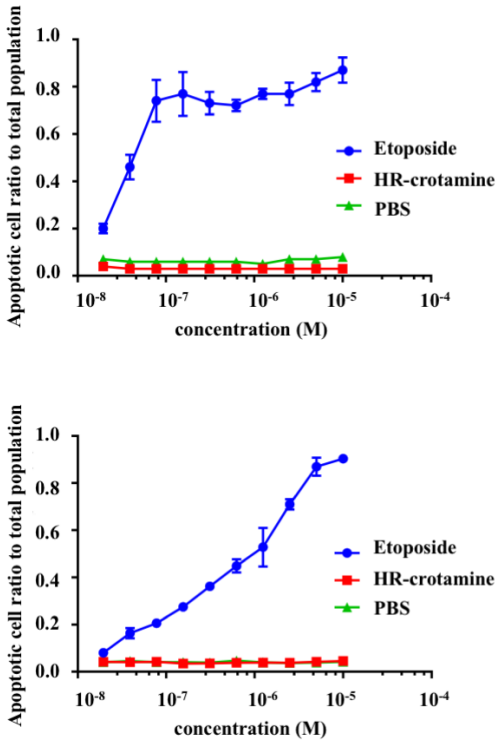

Fig. 8. Measurement of Apoptosis in HR-crotamine -treated Jurkat and HeLa cells Jurkat and HeLa cells were treated with graded concentrations of HR-crotamine or etoposide for 72 hr and the cell was stained by CellEvent™ Caspase-3/7 at the ending

(Fig. 8. Continued)
time point. The stained cells were then applied to the cell segmentation and count. The chart is curve fitted based on each data point. The data points are presented in the mean+/-standard deviation.

Cytotoxicity kinetics

To address the question of whether the growth inhibitory activity of HR-crotamine was attributable to its potential membrane disrupting activity, we compared the kinetics of myotoxin-induced cytotoxicity with that of an established membrane peturbant such as SDS. Multiple cell lines were examined from 0.5 hr to 72 hr after the addition of multiple concentrations of SDS and HR-crotamine to the wells. A concentration of 0.0025% w/v of SDS induced 100% cell death in HEK293T, HeLa, SK-Mel-28, C2C12 and Jurkat cells within 0.5 hr. In the higher concentration of SDS present, 0.02%, the cell apoptosis was trigger as expected. After 4 hr, the apoptotic population was reduced in total population may due to most cells were eliminated within 4 hr. By contrast, in the HR-crotamine treated group, the apoptotic cells were very few at any time points. [Fig. 9] Based on the observation on SDS treated cells, the apoptosis was triggered immediately, once the cytoplasm membrane interrupted. However, the HR-crotamine, even in highest test concentration, was not increase the percentage of apoptotic population. The HR-crotamine may neither impair the cells membrane integrity nor trigger the cell apoptosis.

Fig. 9

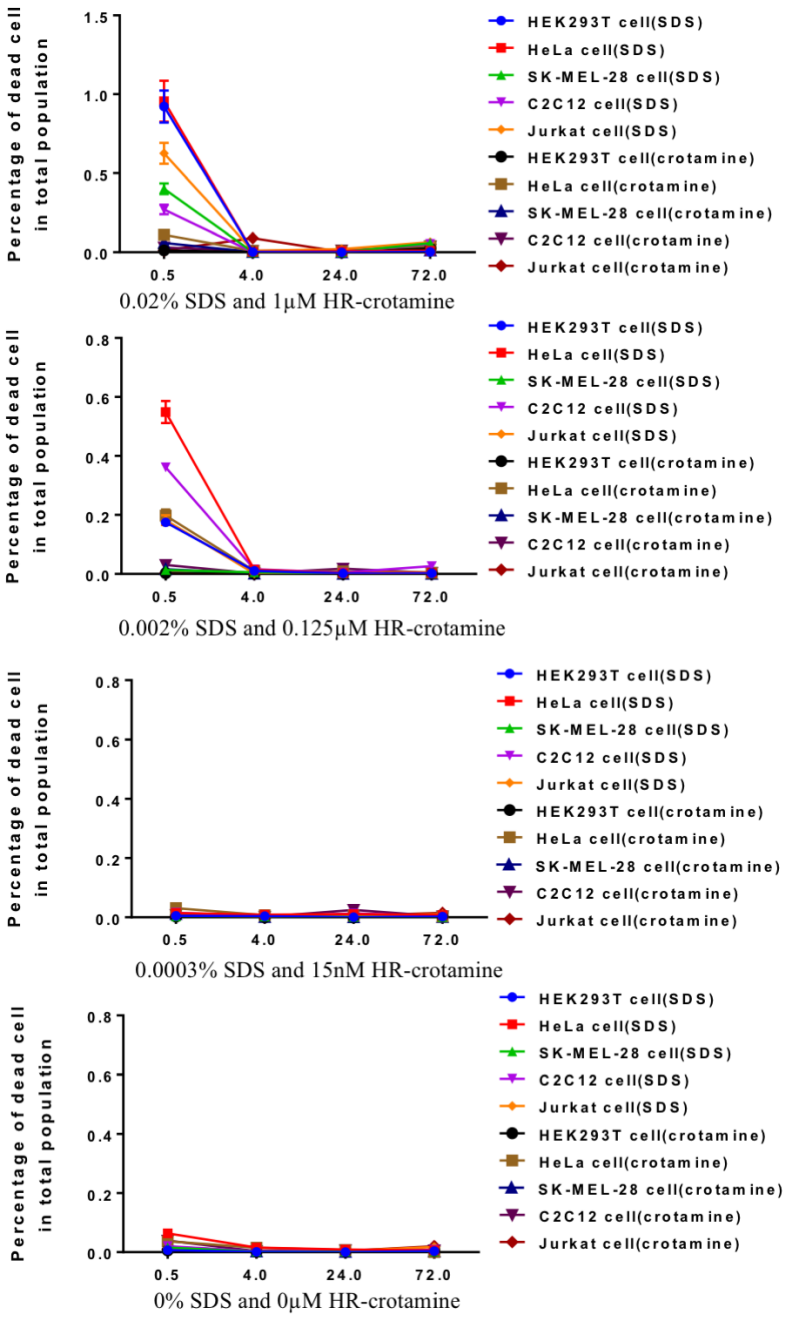

Fig. 9. The comparison for apoptotic population triggered by HR-crotamine or SDS on multiple cell lines.

Several concentrations of SDS and HR-crotamine were applied to multiple cell lines and the percentage of apoptotic cell population in total population was monitored by DRAQ7™ staining and DAPI staining at 0.5 hr, 4 hr, 24 hr and 72 hr. Each data point was present the mean from 4 replicate tests+/-standard deviation.

Comparison of the effect of HR-crotamine on multiple leukemia cell lines

Our initial studies characterized the effects of HR-crotamine of Jurkat cells, a CD3 positive, IL-2 expressing T-cell leukemia cell line isolated from 14-year-old boy. To examine the generality of the observed effects, we compared the activity of HR-crotamine on Jurkat cells with its activity on 2 additional human T-cell leukemia cell lines, CCRF CEM and Molt-3 cell. All 3 cell lines showed inhibition of cell proliferation in response to HR-crotamine as measured by both cell counting and CellTiter-Glo assays but there were modest quantitative differences in the sensitivity of the different cell lines. [Fig.6 A] Molt-3 cells and Jurkat cells were comparable and CCRF CEM cells were less sensitive to the growth inhibitory effects of HR-crotamine. SK-MEL cells and HeLa cells were used as the reference for HR-crotamine insensitive cells. [Fig.10 A] These studies confirmed that the relative sensitivity of Jurkat cells to the growth inhibitory activity of HR-crotamine was not unique to Jurkat cells but was a general property of Human T-cell leukemia cells.

Our hypothesis is that the differential sensitivity of cancer cell lines to cytotoxic activity of HR-crotamine, is based on the differential expression of specific molecular targets (or receptors) that mediate the cytotoxic effects. Based on previous studies carried out on the biological activities of snake venom myotoxins, we considered two specific classes of targets, Kv channels or HSPG's, as the best candidates to account for the differential effects of HR-crotamine of cell proliferative activity. To test this hypothesis, we tested the level of expression of 4 major classes of Kv channels Kv1.1, Kv1.2, Kv1.3 and Kv1.5 (as measured by qPCR) and HSPG's (as measured by ELISA,

on the three “sensitive” leukemia cell lines and HeLa cells, a “resistant” cell line. The results obtained from this study [Fig.10 B and C] showed that all 4 cell lines expressed comparable levels of Kv1.1, Kv1.2 and Kv1.5 but dramatically difference levels of Kv1.3 channel. The Kv1.3 channel transcript was detected in all of the T cell leukemia cell lines but was close to undetectable in HeLa cells. [Fig.10 B] The level of HSPG expression was comparable between the leukemia cells and HeLa, making it unlike that differential expression of these proteins accounted for the selective effects of HR-crotamine on cell proliferation. Based on these results, we narrowed the test of our hypothesis to address the question of whether differential expression of Kv1.3 could account for the selective cytotoxic effects of HR-crotamine on cancer cells.

Fig.10.

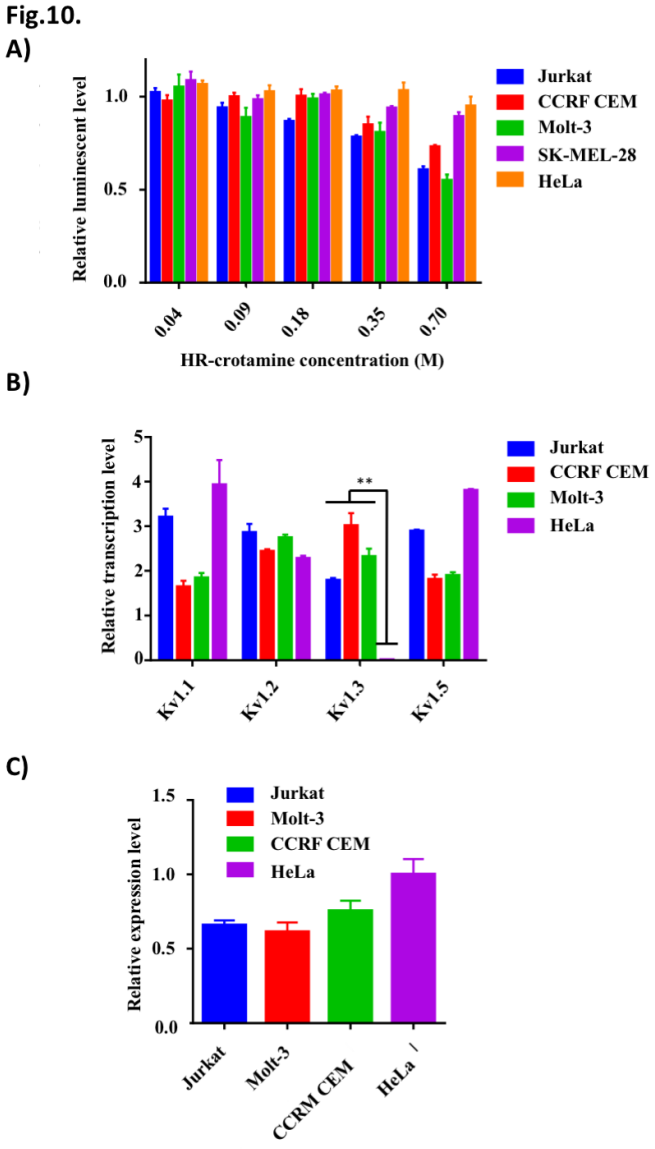

Fig. 10. The relation between cell growth inhibition effect and the expression level of potential binding target.

A) *CellTiter-Glo assay for the effect of HR-crotamine on cancer cell proliferation* Cells treated with graded concentrations of HR-crotamine were cultured for 72 hr. CellTiter-Glo activity was measured by luminescence plate reader. The results shown are the mean+/-standard deviation of the luminescence signal for 4 replicates of CellTiter-Glo test. B) *Measurement of Kv1.1, Kv1.2, Kv1.3 and Kv1.5 channel expression in leukemia cell lines and HeLa cells* Gene specific transcripts were quantitated by real-time qPCR with gene specific primers. GAPDH was used as internal reference. The results shown are the mean+/-standard deviation for 3 replicates of Kv channel transcript level assay.

(Fig. 10. Continued)
C) *HSPG receptor level in leukemia cell lines and HeLa cells* An ELISA assay was used to measure the level of HSPG's in protein samples prepared from the total cell membrane preparation from each of the cell lines. Each bar is normalized to the level of HSPG in HeLa cells. The results shown are the mean+/-standard deviation for 3 replicates of HSPG expression level determinations.

Correlation of susceptibility versus putative targets

Kv's in sensitive versus resistant cells

Transcript and protein expression patterns

Since we have previously profiled the relative sensitivity of multiple cell lines to the growth inhibitory effects of HR-crotamine, we examined the level of endogenous Kv channel expression to determine if these was a relationship between the level of expression of a specific Kv channel and the sensitivity of that cell line to HR-crotamine. For these studies we focused on four Kv channels, Kv1.1, Kv1.2, Kv1.3 and Kv1.5, because previous patch-clamp studies had reported that the first three (Kv1.1, Kv1.2, Kv1.3) were sensitive to inhibition by snake venom myotoxin whereas Kv1.5 was not. (S. Peigneur et al., 2012). We used gene-specific real-time PCR to examine the expression level of the Kv channel transcripts in cDNA prepared from RNA from multiple HR-crotamine sensitive and insensitive cell lines. The real-time qPCR assay that we used was run in 20 μl volume master mix that included 10 μl FastStart SYBR Green Master (Roche, Inc., Switzerland), 1 μl of forward and reverse primer mix, 1 μl of cDNA sample and 8μl of molecular grade water. Each sample was run in triplicate. Beta-actin and GAPDH, two house-keeping genes were used to normalize the data from different cell lines. The real-time qPCR was performed on StepOnePlus™ Real-Time

PCR Systems for 40 cycles. The protocol includes 95ºC at 1 min and 55ºC at 1 min followed by a melting curve step, for each cycle. The calculated final results were presented as the mean+/-standard deviation format. [Fig.11] The results of this study showed that there was absolutely no correlation between the level of expression of Kv1.1, Kv1.2 or Kv1.5 and the sensitivity of the cells to HR-crotamine's cytotoxic activity. There was, however a highly significant negative correlation between the level of expression of Kv1.3 and the IC_{50}, namely the higher the level of expression of the Kv1.3 transcript, the lower the IC_{50} for the growth inhibitory effect of HR-crotamine.

Fig.11

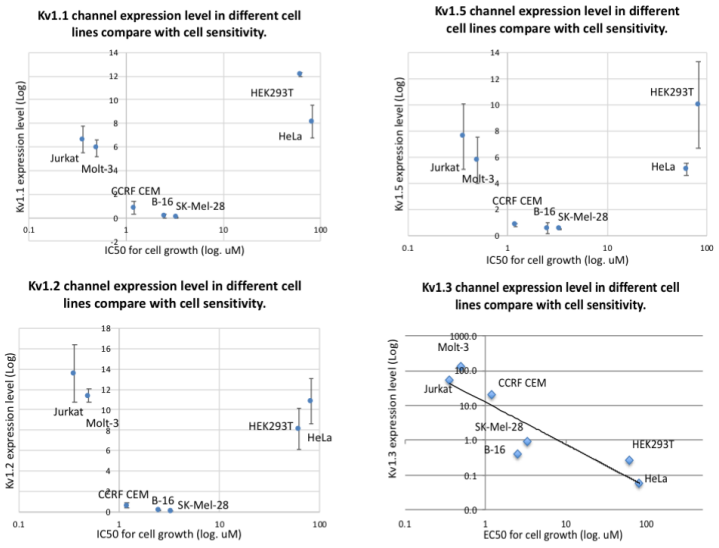

Fig. 11. The Kv channel expression level and HR-crotamine sensitivity correlation analysis

The IC_{50} value for the growth inhibitory effect of HR-crotamine for each of seven cancer cell lines was plotted against the relative level of Kv1.1, Kv1.2, Kv1.3 and Kv1.5 transcript expression. Values are plotted on a logarithmic scale. Error bars indicates the standard deviation. The solid line in the chart for the Kv1.3 channel correlation represents the linear correlation between these two sets of data.

Studies on the Overexpression of Kv Channels in cell lines.

The next step in our studies was to determine whether overexpressing Kv1.3 in cells rendered them susceptible to the growth inhibitory activity of Kv1.3. To achieve this goal, we had to optimize the transfection conditions for cell survival and highest transfection rate.

Kv channels are expressed at very low levels in most cells, making the study of the direct interactions of putative inhibitors with Kv channels technically difficult. In the case of a scorpion toxin that was thought to bind Kv channels, overexpression of the channels in a cell line with very low endogenous Kv channel expression was used successfully to demonstrate direct interactions (Gamper et al., 2002). To generate human Kv channel expression vectors, Kv1.1, Kv1.2, a N-terminal truncated version Kv1.3 that lacks sequences necessary for plasma membrane insertion (Kv1.3 truncate) and Kv1.5 channel was first cloned from commercially available vectors. The full length Kv1.3 channel was cloned from the total mRNA extracted from Jurkat cells. The pcDNA3 mCherry LIC cloning vector(6B) was used to create the eukaryotic overexpress vector suitable for transfection into selected cell lines. This vector includes an mCherry fluorescent tag can be fused in-frame to the C-terminus of the recombinant protein. The inserted sequences were confirmed by both PCR fragment length determination and gene sequencing. [Fig.12 A]

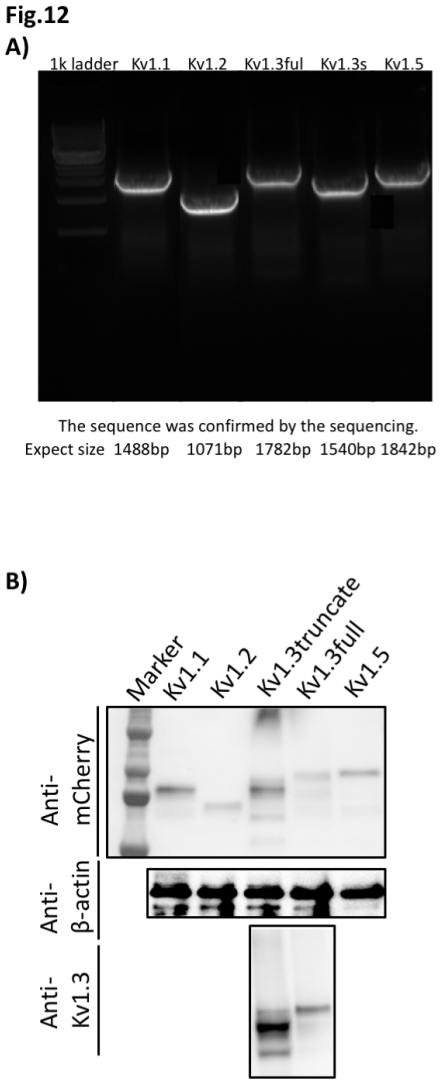

Fig. 12. Overexpression of the Kv channels in HeLa cells
A) *The confirmation of Kv channels insert segment size* Kv1.1, Kv1.2, Kv1.3 full length, Kv1.3 truncate and Kv1.5 cDNA's were cloned using gene specific primers and double digestion with restriction enzymes. The cDNA's were ligated into the pcDNA3 mCherry LIC cloning vector(6B) with T4 ligase and the size of the insert sequences was confirmed by DNA gel analysis. The expected size for each DNA segment is listed at the bottom of the figure. B) *Western blot of the HeLa cell with Kv channels overexpression* The Western blot was applied to the total protein harvested from the HeLa cell with Kv channel overexpression. The rabbit anti-mCherry antibody was applied in 1:1000 dilution while the mouse anti-Kv1.3 channel antibody was diluted in 1:500. The beta-actin amount in each sample loading is also presented at lower panel to indicate the equal amount of protein sample was applied. The expected molecular weight is listed at the bottom of the figure.

To confirm that the expression vectors were generating the anticipated proteins in transfected HeLa cells, the presence of expressed proteins of the correct size was confirmed by Western blot. Total cell proteins harvested from HeLa cells transfected with the individual Kv channel expression vectors, were fractionated by SDS-PAGE and the transfected fusion proteins detected using anti-mCherry antibodies. In the case of Kv1.3 the fusion protein was also detected with an anti-Kv1.3 channel antibody as well. Western blot analysis confirmed the expression of each of the Kv channel proteins with the anticipated correct size. [Fig.12 B]

The final goal of this overexpression model was to determine whether the overexpression of Kv channels impacted the viability of the transfected cells and their sensitivity to growth inhibition by HR-crotamine. The viability of HeLa cells transiently transfected with each of the Kv channel expression constructs (or empty vector as a control) was evaluated after 72 hr treatment with 1 μM of HR-crotamine or negative control (PBS). The results we obtained indicated no significant differences in cell growth were observed (data not shown). There are obviously many possible interpretations to this negative result. It could be due to the limited level of expression of Kv1.3 in the transfected HeLa cells (or the limited fraction of cells expressing adequate levels of Kv1.3 channel on the cell surface). Alternatively, multiple counter-regulatory mechanisms may have suppressed the level of expression of the channel, or its downstream effectors such as Ca^{+2} regulatory systems, in response to the overexpression of the channel. Finally, it is possible that Kv channels are not involved in growth

regulatory activity in HeLa cells or other ion channels may function to compensate for artificially induced changes in Kv1.3 channel expression,

HSPG depletion studies

Our preliminary correlative studies had pointed away from a relationship between the level of expression of HSPGs on multiple cancer cell lines and their sensitivity to the growth inhibitory activity of HR-crotamine. The quantitative results of ELISA were summarized in the bar chart. [Fig.13 A] The levels of HSPG on the surface of C2C12 cell, HeLa cell and SK-Mel-28 cell are very close. Jurkat cells had lower levels of HSPG's than the other cells lines. To ensure that the level of HSPG's on the surface of cells was not a contributor to the sensitivity of the cells to the growth inhibitory activity of HR-crotamine, we next carried out depletion studies using heparinase III to reduce the levels of HSPG's on both myotoxin sensitive and insensitive cell lines. Cells treated with buffer alone served as a negative control while digestion with Trypsin/EDTA served as a positive control. As shown in Fig. 13 A, treatment with heparinase III resulted in a major decrease in HSPGs (as measured by ELISA using mouse anti-HSPG/Heparin) on the surface of all three cell lines tested. The next step was to determine whether the reduction in HSPG content on the surface of the cells reduced their sensitivity to growth inhibition by HR-crotamine. [Fig.13 B] The results obtained showed clearly that HR-crotamine was effective in reducing the proliferative activity in heparinase III-treated Jurkat cells. There were minimal effects on HR-responsiveness in the two "unresponsive" melanoma cell lines. These studies confirmed the observation

that while HSPG's may bond to myotoxins, this effect is not essential for the growth inhibitory activity of the myotoxin.

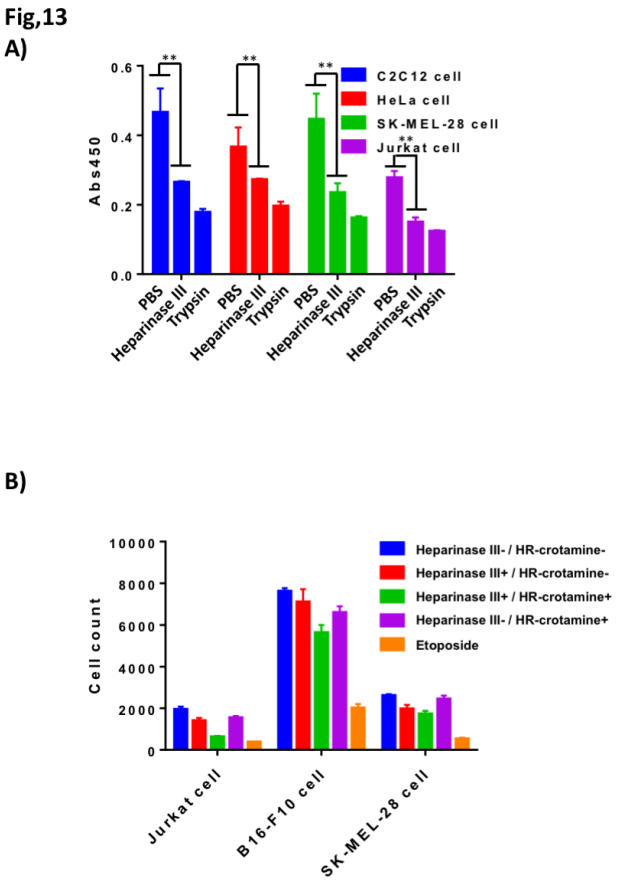

Fig. 13. Heparinase III digestion of HSPG's and the effect of HSPG depletion on HR-crotamine's antiproliferative activity
A) Measurement of cell surface HSPG levels in Heparinase III-treated cells. C2C12, HeLa, SK-Mel-28 and Jurkat cells were treated with Heparinase III and the levels of HSPG's in the cell membrane prep were determined by first lysing the cells in a detergent cocktail, sediment the cell membranes and solubilizing membrane proteins was in 0.5% Triton-X100. Both solubilized membrane proteins and the pellets were analyzed using an indirect ELISA with mouse anti-HSPG/Heparin in 1:2000 dilution. All determinations were in triplicate and the values represent the mean+/-standard deviation. The PBS group represent the baseline HSPG levels in each of the cell lines. The trypsin-treated group represents the maximal reduction of cell surface HSPG's achievable by non-specific protease digestion. B) *Cell growth analysis for Heparinase III and HR-*

(Fig. 13. Continued)
crotamine treated cells. Jurkat and two skin melanoma cell lines, B16-F10 and SK-Mel-28, were treated with 7 unit/ml Heparinase III for 3 hr and then washed with PBS. The cells were then continued to be cultured with Heparinase III present with or without the addition of HR-crotamine (1 μM). Etoposide (0.1 mM) served as the positive control and PBS as the negative control. The result indicate that the Heparinase III has a small effect on cells proliferation but significant growth inhibition was observed in the cells treated with both Heparinase III and HR-crotamine. For all three cell lines, the Heparinase III-treated cells are more sensitive than the Heparinase III- untreated cells.

In summary, the preceding studies have suggested that the cytotoxic activity of HR-crotamine are not readily explained by the potential interactions of the myotoxin with the cell's lipid bilayer membrane nor with cell surface HSPG's (Nascimento et al., 2007). The results we have obtained point to the anti-proliferative activity of the myotoxin are most likely due to interactions with one or more targets (i.e. receptors) on the cell surface that are responsible for the transfer of the anti-proliferative activity to the interior of the cell.

Discussion

Implications for selectivity

Malignant versus normal cells

The basic question we have been addressing is why certain cancer cells and cancer cell lines are more sensitive than others or normal cells to the cytotoxic activity snake venom myotoxins. Although a number of different explanations, such as differences in doubling time or metabolic activity, interactions with membrane lipid bilayers, presence or absence of cell surface sulfated proteoglycans or specific ion

channels, have been advanced to account for this selective activity, none has been definitively demonstrated to account for the anti-proliferative activity of this class of toxins. The preliminary studies we have carried out with sensitive versus insensitive cancer cell lines have eliminated most of the potential mechanisms proposed by others. Our results have pointed towards a specific interaction with one or more classes of membrane receptors as serving as the most likely mechanism for the action of these proteins.

The Jurkat cell model for HR-crotamine study

In an initial survey of myotoxin sensitive versus insensitive cell lines suggested that Jurkat cells would make a useful model system for a sensitive cell line and HeLa cells were a good example of an insensitive cell line. The Jurkat cells were not unique, in their sensitivity to HR-crotamine, several other human T-cell leukemia cell lines exhibited comparable sensitivity. Similarly, the insensitive properties of HeLa cells were shared with other cell lines including melanoma and epithelioma cell lines. Jurkat cells were readily transfect-able and were convenient for long term culture studies and had a relatively short doubling time. These properties were important for future studies which would require specialized analysis such as the measurement of cell surface binding activity or the construction of stably-transfected cell lines.

Proposed mechanism based on observations

No correlation between HSPG expression level and sensitivity of cells to HR-crotamine

The human T-cell leukemia cell lines, Jurkat, CCRF-CEM and Molt-3, are small spherical cells that grow in suspension, with relatively low cell surface area/volume ratio and large nuclear/cytoplasmic volumes compared with other attached malignant cell lines. We have found that these cell lines were the most sensitive to HR-crotamine among the cell lines tested. Some groups have proposed that the cytotoxic activity of myotoxins such as HR-crotamine are dependent on their internalization in a receptor-mediated, energy required process. They have suggested that the principal receptors for this process could be syndecan-3 and its heparan side chain(Nascimento et al., 2007). In our studies, we found no evidence for HR-crotamine internalization and no relationship between HSPG expression or levels and the growth inhibitory activity of the myotoxin.

Kinetics: Receptor-mediated versus biophysical effect

Some studies from other groups have suggested that the cytotoxic activity of myotoxins may be due to its cell penetrating due to the high positive charge of the molecule at physiological *pH* and its potential ability to interfere with the cell membrane's lipid bilayer structure. The presence of a large amphipathic surface on the crotamine molecule is hypothesized to permit its breaching of the lipid bilayer structure subsequent disruption of the membrane structure. We do not believe this type of mechanism accounts for the bio-activity of HR-crotamine because the interaction

between the lipid bilayers and the detergent/or detergent-like molecules are very rapid and generally very complete (Schilling, Kamholz, & Yager, 2002). We demonstrated the kinetics of this type of effect in studies that compared the cytotoxic activity of a membrane-disrupting detergent such as SDS with HR-crotamine. Even very low concentrations of the detergent have effects on cell viability that are readily detected within 30min. HR-crotamine on the other hand requires many hours of exposure to decrease the proliferative activity of sensitive cells. These studies make it very likely that the myotoxin exerts its anti-proliferative activity not via a detergent-like biophysical disruption of cell membrane bilayer structures.

According to the previous study, the toxins may achieve toxic effects by plugging into ion channel pores and occlude it (Yount et al., 2009). Thus, the ability of structurally divergent toxins to interact with a particular Kv channel relies on a certain spatial distribution of amino acid residues that are keys to the toxin-channel interaction. Based on their structure, these toxins were classified into three groups: 1) myotoxins of the crotamine type, which is considered as voltage channel modulators; 2) "three fingers" toxins; and 3) substances homologous to protease inhibitors and Kv1 channels blockers (Kordis & Gubensek, 2000). Most of these toxins are 23-64 residues in length and are tightly packed by three or four disulfide bridges. They can modify potassium permeability in excitable and non-excitable cells at nanomolar concentration level or below(Soares et al., 2000).

The particularly high binding affinities of channels, such as Kv1.3 channel, to several toxins, are proposed based on the charge and 3-D molecule structure. The toxins

that carry charges of between +5e and +8e are drawn toward the negatively charged receptor site, near the entrance of the selectivity filter, where they physically occlude the conducting pathway of K^+ ions based on the molecule shape (Swartz & MacKinnon, 1997). The crotamine contains a large number of cationic residues and have a +7.6e at *pH*. 7.4 (I. Kerkis et al., 2010). Thus, in human normal blood *pH*. range, the crotamine have all of the prerequisite property to bind to the channels. Based upon the analysis of the sequences, it suggests that the toxins may bind to channel may via two basic charge residues, lysine and arginine. Due to the unique distribution of the charge in myotoxin molecule, several H-bonds are formed between the toxin and channel to stabilize the binding after the initial binding(Ward, Chioato, de Oliveira, Ruller, & Sa, 2002).

Type of cytotoxic activity (proliferation inhibition versus necrosis versus apoptosis)

We used a variety of experimental techniques to demonstrate that, under the conditions used to show significant decreases in cell proliferation, that HR-crotamine does not induce either cell necrosis or cell apoptosis. Even after 72 hr of incubation with 1μM HR-crotamine and in the presence of major growth inhibition, no significant increase in the number of dead or apoptotic cells was detected. Our data suggests that under our conditions HR-crotamine can have a purely anti-proliferative effect on susceptible cells.

CHAPTER II

IDENTIFICATION OF THE CELL SURFACE TARGET THAT MEDIATES THE ANTI-PROLIFERATIVE ACTIVITY OF HELLERIED CROTAMINE

Introduction

The identification of the cell surface protein that is the target for HR-crotamine binding is the critical first step in establishing the molecular mechanisms involved in the anti-proliferative activity of the myotoxin (Campelo et al., 2016). In our previous studies we have identified, HR-crotamine sensitive and insensitive cells and have provided evidence in support of the hypothesis that cell surface Kv receptors are candidates for mediating the cytotoxic activity of HR-crotamine (S. Peigneur et al., 2012). To test the hypothesis that a subset of Kv channels serve as the functional targets of HR-crotamine target, we have employed a set of molecular and pharmacologic approaches to characterize HR-crotamine binding on sensitive and insensitive cell lines.

Methods

Cell Surface Binding Assay

We used two binding assay protocols, direct binding using varying concentrations of FITC HR-crotamine and a competitive binding assay using a fixed concentration of FITC HR-crotamine and varying concentrations of unlabeled HR-crotamine, to measure the binding of HR-crotamine to intact Jurkat cells. The FITC conjugated HR-crotamine used in these experiments was produced using the DyLight

labeling kits (Thermo Fisher Scientific, MA) follow the vendor's recommended protocol. In the direct binding assay, $1X10^6$ Jurkat cells were incubated with graded concentrations (9 μM-100 nM, in half fold dilution) of FITC labeled HR-crotamine 20 min on ice to limit endocytosis. The cells were then washed with ice-cold PBST buffer (0.5% v/v Tween-20) to reduce non-specific background binding The PBS without FITC HR-crotamine served as the negative control. The cells were then analyzed for bound FITC HR-crotamine with a LSRII flow cytometer. The results were normalized within the signal window between the positive and negative controls to reduce the interference from the background and non-specific binding.

In the competitive binding assay, graded concentrations (from 0 μM to 20 μM, in) of unlabeled HR-crotamine (from 20 μM-0 μM, in half fold dilution) was mixed with 1 μM of FITC labeled HR-crotamine before addition to $1X10^6$ Jurkat cells, the cells and the pre-mixed HR-crotamine were incubated on ice for 20min as described above. The PBS buffer served as the negative control and FITC HR-crotamine alone served as the positive control to generate the signal window boundaries. After incubation, cells were washed, processed by fluorescent flow cytometry and the data analyzed as described for the direct binding assay.

Overexpression of Kv channels and binding study

The pCIG3 (pCMV-IRES-GFP version 3) lentiviral expression vector (from Add gene, MA) [Fig.14 A] was used to construct Kv channel expression vectors (Kv1.1, Kv1.2, full length and truncated Kv1.3 and Kv1.5). in which the C-terminal of the

recombinant channel cDNA is fused, in frame, to a Flag tag. This expression vector system also has ERIS-GFP to facilitate positive clone selection. The gene-specific primers used to characterize the inserts are listed in Table 4. HEK293T were transfected with the expression vector constructs, psPAX2 and pMD2G vector using Lipofectamine® 3000 reagent (Thermo Fisher Scientific, MO) following the vendor's recommended protocol. After 48 hr, the culture medium was harvested to collect the lentivirus, and the lentivirus was used to transfect Jurkat cell using a protocol in which 400 μl of lentivirus media and the Jurkat cells were mixed and centrifuged at 2000 rpm for 120 min to increase the transfection efficiency. The transfected Jurkat cells was ready for FACS sorting after 48 hr of cell culture. [Fig.14 B]

The overexpression of each Kv channel in Jurkat cells was tested and confirmed by Western blot (with mouse anti-Flag antibody,1:2000) and cell surface staining of non-permeabilized cells with anti-Flag antibodies. In the surface staining experiments, cells were stained with (1:1000) mouse anti-Flag antibody following a conventional surface staining protocol. Both the stained cells and Western blot membranes were treated with 1:5000 anti-mouse secondary antibody. The Western blot result was visualized by ECL buffer (Thermo Fisher Scientific, MO). Immunofluorescent images were collected using a DeltaVision Elite high-resolution microscope (GE healthcare, IL).

Table 4. Gene specific primers used to amplify the Kv channel sequences prior to cloning in the pCIG3 vector

Gene's name		Clone primer sequence for pCIG3 (pCMV-IRES-GFP version 3)
Kv1.1	F	5-CGG CTCGAG ATGACGGTGATGTCTGGGGAGAA-3
	R	5- CGG GGATCC TTA CTTGTCGTCATCGTCTTTGTAGTC AAC ATC GGT CAG TAG CTT GC-3
Kv1.2	F	5-CGG CTCGAG ATGACAGTGGCCACCGGAGA-3
	R	5- CGG GGATCC TCA CTTGTCGTCATCGTCTTTGTAGTC ATA CAT CCT GTG CAA TGT AGT TAC AGC -3
Kv1.3 full	F	5-CGG CTCGAG ATGGACGAGCGCCT-3
	R	5- CGG GGATCC TTA CTTGTCGTCATCGTCTTTGTAGTC AAC ATC GGT GAA TAT CTT TTT GAT G-3
Kv1.3 truncate	F	5-CGG CTCGAG ATGACCGTGGTGCCC-3
Kv1.5	F	5-CGG CTCGAG ATGGAGATCGCCCTGGTGCC-3
	R	5-CGG TTAATTAA TCA CTTGTCGTCATCGTCTTTGTAGTC CAA ATC TGT TTC CCG GCT GG-3

Fig. 14
A)

Fig. 14. The lentiviral expression vector system used to manipulate (overexpression and knockdown) of Kv channels in Jurkat cells.
A) *The gene map of the lentiviral expression vector (pCIG3) that was used for the expression of Kv channels in the Jurkat cells.* The vector contains the ampicillin resistance gene and IRES EGFP domain for clonal selection.

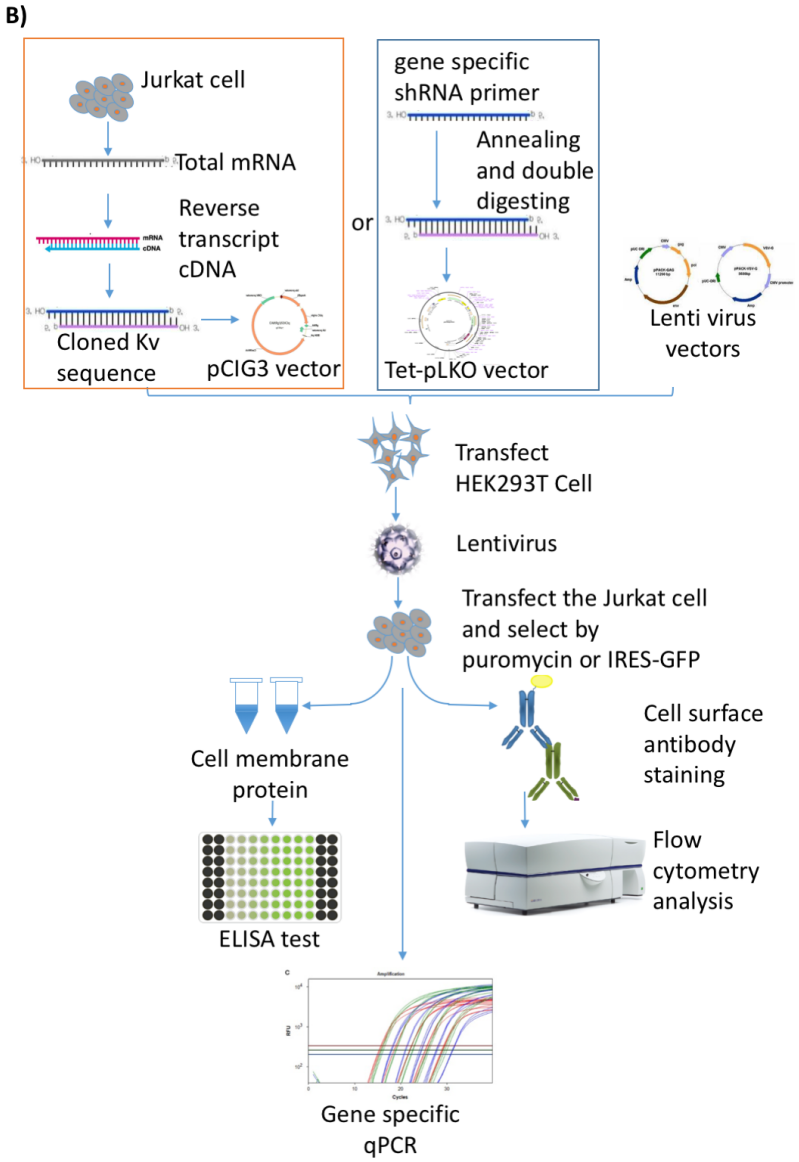

(Fig. 14. Continued)
B) *The protocol used for the overexpression and knock down of Kv channels in Jurkat cells.* Individual Kv channels were amplified from Jurkat cell cDNA's and cloned into the *pCIG3 expression vector*) or the knockdown vector (Tet-pLKO-puro). Lentivirus constructs were applied to Jurkat cell. Positive clones were selected by GFP sorting or puromycin selection. The level of overexpression and the efficiency of knock down was tested by gene specific real-time qPCR, cell membrane protein ELISA or indirect immunofluorescent cell staining.

C)

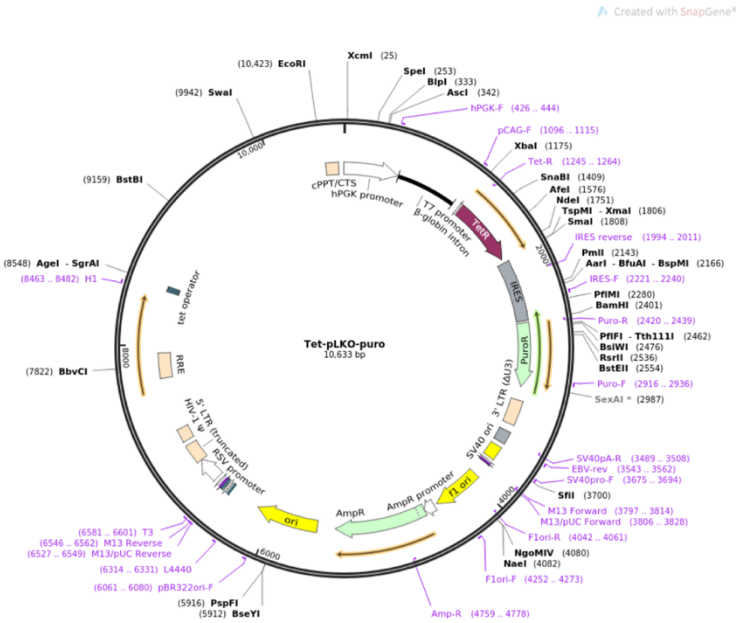

(Fig. 14. Continued)
C) *The gene map for the Tet-pLKO-puro vector* This vector was used to generate shRNA's, which were used to knock down Kv channel transcripts in Jurkat cells. The vector includes a doxycycline-inducible expression system and a puromycin resistance gene for clonal selection.

To measure the binding of HR-crotamine to cells, 1 µM of FITC-conjugated HR-crotamine was applied to pre-chilled Jurkat cells (native cells as well as cells transfected with either lentiviral expression vectors for each of the Kv channel constructs or Tet-pLKO-puro shRNA expression constructs for Kv channels knockdown studies) for 30 min, on ice. The control for these experiments were Jurkat cells transfected with the empty pCIG3 vector (or Tet-pLKO-puro vector with scramble shRNA). After a wash step, cells were fixed and analyzed by flow cytometer. The mean of each cell populations' fluorescent intensity was calculated and normalized to the negative control.

Western blot for Kv channel overexpression

Both membrane proteins and cell cytoplasm preparations (80 μg/lane) were fractionated by SDS-PAGE and transferred to membranes using standard protocols. Membranes were probed with anti-Flag anti-body (1:2000) and secondary antibody (1: 5000). Bound antibodies were detected with ECL substrate plus reagent (Thermo Scientific, MA).

Immunostaining of Kv channels

Transfected cells grown on glass coverslips coated with poly-D-lysine were fixed by 4% PFA buffer and blocked with 5% BSA or non-fat milk followed by washing twice in PBS. The cells were then stained with primary antibody (1:2000) in TBS buffer with 5% BSA for 2 hr on ice. Secondary antibody was applied in a 1:2000 dilution in TBST buffer for 2 hr on ice. The cells were mounted using slow-fade buffer and analyzed using a DeltaVision Elite deconvolution microscopy system.

Membrane protein isolation

Cell membrane and the cytoplasmic protein preparations were generated using the Mem-PER Plus membrane protein extraction kit (Thermo Fisher Scientific, MA) following the vendor's recommended protocol. Briefly, cells were harvested by washing them from the culture plate by flushing with PBS addition of proteinase to avoid cell membrane protein degradation. All reagents were pre-chilled to minimize protein degradation. Cells ($5X10^6$) were washed twice with the kit's wash buffer and

permeabilized by mixing with 0.75 ml of permeabilization buffer. After 15min incubation at 4°C, the cytoplasmic protein fraction was generated by centrifugation for 15min at 16,000 x g with collection of the supernatant. The cell pellet was mixed with 0.5 ml solubilization buffer to extract the membrane proteins. [Fig.3 A] After 30 min incubation at 4°C, the membrane protein was separated from the insoluble fraction by centrifugation for 15min at 16,000 x g. The membrane and cytoplasm proteins were fractionated by SDS-PAGE and probed for specific proteins by Western blot analysis.

Biotinylation of HR-crotamine

To bind HR-crotamine to Dynabeads M-280 streptavidin beads, HR-crotamine was biotinylated using the EZ-Link Sulfo-NHS-Biotin kit. The amounts of the HR-crotamine and Sulfo-NHC-LC-Biotin was calculated for an optimal reaction ratio and the mixture of 10 mM Sulfo-NHS-LC-Biotin and HR-crotamine was incubated on ice for 2 hr. Excess biotin reagent was removed by a desalting column and the biotinylated HR-crotamine was recovered and confirmed by the HABA assay.

Pull down analysis of HR-Crotamine Binding proteins

Pull-down analysis was performed with Dynabeads M-280 streptavidin beads; biotinylated HR-crotamine and the cell protein preparations (cell membrane or cytoplasm protein fractions). The Dynabeads M-280 beads were washed 3 times and then incubated with 15 μM of biotinylated HR-crotamine at 4°C for 3 hr. The beads with immobilized HR-crotamine were blocked with 5% BSA for 1 hr to reduce the possible

background. The blocked beads were washed 3 times with PBS to remove unbound HR-crotamine and BSA. Membrane proteins from Jurkat cells expressing Flag tag-fused Kv channels were incubated with the beads at 4^{o}C overnight with Dynabeads M-280 without bound HR-crotamine serving as the background control. The beads with pull-down proteins were washed with PBS buffer for three times (15 min each) and prepared for SDS-PAGE, followed by silver staining and Western blot analysis.

Knockdown of Kv Channel in HR-crotamine sensitive cell lines

Knockdown of Kv1.3 and Kv1.5 channels were performed using an RNA interference silencing system. The shRNA sequences that target to each Kv channel were designed to achieve the best knockdown efficient. For each gene, two shRNA sequences were designed and tested. The gene-specific shRNA was obtained from IDT DNA synthesis facility and the backbone of the transfection vector is Tet-pLKO-puro. The gene-specific shRNA's designed as described in Table 5 and the primers were annealed using a gradual temperature reduction protocol. Specifically, 250 μg of each strand primer was added to a 50 μl reaction system that was heated to 95^{o}C and then cooled with a temperature decrement rate of 1^{o}C per 10 min, until the reaction reached room temperature. The processed shRNA sequence and plain vector was digested with *AgeI* and *EcoRI*. [Fig.14 C] After the gel purification step, the annealed insert sequence and the cleaved vector was ligated by T-4 ligase at the vendor recommend condition (16^{o}C, overnight). Due to utilize the isocaudomers' sequence for the adaptor, the ligation was treated with *EcoRI* restrict enzyme for 3 hr to ensure the quality and the plasmid was

transferred into One Shot® Stbl3™ Chemically Competent Cells. The positive clone was selected by ampicillin selection pressure, and the positive colony was picked for expansion. The purified plasmid from an expanded single clone was sequenced in order to confirm the correct clone.

HEK293T were transfected using a lentivirus system that included the Tet-pLKO-puro vector containing the gene-specific shRNA sequences and psPAX2 and pMD2G vectors. The lentivirus was generated in HEK293T cells serving as the host cell for lentiviral assembly. Briefly, the HEK293T cell was seeded in 6-well plate and the cell was transfected with constructed 3 μg of Tet-pLKO-puro, 1.5 μg of pSPAX2 and 1μg of pMD2G vector. The cell was transfected with lipofectamine 3000 at the 70-80% confluence. The cells were cultured for 48 hr until the supernatant culture media collected for Jurkat cell transfection.

For lentivirus transfection, $1.5X10^5$ Jurkat cells were cultured in FBS-free media for 2 hr and then mixed with the lentivirus – containing media (0.8ml of virus content media+0.8 ml of RPMI1640 complete medium) followed by centrifugation at 2000 rpm for 2hr. After an additional 6 hr of incubation, the transfected Jurkat cells were placed into complete RPMI-1640 media and incubated for 24 hr to allow for resistance gene expression prior to the addition of 2 μg/ml of puromycin for 3 weeks of positive clonal selection. Knockdown activity was induced by the addition of 1 μM of doxycycline and the efficiency of knockdown was determined via gene-specific qPCR.

The real-time qPCR test was applied to the Jurkat cell that transfected with lentivirus content the Kv channel specific shRNA sequence. Total mRNA was isolated

from cell samples using E.Z.N.A.® Total RNA kit (Omega Bio-tek, GA). The quantity and purity were measured by Nanodrop 2000 spectrophotometer (Thermo Fisher Scientific, MA). Total mRNA was converted to cDNA using SuperScript III first-strand synthesis system following vendor's instructions (Thermo Fisher Scientific, MA). The transcription level of Kv channels was determined by quantitative real-time qPCR by using FastStart Universal SYBR Green Master (Roche, Switzerland). The primers for the real-time qPCR was specifically designed for Kv channels (Kv1.1, Kv1.2, Kv1.3 and Kv1.5, detail in table 2) and two standard internal references primers (GADPH and beta-actin) was used. The program for qPCR reaction followed the conventional protocol with annealing temperature at 50^{o}C and all the reactions were carried out in triplicates format to achieve the improved reliability.

The knockdown efficient was also confirmed by the ELISA of the level of the Kv channels in a total cell membrane protein using both mouse anti-Kv1.3 channel and mouse anti-Kv1.5 channel antibodies (Alomone Lab, Israel) and a standard indirect ELISA assay protocol.

Table 5. The shRNA sequences used to knock down each Kv channels in Jurkat cell

Gene's name		Forward primer of shRNA	Reverse primer of shRNA
Kv1.1	1	5-CCGGCAGAACAAGATGATCACTTAGCTCGAGCTAAGTGATCATCTTGTTCTGTTTTT -3	5-AATTAAAAACAGAACAAGATGATCACTTAGCTCGAGCTAAGTGATCATCTTGTTCTG -3
	2	5-CCGGCACGGTCATCTACAATTCCAACTCGAGTTGGAATTGTAGATGACCGTGTTTTT -3	5-AATTAAAAACACGGTCATCTACAATTCCAACTCGAGTTGGAATTGTAGATGACCGTG -3
	3	5-CCGGTCCTCTACTATGAGCAAGTATCTCGAGATACTTGCTCATAGTAGAGGATTTTT -3	5-AATTAAAAATCCTCTACTATGAGCAAGTATCTCGAGATACTTGCTCATAGTAGAGGA -3
Kv1.2	1	5-CCGGACCATTAGTAAGTCTGATTACCTCGAGGTAATCAGACTTACTAATGGTTTTTT -3	5-AATTAAAAAACCATTAGTAAGTCTGATTACCTCGAGGTAATCAGACTTACTAATGGT -3
	2	5-CCGGGCAAGTGACAAGCTGTCCAAACTCGAGTTTGGACAGCTTGTCACTTGCTTTTT -3	5-AATTAAAAAGCAAGTGACAAGCTGTCCAAACTCGAGTTTGGACAGCTTGTCACTTGC -3
	3	5-CCGGGCCTGCCAGGATTATAGCTATCTCGAGATAGCTATAATCCTGGCAGGCTTTTT -3	5-AATTAAAAAGCCTGCCAGGATTATAGCTATCTCGAGATAGCTATAATCCTGGCAGGC -3
Kv1.3	1	5-CCGGCGAACAATAATCCCAACTCTTCTCGAGAAGAGTTGGGATTATTGTTCGTTTTT -3	5-AATTAAAAACGAACAATAATCCCAACTCTTCTCGAGAAGAGTTGGGATTATTGTTCG -3
	2	5-CCGGGCTCCGCAACGAGTACTTCTTCTCGAGAAGAAGTACTCGTTGCGGAGCTTTTT -3	5-AATTAAAAAGCTCCGCAACGAGTACTTCTTCTCGAGAAGAAGTACTCGTTGCGGAGC -3
	3	5-CCGGGCACATCAATTCGTAGTAAATCTCGAGATTTACTACGAATTGATGTGCTTTTT -3	5-AATTAAAAAGCACATCAATTCGTAGTAAATCTCGAGATTTACTACGAATTGATGTGC -3
Kv1.5	1	5-CCGGCCTAGAGAAGTGTAACGTCAACTCGAGTTGACGTTACACTTCTCTAGGTTTTT -3	5-AATTAAAAACCTAGAGAAGTGTAACGTCAACTCGAGTTGACGTTACACTTCTCTAGG -3
	2	5-CCGGGCTGACAACCAGGGAACCCATCTCGAGATGGGTTCCCTGGTTGTCAGCTTTTT- 3	5-AATTAAAAAGCTGACAACCAGGGAACCCATCTCGAGATGGGTTCCCTGGTTGTCAGC -3
	3	5-CCGGACATTATACCGCAGAGTATTTCTCGAGAAATACTCTGCGGTATAATGTTTTTT -3	5-AATTAAAAAACATTATACCGCAGAGTATTTCTCGAGAAATACTCTGCGGTATAATGT -3

The cell viability assay used in the Kv channel knockdown and inhibitor studies was the same as the cell viability assay described in Chapter I, with the modification that Jurkat cells transfected with lentivirus with scrambled shRNA served as an additional control.

Binding target cross-blocking assay

In the cross-blocking assay, the cell binding protocol used was same as the competitive binding assay described previously except that graded concentrations of a chemical channel blocker, 0-20 μM CP-339818 (Sigma-Aldrich, MO) was added to the incubation mix to compete with 1 μM FITC-conjugated HR-crotamine binding prior to incubation with $1X10^6$ Jurkat cells on ice for 20min. The cells were then analyzed for bound FITC HR-crotamine with a LSRII flow cytometry system using the same protocol used for the competitive binding assay.

Result

Binding of HR-Crotamine to Jurkat cells

The first step in our search for the HR-crotamine target was to determine whether or not there was a saturable binding site for the myotoxin on the surface on intact HR-crotamine-sensitive cells such as Jurkat cells. A cell surface binding assay was performed using graded concentrations (300 nM, 1 μM, 3 μM and 9 μM) of FITC labeled HR-crotamine: incubated with intact Jurkat cells for 20 min on ice and cell-bound FITC -HR-crotamine detection using flow cytometry (for experimental details see Methods e. Cell Surface Binding Assay). The results of this ligand binding assay showed a single component binding curve at approached saturation at >2 μM and exhibited an EC_{50} of 1.3 μM. [Fig.15 B] The lack of complete saturation at higher concentrations is likely due to a modest contribution of non-specific (i.e. non-saturable) binding activity. Imaging of the FITC-HR-crotamine bound to Jurkat cells showed a narrow band on

florescence excluded from the nuclear and intracellular compartments and fully compatible with a specific cell surface binding activity. [Fig. 15 A]

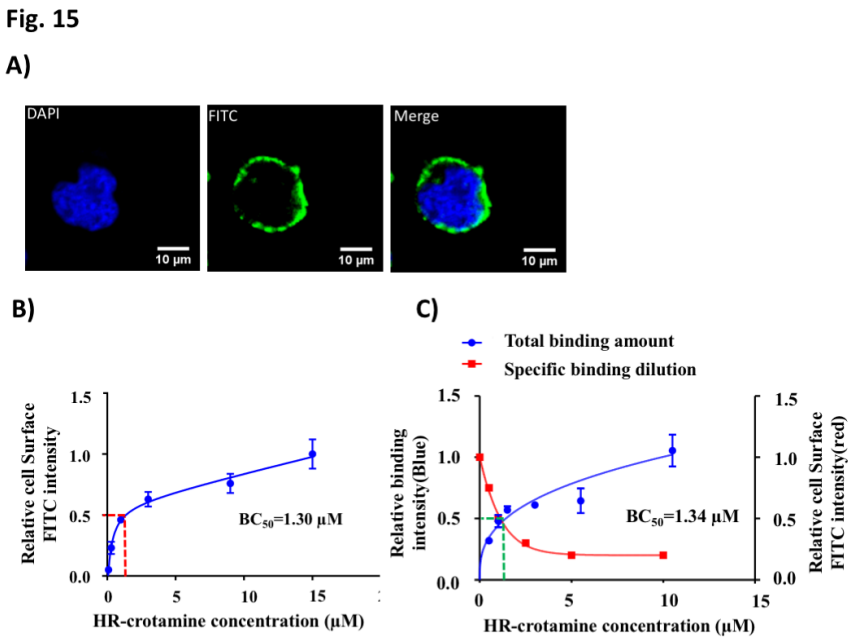

Fig. 15. Binding of FITC-labelled HR-crotamine to intact Jurkat cells.
A) *Direct visualization of FITC HR-crotamine bound to intact Jurkat cells* Cells were stained with FITC conjugated HR-crotamine for 20 min on ice. Images were collected using a 40X objective and epifluorescence microscopy. DAPI staining was used to mark the cell nucleus. B) *Direct binding assay for FITC-HR-crotamine binding to intact Jurkat* using the Cell Surface Binding Assay as described in Methods using *a* fixed concentration of FITC-HR-crotamine and graded concentrations of unlabeled HR-crotamine. The total binding data curve (red) and BC_{50} were calculated from the total concentration of FITC-labelled and unlabeled HR-crotamine in the binding assay. The dilution curve (green) is the amount of FITC-HR-crotamine bound to the cells in the presence of increasing concentrations of unlabeled HR-crotamine. The result is the mean+/-standard deviation of triplicate determinations.

To confirm the results obtained with the direct binding assay and to ensure that the observed binding was not reflecting a selective binding of FITC-conjugated HR-

crotamine as opposed to unlabeled HR-crotamine, we carried out a competitive binding using a fixed concentration of FITC-conjugated HR-crotamine (1 μM) and increasing concentrations of unlabeled HR-crotamine. [Fig. 15 C] The results obtained indicated a robust dilution in the binding of FITC-HR-crotamine by unlabeled HR-crotamine (Green line Fig. 15 C) confirming the presence of a saturable and compete-able binding site on the surface of Jurkat cells. The total binding curve (red line Fig. 15 C) was comparable to the direct binding assay as the BC_{50} 1.34 μM was essentially the same as the BC_{50} obtained with the direct binding assay, confirming that the binding constant reflected the binding of HR-crotamine to the cell.

The Kv channel overexpression and localization was confirmed

To test our hypothesis that the target for HR-crotamine binding to Jurkat cells are members of the Kv channel family, we first tested whether HR-crotamine binds to Kv channels by overexpressing Kv channels in Jurkat cells and then testing whether the overexpression of individual channels leads to increased HR-crotamine binding. The first step in this study was to demonstrate the ability to overexpress Kv channels in Jurkat cells. Due to the fact that endogenous Kv channels are expressed at low abundance in the Jurkat cells, we found it was necessary to overexpress the Kv channels in the cells to demonstrate their myotoxin binding activity.

We constructed a series of recombinant pCIG3 (pCMV-IRES-GFP version 3) lentiviral vectors that included full length inserts for Kv1.1, 1.2, 1.3 and 1.5 and a truncated insert for Kv1.3 that deleted its plasma membrane insertion sequence, each

including a C-terminal Flag tag (for details see Methods a. Overexpression of Kv Channels). We transfected Jurkat cells with each of these lentiviral expression vectors and then identified the expressed of Kv proteins by Western blot analysis of whole cell lysates using an anti-Flag antibody. [Fig. 16 A] Each of the transfected cells expressed a flag fusion protein with a size that was appropriate for the Kv channel-Flag fusion protein. The Kv1.1, truncated Kv1.3 and Kv1.5 transfected cells exhibited two to three additional, lower molecular weight bands that are likely due to proteolytic degradation of transfected Kv channels.

Immunofluorescence analysis of Jurkat cells transfected with the Kv channel expression constructs showed clear expression of full length Kv1.1, 1.2, 1.3 and 1.5 both in the cytoplasm and at the cell periphery, indicating expression and insertion of the channel proteins into the Jurkat cell membrane. [Fig. 16 B, C] In contrast, cells transfected with the truncated Kv1.3 construct (which lacks the membrane insertion sequence) showed only diffuse cytoplasmic expression of the transfected protein. We also noted that over-expression of the full-length Kv1.3 channel but not the truncated Kv1.3 channel protein resulted in a noticeably more roundish shape to the transfected cells. Similar shape changes, but to a lesser degree were noted in cells transfected with full length Kv1.1, Kv1.2 and Kv1.5 channels.

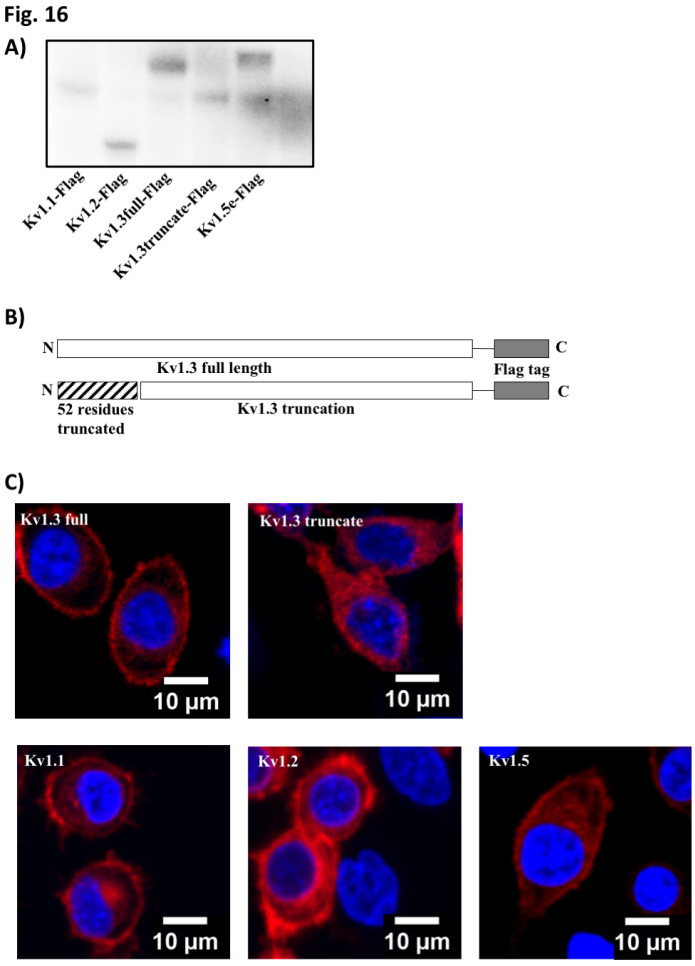

Fig. 16. Kv channel overexpression in Jurkat cells
A) *Western Blot analysis Kv channel overexpression.* Jurkat cells were transfected with lentivirus expression system containing inserts for Kv1.1, Kv1.2, full-length and a truncated Kv1.3 and Kv1.5 constructs each with a fused Flag tag. Cell lysates were fractionated by SDS-PAGE, transferred to PDF membranes and probed with anti-Flag antibody using a protocol described in Methods b. for Kv Channel Overexpression Western Blot B) *Full length and truncated Kv1.3 channel inserts.* The difference between the full length Kv1.3 and the truncated Kv1.3 constructs is the deletion of 52 amino acids (shaded part) at the N-terminal that abolishes plasma membrane insertion activity C) *Immunofluorescence detection of Kv channel fusion proteins in Lentivirus transfected Jurkat cell*. Jurkat cells grown on poly-lysine coated cover slips were transfected with lentivirus expression vectors containing Kv channel constructs fused to a Flag tag. After 48 hr, cells were fixed, permeabilized and stained with anti-Flag primary antibody and fluorescent second antibody under conditions described in detail in Methods c. Immunostaining of Kv channels. Cell nuclei were stained with DAPI. Images were collected at 60X power.

Effect of Kv channel overexpression on HR-Crotamine binding

With the ability to overexpress Kv channels on Jurkat cell, we were now in a position to determine if overexpression of specific Kv channels impacted HR-crotamine binding. The HR-crotamine binding activity of Jurkat cells overexpressing full length Kv1.1, Kv1.2, Kv1.3 and Kv1.5 were compared with the cell surface binding activity of non-transfected cells and cells transfected with an empty vector. [Fig.17 A] Expression of either Kv1.1, Kv1.2 and Kv1.3 on the surface of Jurkat cells significantly ($P<0.05$) increased HR-crotamine binding. Expression of Kv1.5 had no effect on myotoxin binding. To determine whether expression on the cell surface was essential for HR-crotamine binding, we compared the binding activity of Jurkat cells overexpressing full length Kv1.3 with cells expressing a truncated version of the channel protein that was restricted to the cytoplasm. The results of this experiment showed clearly that expression of the Kv on the cell surface was required for HR-crotamine binding activity. [Fig. 17 B]

Fig. 17

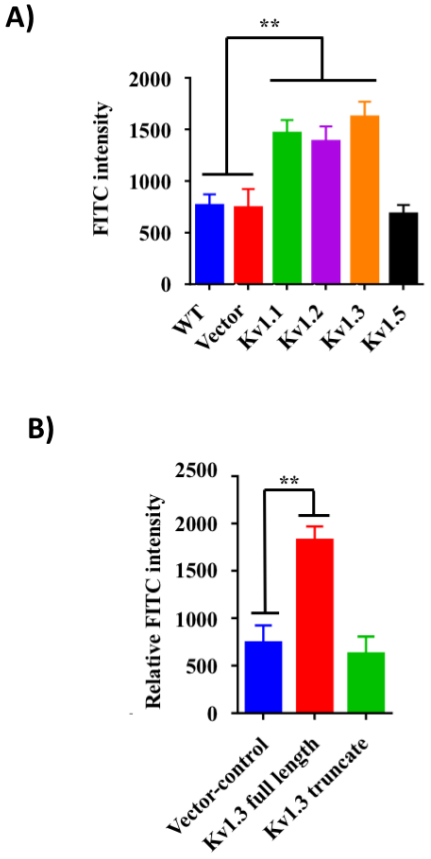

Fig. 17. Effect of Kv channel overexpression on HR-crotamine Binding
A) *Effect of Full Length Kv channel overexpression on HR-crotamine binding Jurkat cell* FITC-labeled HR-crotamine (1 μM) was incubated with Jurkat cell overexpressing specific full-length Kv Channels and the level of cell bound FITC-conjugated HR-crotamine determined as described previous. Non-transfected Jurkat cells (WT) and Jurkat cells transfected with empty lentiviral vector (Empty Vector) served as the controls. The results are the mean+/-standard deviation of triplicate determinations. Statistical significance was determined by Student's T-test and the (**) indicates $P<0.05$.
B) *Comparison of full length versus truncated Kv1.3 expression on HR-crotamine Binding.* FITC-labeled HR-crotamine (1 μM) was incubated with Jurkat cell overexpressing either full-length or NH_2-terminal truncated Kv1.3, in Fig. 16 B, and the level of cell bound FITC-conjugated HR-crotamine determined as described previous. Jurkat cells transfected with empty lentiviral vector (Empty Vector) served as the controls. The results are the mean +/-standard deviation of triplicate determinations. Statistical significance was determined by Student's T-test and the (**) indicates $P<0.05$.

Pull down analysis and Co-immunoprecipitation (co-IP)

As an independent test of the interaction of HR-crotamine with KV channel proteins we performed a pull-down analysis using beads coated with HR-crotamine and membrane proteins purified from cells overexpressing the Kv channel proteins. The results of these experiments confirmed that HR-crotamine can bind to KV1.1, 1.2 and 1.3 expressed in the membranes of Jurkat cells. [Fig. 18]

Fig. 18

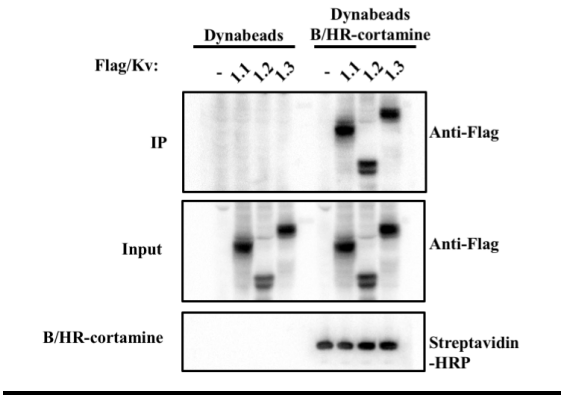

Fig. 18. Pull-down analysis of the binding of HR-crotamine to membrane associated Kv 1.1, 1.2 and 1.3.
The Jurkat cell was transfected with Kv channel overexpression vector (pCIG3 vector). The cell membrane protein was prepared by the Membrane Prep kit. Total cell membrane proteins prepared from Jurkat cells transfected with lentiviral vectors expressing Flag-tagged Kv1.1, Kv1.2 and Kv1.3 were incubated streptavidin Dynabeads coated with biotinylated HR-crotamine (see Methods g. Pull-down analysis of HR-crotamine binding proteins). After washing proteins bound to the beads were solubilized, fractionated by SDS-PAGE and probed by Western Blot with anti-Flag antibody. Dynabeads with no immobilized HR-crotamine served as the control. The size of the Flag-tag fused Kv channel is: Kv1.1, 58 kDa; Kv1.2, 42kDa and Kv1.3, 65 kDa. B/HR-crotamine: biotinylated HR-crotamine.

Knockdown of the Kv channels in Jurkat cell

The preceding studies used the overexpression of Kv channels in Jurkat cells to demonstrate the selective binding of HR-crotamine to Kv1.1,1.2 and 1.3 but not Kv1.5

when the channel proteins were expressed on the surface of Jurkat cells. They did not however address the question of whether HR-crotamine bound to the endogenous Kv channels expressed on the surface of these cells. To address this question, we first developed inducible lentiviral shRNA expression constructs for each of the four Kv channels of interest (Kv1.1, 1.2, 1.3 and 1.5) and established experimental conditions under which induction of the shRNA's led to a profound suppression (60-80% suppression) of Kv channel expression [Fig. 19 A] as measured by real-time qPCR. We then used these conditions to examine the effect of the knock-down of each channel on HR-crotamine binding activity. The results of this experiment [Fig. 19 B] showed that suppression of Kv1.1, 1.2 and 1.3 expression resulted in a significant decrease in HR-crotamine binding in Jurkat cells whereas suppression of Kv1.5 had no effect. The suppression of each individual channel protein resulted in a fractional decrease in HR-crotamine binding. Suppression of Kv1.1 expression resulted in a 20% reduction in myotoxin binding, suppression of Kv1.2 reduced binding by 25% and Kv1.3 by 30%. When combined the suppression of Kv channels, the expression appears to account for a minimum for 75% of the specific binding of HR-crotamine to intact Jurkat cells. This is a minimal estimate because the quantitative analysis of the Kv channel transcripts indicates that the suppression of expression of each transcript ranged from 60-80%. [Fig. 19 A] These results provide strong evidence that Kv channels serve as the major target for HR-crotamine activity in Jurkat cells.

Cross competitive binding test with Kv1.3 blocker

As an independent test for the hypothesis that Kv channels serve as a target for HR-crotamine binding to Jurkat cells, we investigated the ability of a well-characterized Kv 1.3 channel inhibitor, CP-339818 (Jimenez-Perez et al., 2016; Wulff, Castle, & Pardo, 2009) to interfere with HR-crotamine binding to endogenous Kv channels in Jurkat cells. [Fig. 19 C] In this experiment, cells were incubated with FITC-conjugated HR-crotamine (1 μM) and increasing concentrations (0 μM to 20 μM) of CP-339818. After a 30 min incubation on ice, cells were washed, fixed and cell-bound fluorescence determined by flow cytometry as described previously. For these experiments SKF-96365, a Ca^{+2} channel inhibitor with no know interactions with Kv channels served as the negative control. The results of this experiment [Fig. 19 C] showed clearly a dose-dependent inhibition of HR-crotamine binding by the Kv channel inhibitor but not by the Ca^{+2} channel inhibitor. This study confirms independently that endogenous Kv channels serve as the targets for HR-crotamine binding and further suggest that CP-339818 which is known to inhibit Kv channel activity by occluding the extracellular component of K^+ channel and HR-crotamine share overlapping binding sites on the surface of the channel protein.

Fig. 19

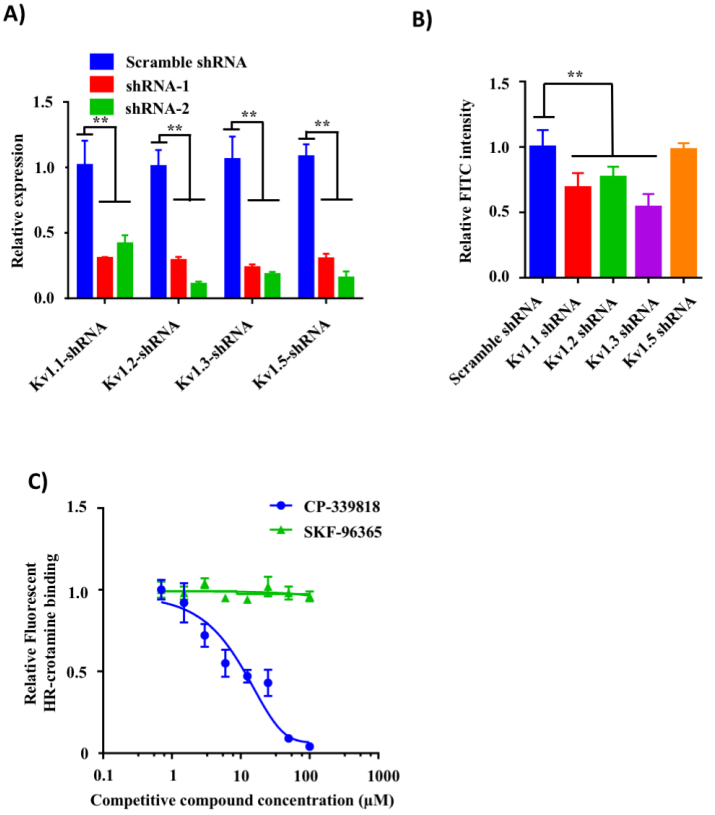

Fig. 19. Effect of Knockdown/Inhibition of Endogenous Kv channels on HR-crotamine binding to Jurkat cells

A) *Knockdown efficient test* Two shRNA's for each of the targeted genes (Kv1.1, Kv1,2, Kv1.3 and Kv1.5) were cloned into an inducible lentivirus expression system (for experimental details see Methods h. Knockdown of Kv Channels in HR-crotamine sensitive cells). Jurkat cells were transfected with the expression vectors and transfected cells were selected with puromycin. Jurkat cells transfected with the same vector containing scrambled shRNA sequences served as a negative control. After 72hr of doxycycline induction, cells were harvested for RNA isolation and transcript quantification. The level of each Kv channel transcript in control and shRNA transfected cells was determined using real-time PCR with gene-specific primers. Transcript levels were normalized to the GAPDH internal references and the efficiency of knockdown was scaled to the level of expression of the transcript in control cells. Results are the mean+/-standard deviation of triplicate determinations B) *Binding of HR-crotamine to Kv knockdown Jurkat cells* Kv channel transcripts in Jurkat cells were knocked down by transfection with an inducible lentiviral shRNA expression system for Kv1.1, Kv1.2, Kv1.3 and Kv1.5. Jurkat cells transfected with a scrambled shRNA vector served as the control. HR-crotamine binding was determined by incubation with FITC-conjugated HR-crotamine (1 μM) followed by quantitation by flow cytometry. Results are the

(Fig. 19. Continued)
mean+/- standard deviation of triplicate determinations. C) *Effect of a Kv channel-specific inhibitor on HR-crotamine binding to Jurkat cells* Jurkat cells were incubated with FITC-conjugated HR-crotamine (1 μM) and increasing concentrations CP-339818, a Kv1.3 channel inhibitor or SKF-96365, calcium channel inhibitor that served as a control. The inhibition of binding curve was generated by curve fitting to the data points. Results represent the mean +/-standard deviation of triplicate replications.

Discussion

The results we have obtained on the direct binding of HR-crotamine to Kv channels expressed on the surface of Jurkat cells fits nicely with previous patch clamp data that reported that crotamine, a related myotoxin, can inhibit the conductance of the Kv1.1, Kv1.2 and Kv1.3 channels but not of Kv1.5 channel (S. Peigneur et al., 2012).

The studies we carried out using the overexpression of Kv channels in Jurkat cells demonstrated the ability of HR-crotamine to bind to Kv1.1, 1.2 and 1.3 but not the closely related to Kv1.5. The results obtained by comparing the myotoxin binding activity of full-length versus a truncated Kv1.3 expression construct suggested strongly that expression on the surface of the cell is a necessary pre-requisite for myotoxin binding although we cannot rule out the possibility that the simple mis-folding of the truncated protein may have abolished its crotamine binding activity.

The studies that manipulated the level or activity of the endogenous Kv receptors on Jurkat cells provide strong evidence that these proteins are very likely to play a critical role as the targets for the anti-proliferative activity of myotoxins in these cells. There is extensive evidence in the literature that the Kv1.1 and Kv1.2 channels play a critical role in the transmission of electrical in excitable cells.(Hyun et al., 2015; Perez-Garcia, Cidad, & Lopez-Lopez, 2018; Yuan et al., 2018) Kv1.3 however has been

thought to play a much more important role in the regulation of cell cycle activity and cell proliferation, particularly in T-cells. These observations provide a solid basis for our hypothesis that targeted interactions of HR-crotamine with the endogenous Kv1.3 channel in T-cell leukemia cells, such as Jurkat cells, may play a crucial role in the anti-proliferative activity of the toxin.

CHAPTER III

MECHANISM AND CONCLUSIONS FOR ANTI-PROLIFERATIVE ACTIVITY OF HELLERIED CROTAMINE

Introduction

Potassium channels are widely distributed in cells and tissues and have diverse electrophysiological and biologic functions (Littleton & Ganetzky, 2000). In the most general sense, all potassium channels function to allow the conductance of potassium ion down their electrochemical gradient (Hille, 2001) maintaining or adjusting the resting membrane potential. At the most basic level the function of potassium channels is involved in neural conduction, the maintenance of vascular tone and cardiac contraction and multiple secretory processes such as insulin secretion (Checchetto et al., 2013). A specific member of the potassium channel family, Kv1.3 channel (encoded by the KCNA3 gene) plays a unique role in the regulation of T-cell and B-cell function and proliferation.

There are a large number of different types of potassium channels that can be grouped into four major classes: i) the calcium-activated potassium channels, ii) the inwardly rectifying potassium channel, iii) the tandem pore domain potassium channels and iv) the voltage-gated potassium channels (Rang, 2006). Our studies on the biological activity of snake venom myotoxins such as HR-crotamine and their membrane targets have focused on their interactions with the voltage-gated potassium channel (Kv). The Kv1.1 and 1.2 channels, encoded by the KCNA1 and KCNA2 genes, are ubiquitously

expressed in most cells and tissue where they play a vital role in the signal transmission and the conduction of action potentials through excitable cells such as neurons and various types of muscle cells (Curran, Landes, & Keating, 1992; Gutman et al., 2005).

As mentioned previously, Kv 1.3 channel, encoded by the KCNA3 gene, has a unique role in regulating the immunologic and proliferative activity of T- and B-cells. Kv1.3 channel is classified as a member of the delayed rectifier (slowly inactivating) family of potassium channel related the *"shaker"* gene in Drosophila. *Shaker* gene mutations cause of host of neurological and physiological anomalies in fruit flies. In T- and B-cells much of the activity of Kv1.3 channels are related to its close coupling to the electrochemical systems that control transmembrane Ca^{+2} flux and the intracellular concentration of Ca^{+2}. In lymphocytes, the Kv1.3 channel is only expressed in the G1/S stage of the cell cycle (Comes et al., 2013). During this transient period, the Kv1.3 channel acts in concert Ca^{+2}-activated potassium channel, Kca3.1 to maintain the membrane potential during the early stage of cell proliferation (Chiang et al., 2017). The resting cell, the cytoplasmic Ca^{+2}- level is about 0.1 μM (in the face of an extracellular Ca^{+2} concentration of 1000 μM). Calcium influx into the cytoplasm of T-cells and B-cells occurs through the CRAC/ORAI1 channel. The driving force for this influx is the large negative intracellular potential (about -60 mV), which is continuously maintained by the Kv1.3 channel. The Kv1.3 channel functions to allow for potassium ion efflux out of the cell in order to compensate for the depolarizing effect of calcium influx. Once cytoplasmic Ca^{+2} levels reach 1 μM, or higher, the Ca^{+2} concentration is sufficient to activate calmodulin which in turn activates the Kca3.1channel and calcineurin, a Ca^{+2}

dependent protein phosphatase. Activated calcineurin will dephosphorylate the transcription factor—NFAT and dephosphorylated NFAT translocate to the nucleus and control the transcription for cell proliferation-related genes (Bradding & Wulff, 2009). Therefore, through NFAT pathway, the Kv channel's activity can directly control the activation and proliferation of both T-cells and B-cells. [Fig. 20 A, B]

Our observation that HR-crotamine targets KV channels and Kv1.3 in particular, is not unique. There are numerous toxins that have been identified in the venoms of many different types of venomous creatures, that have been found to target this channel. For instance, several scorpion toxins, including ADWX1, OSK1, margatoxin, kaliotoxin, charybdotoxin, noxiustoxin, anuroctoxin as well as some sea anemone toxins including ShK family and BgK toxin have been shown to function as Kv channel inhibitors. In addition, several chemical compounds, including CP339818, PAP-1, correolide, benzamides, progesterone and the anti-lepromatous drug(clofazimine) are also able to inhibit the Kv1.3 channel with different degrees of specificity and potency (Garcia-Calvo et al., 1993; Han et al., 2008; Nguyen et al., 1996). Some of these compounds have been developed as potentially clinically useful drugs based on their Kv1.3 channel blocking activity.

Fig. 20

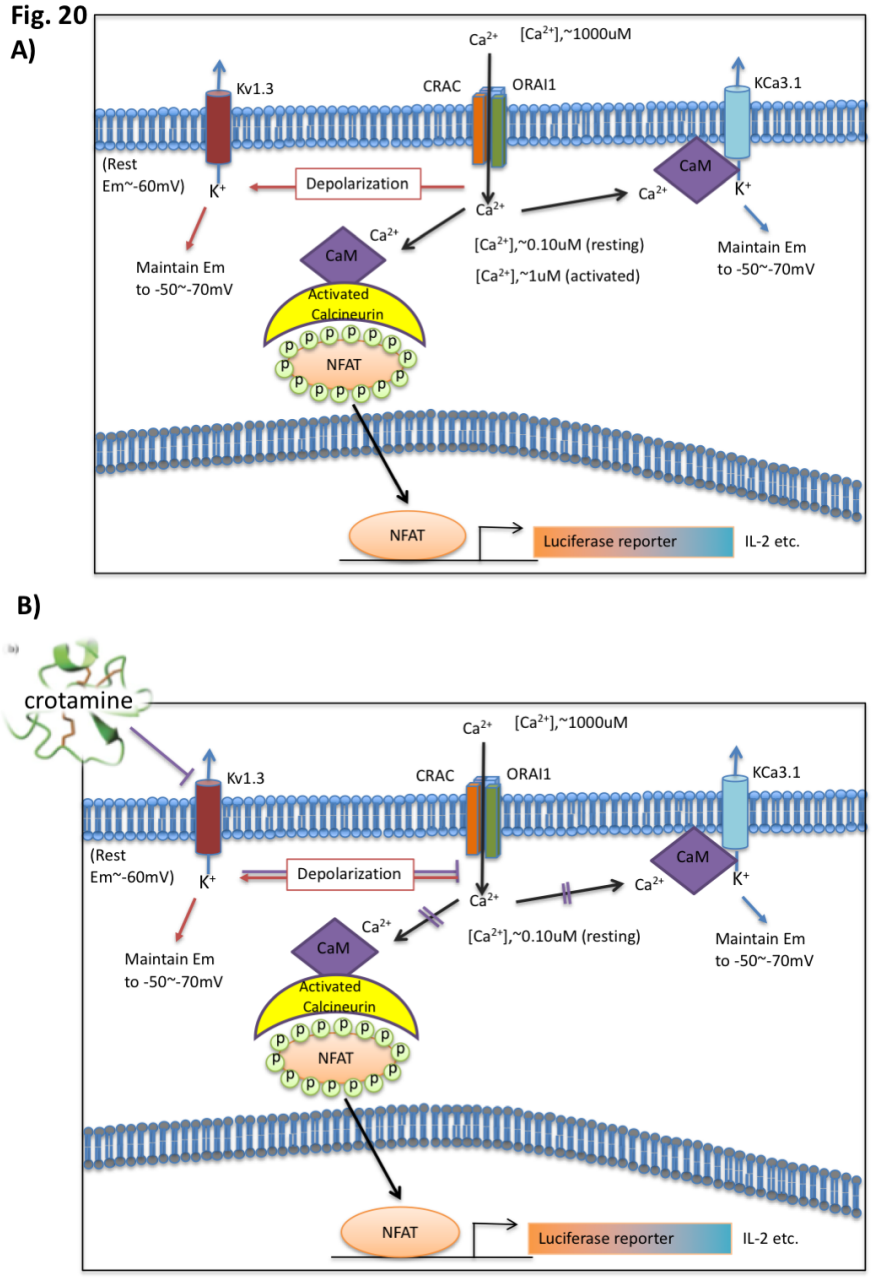

Fig 20. A proposed model for the effect of HR-crotamine's on calcium influx in T- and B- cell lymphocytes

A) *Calcium mediated signaling pathway*s The figure illustrates the function of Kv1.3 as an indirect regulator of proliferation-related calcium signaling pathways in cells. B) *The proposed effect of HR-crotamine dependent inhibition of Kv1.3 activity on calcium mediated signaling pathways,* A proposed model for the consequences of HR-crotamine induced Kv1.3 inhibition and its effect on calcium – regulated cell proliferation.

(Fig. 20. Continued)
Inhibition of Kv1.3 is hypothesized to prevent membrane hyperpolarization and thereby reduce calcium influx resulting in a lower level of intracellular calcium ion concentration. As a consequence, calcium-dependent activation of calmodulin is suppressed, resulting in reduced calcineurin activation. Decreased activation of calcineurin results in persistent NFAT phosphorylation and a resulting decrease in the translocation of NFAT into the nucleus. Decreased NFAT activity decreased the expression of proliferation-related genes and an inhibition of cell proliferation.

To explain our observation of the anti-proliferative activity of HR-crotamine in Jurkat cells, we hypothesize that as an inhibitor of Kv1.3 activity, HR-crotamine, will prevent membrane hyperpolarization and thereby decrease calcium influx. The net effect will be a blunting of the calcium-calmodulin-calcineurin-NFAT regulatory system and a down regulation in the transcription of genes essential for lymphocyte proliferation. [Fig. 20 B] The Kv1.3 channel has also been reported to be expressed in mitochondria where it is thought to play a role in mitochondrial membrane polarization. There have been suggestions that malfunctioning of mitochondrial Kv1.3 channels could be linked to the induction of the NOS-mediated cell apoptosis in malignant cell (Cirrone et al., 2017; Leanza et al., 2017). We do not think this potential cytotoxic mechanism plays a role in the effects of HR-crotamine in Jurkat cells since we have seen no evidence that HR-crotamine gains access to the interior of Jurkat cells and no evidence that HR-crotamine induces either apoptosis or necrosis under the conditions used in our studies. Our mechanistic hypothesis related entirely to the anti-proliferative effect of the myotoxin in Jurkat cells, and by extension, in lymphocytes.

In this chapter, we will test the validity of our hypothesis by investigating the intracellular mechanisms that mediate HR-crotamine's growth inhibitory activity. We

will compare the activity of HR-crotamine with well-established Kv1.3 channel inhibitor to understand the common points and the variances in their property. In the end, our goal is to establish the overall mechanism by which HR-crotamine, and by extension other myotoxins, act as anti-proliferative agents in lymphoid cells.

Material and Methods

Cell culture condition

Jurkat cell and Jurkat-Lucia™ NFAT Cells were cultured in RPMI complete media as described in Chapter I. HEK293T cell were cultured in DMEM complete media with the same culture conditions as Jurkat cells. The Jurkat and Jurkat-Lucia™ NFAT cells model with Kv channels knockdown was established as described in the Method h. Knockdown of Kv Channel in HR-crotamine sensitive cell lines in Chapter II.

Western blot for biomarkers of apoptosis and cell growth inhibition

Western blot analysis was used to detect biomarkers of apoptosis. Cells were treated with 1 μM of HR-crotamine for 24 hr and harvested after a PBS wash step. In parallel, cells treated with PBS only were used as a negative control while cells treated with 1 μM Etoposide was used as a positive control. Cells were lysed by SDS-PAGE loading buffer and the protein samples were denatured and reduced by heating in the presence of DTT at 95^{o}C for 5 min. The samples were then loaded onto 4%-12% gradient SDS-PAGE gels and then electrophoresed at 150 volts for 40 min. Proteins were transferred to PVDF membrane at 300 mA for 2 hr (on ice). The membrane was

blocked with 5% W/V dry milk for 2 hr and the target protein, cleaved Caspase-3, was detected using mouse anti- cleaved Caspase-3 antibody (at 1:1000 dilution). An HRP conjugated secondary rabbit anti-mouse antibody (1:5000 dilution) and ECL buffer was used to detect the bound anti- cleaved Caspase 3 antibody. The membrane was imaged with a Bio-rad ChemiDoc XRS+ system. The level of beta-actin in each sample was also visualized with an anti-actin antibody to ensure the equal cell extract loading in each sample.

Cell cycle analysis

To measure cell doubling times, Jurkat, HeLa and SK-Mel-28 cells were diluted to 1 x10^6cells/ml and then loaded with CellTrace™ Far Red (ThermoFisher Scientific, MA) following the vendor's suggested protocol. The adherent cells were then plated and allowed to attach while the Jurkat cells were maintained in suspension culture. Cells were then incubated with HR-crotamine at multiple concentration (2 µM, 1 µM, 500 nM, 250 nM and 100 nM), 20µM SKF-96365 (negative control) or 10 µM CP-339818 (positive control). After 72 hr incubation, the cells were harvested and fixed for flow cytometry analysis. The results generated by the flow cytometer was analyzed with Flowjo software.

As an independent measure of cell cycle, we used the expression of P21 (measured by Western blot) as a biomarker of cell cycle arrest. Cells were pre-incubated with 0.5 µM HR-crotamine or 10 µM of CP-339818 (positive control) or PBS (negative control) for 72 hr and then harvested and the extracts prepared for Western blot analysis

as described previously. P21 was detected using a mouse anti-P21 antibody (1:2000, Cell signaling technology, MA). Beta-actin was used as a reference marker for sample loading.

Cell cycle arrest analysis

A cell cycle arrest analysis was conducted using Propidium Iodide (PI) staining. The cells were cultured with HR-crotamine (at 1μM, 0.5 μM, 0.25 μM) or 10 μM CP-339818(positive control) or PBS (negative control). After 24 hr incubation, cells were washed and fixed with 70% ethanol solution and then stained with PI dye prior to flow cytometry. The fraction of cell population in G1/S stage and G2/M stage of the cell cycle were quantitated with Flowjo software.

Cell viability assay with Kv channel knockdown cells

Jurkat cells with different Kv channel knockdowns were used for the cell viability assay. Cells were seeded in 384-well plates at an appropriate density to support exponential growth for 72 hr. Medium containing graded concentrations of HR-crotamine or the positive control (CP-339818) was added to the cells. After 72 hr, cells were DAPI (Sigma-Aldrich, MO) stained and imaged in an InCell 6000 system (GE healthcare, CT). Cell counts were determined from the images using cell segmentation software and the cell counts were used to quantify cell viability.

The degree of growth inhibition due to various interventions was expressed as the ratio between the increase in cell number at 72 hr in the treated group versus the

increase in the PBS-treated control group (expressed as a % inhibition). Dose-dependent changes in growth inhibition were used to the IC_{50} (concentration producing 50% of maximal inhibition of cell growth).

For the time course studies of cell viability, Jurkat cells with Kv channels knockdown were counted at 0 hr, 24 hr, 48 hr and 72 hr, based on DAPI staining and automated cell counting using cell imaging segmentation.

Intracellular calcium activity analysis

To measure the activity of intracellular calcium, $5x10^3$ of Jurkat-Lucia™ NFAT cells (Invivogen, CA) were pre-incubated with graded concentrations of HR-crotamine (0-4 μM, half-fold dilution), 0-40 μM of CP-339818 (as a positive control for Kv1.3 channel inhibition) and 0-80μM of SKF-96365(as positive control for inhibition of calcium influx) for 1hr on ice. PBS served as the negative control. Calcium influx and activation of the NFAT/NF-kB pathways were achieved by addition of 30ng/ml phorbol myristate acetate (PMA, Sigma-Aldrich, MO) and 1.5 μM ionomycin (Sigma-Aldrich, MO). After 12 hr of incubation to allow for luciferase reporter protein expression cells were lysed and reporter protein activity was measured on a multi-mode detector plate Reader with Bright-Glo™ Luciferase assay system (Promega, WI). Averaged data from triplicate determinations was normalized and analyzed by curve fitting.

IL-2 ELISA assay

Jurkat cells and peripheral blood CD4+ T cells (PBTC) were seeded in U-bottom 96-well plate at $5X10^4$ cell/well density. After the application of graded concentrations of HR-crotamine (0-4 μM) and CP339818(0-40 μM), phytohemagglutinin (PHA) and phorbol ester were added to the cells for 24 hr to activate IL-2 expression and secretion. Aliquots of cell-free culture media were collected and the IL-2 concentration was measured with a Human IL-2 ELISA Kit (Thermo Fisher Scientific, MO) according to the manufacturer's protocol. The averaged absorbance values at 550 nm and 450 nm from triplicate samples were used to calculate IL-2 concentration based on a standard curve obtained in parallel from the same test plate. The final results were normalized to with the min/max value of the observation.

Statistical analysis

The results from the experiments were summarized in mean+/- standard deviation format (n>=3). Inhibition or activation curves were generated by appropriate curve fitting and the calculation of IC_{50} and BC_{50} were conducted by interpolation of curve fitted data. Statistical significance ($P<0.05$) was calculated using a Student's t-test (or Analysis of Variance test) and marked with ** on all figures.

Result

HR-crotamine induces the cell growth inhibition rather than apoptosis

When we had tested the effect of HR-crotamine on cell growth for 72 hr in multiple cell lines (as described in Chapter I), most of the cell lines showed decreased cell numbers compared to the negative control. In the cell proliferation assay, the time course also provides indirect evidence for the growth inhibitory effect of HR-crotamine. To investigate the intracellular mechanism of HR-crotamine activity, we first need a direct determination of HR-crotamine's growth inhibitory activity and a direct demonstration as to whether or not there is any evidence of HR-crotamine – induced apoptosis or cell death. The activations of Caspase-3 is a widely utilized biomarker of apoptosis. In normal cells, the cleaved Caspase-3 level and the fraction of cleaved Caspase-3 positive cells should be very low. In apoptotic cells, there will be a significant accumulation of cleaved Caspase-3 that can be observed by either immunoblot of the protein or biomarker staining for cleaved Caspase-3 positive cells. To confirm our previous conclusion that HR-crotamine did not induce apoptosis in Jurkat cells, the cells were treated for 24 hr with graded concentrations of HR-crotamine or Etoposide (serving as a positive control) and then the level of cleaved Caspase-3 in cell extracts was detected by Western blot analysis. [Fig. 21 A] The results of this experiment showed clearly that while the positive control (Etoposide) showed a major cleaved Caspase-3 band there was no evidence for any induction of apoptosis in Jurkat cells under the conditions used for these experiments.

Effect of HR-crotamine on cell cycle

Cell growth inhibition is generally reflected in a longer doubling time reflecting a delay in progression through the cell cycle. We used cells CellTrace™ proliferation assay to investigate the effect of HR-crotamine on cell cycle kinetics in Jurkat cells. In this assay, T_0 cells are loaded with the DNA dye-CellTrace™ and extracellular dye is then removed by washing. During subsequent cell cycles, the dye loaded cells will synthesize the half of their DNA strands with new dNTP molecule resulting in a half fold dilution of the dye-labelled DNA for each subsequent cell cycle. Using this method, the number of completed cell generations can be measured by analyzing the fluorescent intensity of the cell and the percentage of the cell in each generation (ie. the fraction of cells that have undergone replication) can be determined. [Fig. 21 B] The results of this experiment are that, after 72 hr, the negative control cells (PBS treated only) indicates 5 peaks with each peak having <50% less fluorescent intensity. By comparison, in cells treated with graded concentrations of HR-crotamine, there is clear evidence for a reduction in the number of peaks. Cells treated with 1 μM and 2 μM of HR-crotamine show only one peak, indicating a complete arrest of proliferative activity in these cells. Cells treated 0.5 μM and 0.25 μM HR-crotamine show some evidence of proliferative activity but much less than the control. In the 0.5 μM HR-crotamine treated cells, two generations of cell proliferation can be observed; and in 0.25 μM HR-crotamine treated cells, three generations of proliferation are detected. Cells treated with 0.1 μM HR-crotamine are very similar to the control cells, indicating very little inhibitory effect on cell proliferation. As expected, cells treated with 10 μM of CP-339818, a Kv1.3 channel

blocker, demonstrate only one peak of fluorescent labelling, indicating a complete inhibition of cell proliferation. The right-side panel in Fig. 21 B summarizes the effects of HR-crotamine (0.5 μM) and 10 μM of CP-339818, compared to control at T_0, T_{24}, T_{48} and T_{72} hours. The results show clearly the statistically significant effect of HR-crotamine on the proliferative activity of the Jurkat cells.

As an independent test for the anti-proliferative activity of HR-crotamine in Jurkat cells we used a biochemical biomarker assay, the induction of P21 protein, to test whether the HR-crotamine induced interference with cell proliferation was reflected in the induction of a critical inhibitor of cell cycle progression. P21 inhibits E/CDK2, D/CDK4,6 and ICBP90 to arrest cells at G1 stage; it also inhibits Cdc2 to arrest cells in G2. P21 also arrests cells in the G1/S boundary by inhibiting or interfereing with the expression/activation of A/CDK1,2, NFkB, D, E/CDK2,6, D1 and CDK2,4/cyclin D, E. P21 accumulation is a generally accepted biomarker for cycle arrest in most types of proliferating cells. We therefore measured the level of P21 expression in cells treated with CP-339818 (a positive control for Kv1.3 inhibition) and graded concentrations of HR-crotamine. [Fig. 21 C] The results obtained demonstrated a marked increase in the cells treated with CP-339818 and a dose-dependent increase in the level of P21 in the HR-crotamine treated cells. The estimated for the induction of P21 which is 0.25-0.5 μM matches the estimated EC_{50} for the inhibition of cell cycle progression estimated by the dye dilution assay.

Delayed progression could reflect a generalized slow-down in proliferative activity or a specific block in progression past a specific point in the cell cycle. The

address this issue, we used Propidium Iodide to stain cellular DNA and then used flow cytometry and Flowjo analysis to quantitate the fraction of the cells in G1, S or G2 phases of the cell cycle. [Fig. 21 D] In the control cells (PBS treated), the majority of cells are in G1 (43.8%) with smaller fractions in S and G2 (30.8% and 25.3% respectively). Inhibition of Kv1.3 by CP-339818, results in a reciprocal increase in the fraction of cells in G1 (67.0%) and a decrease of cells in S phase (9.2%). The fraction of cells in G2 is not much affected. These results demonstrate that the Kv1.3 inhibitor introduces a block in the G1 to S phase transition. The graded concentrations of HR-crotamine have a dose- dependent effect very similar to the effect of CP-339818. Graded concentrations of the myotoxin progressively increase the number of cells in G1 and produce a reciprocal inhibition in the fraction of cells in S-phase. There is little effect on the fraction of cells in G2. These results demonstrate clearly that HR-crotamine delays cell proliferation by inducing a G1/S phase block in cell cycle progression. The location of this blockade is entirely in line with its presumed mechanism of action as a Kv1.3 inhibitor. In Jurkat cells, it has been previously established that the expression of Kv1.3 is cell cycle dependent with the protein being transiently expressed at the later stages of G1 (Hu et al., 2012). It is thought that the transient expression of the channel protein results in a transient hyperpolarization of the membrane potential this increase calcium influx. This transient calcium signal is thought to play a role in progression of the cell through the G1/S phase boundary. In this model, inhibition of Kv1.3 activity, either by a chemical inhibitor such as CP-339818 or HR-crotamine will interfere with this process

and delay progression of the cells through the boundary, thereby decreasing the proliferative rate of the cells.

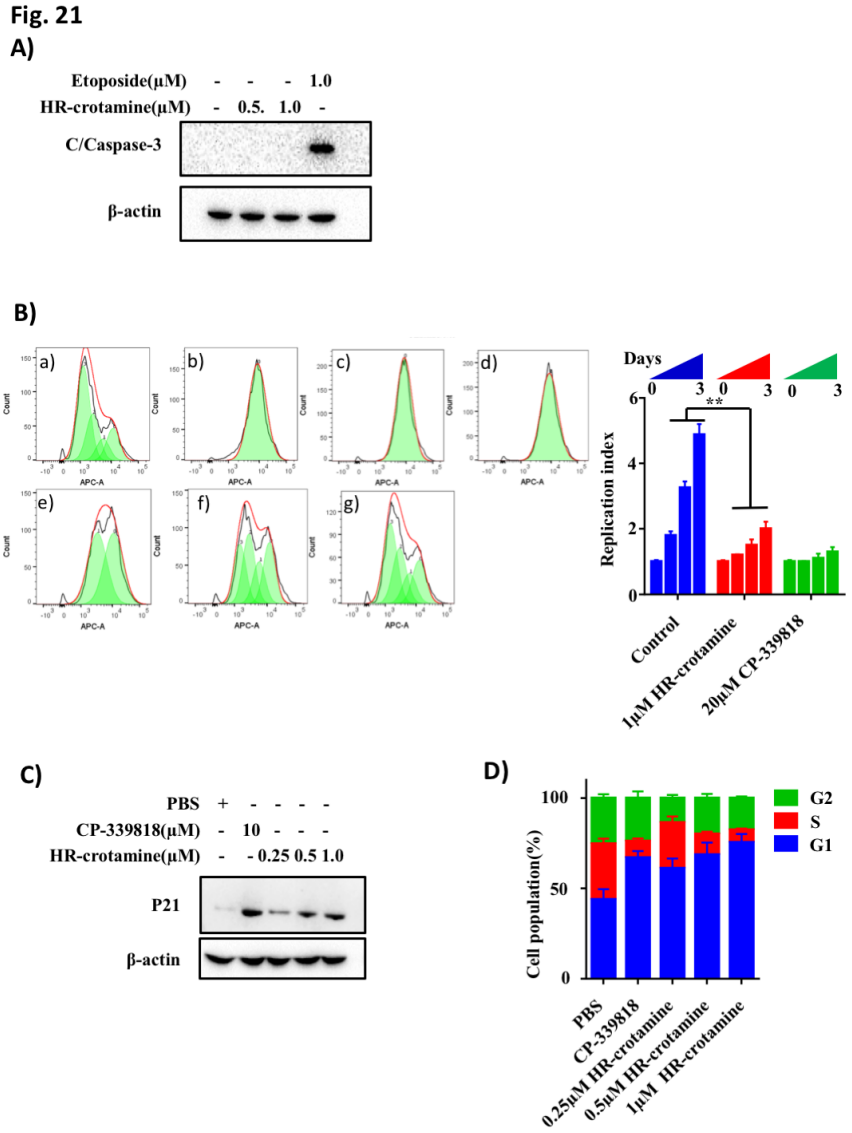

Fig. 21. The effects of HR-crotamine on the proliferative and apoptotic activity of Jurkat cell

A)*Western blot analysis of cleaved Caspase-3 protein levels in HR-crotamine treated Jurkat cells* Jurkat cells were treated with increasing concentrations of HR-crotamine or Etoposide (positive control) for 24 hr and the levels of activated Caspase-3 detected by Western blot analysis (see Methods-b. Western blot procedure of markers of cell proliferation and apoptosis using anti-cleaved human Caspase-3 antibody (1:2000 dilution) B) *Analysis of cell cycle kinetics in HR-crotamine treated Jurkat cells.* Jurkat

(Fig. 21. Continued)
cells were loaded with CellTracer (far red) dye at T_0 and then were treated with graded concentrations of HR-crotamine (0.1-2 μM) or 20 μM CP-339818 (a positive control for Kv1.3 inhibition) for 72 hr followed by flow cytometric analysis. (for details see Methods c. Cell Cycle Analysis) The green peaks for each cell generation was calculated by Flowjo analysis and the generation numbers were marked on the top of peak. The mathematically smoothed model for the distribution of fluorescent cells was represented by the red line. a) negative control, untreated cells b) positive control, cells treated with 20 μM CP-339818, c) cells treated with 2 μM HR-crotamine, d) cells treated with 1 μM HR-crotamine, e) cells treated with 0.5 μM HR-crotamine, f) cells treated with 0.25 μM HR-crotamine, g) cells treated with 0.1 μM HR-crotamine The panel on right displays the replication index (number of cell cycles) for cells treated with PBS(negative control), 0.5 μM of HR-crotamine and 20 μM of CP-339818(positive control) at T_0, T_{24}, T_{48} and T_{72} hr. Significant decreases in replication index ($p<0.05$) for HR-crotamine treated cells indicated by ** C) *Western blot analysis of P21 protein levels in HR-crotamine treated Jurkat cells* Jurkat cells were treated with increasing concentrations of HR-crotamine or 10 μM CP-339818 (positive control for Kv1.3 channel inhibition) for 24 hr and the levels of activated P21 detected by Western blot analysis (see Methods-b. Western blot procedure of markers of cell proliferation) and apoptosis using rabbit anti-human P21 (1:2000) and an HRP-conjugated anti-rabbit secondary antibody. D) *Cell cycle analysis of Jurkat cells treated with HR-crotamine* Jurkat cells were treated with increasing concentrations of HR-crotamine or 10 μM CP-339818 (positive control for Kv1.3 channel inhibition) for 24 hr and then were fixed, permeabilized and stained with Propidium Iodide to quantitate DNA content (see Methods-d. cell cycle arrest analysis), Stained cells were analyzed by flow cytometry and the fraction of cells in G1, S or G2 phases of the cell cycle were calculated using Flowjo software. Values reflect the mean+/-standard deviation for triplicate determinations.

The HR-crotamine's effect on the Jurkat cell can be affected by Kv channel knockdown

Our previous studies had suggested that the effects of HR-crotamine's activity in Jurkat cells was focused on the inhibition of Kv1.3 activity. We tested the dependence of Jurkat cells proliferation on Kv1.3 in two ways, both by evaluation the activity of a specific Kv1.3 channel inhibitor and knocking down the level of expression of Kv1.3 using an inhibitory shRNA construct. The results are summarized in Fig. 22 A and B. A quantitative evaluation of the activity of the specific Kv1.3 inhibitor CP-339818 [Fig. 22 A], showed that inhibition of the channel by concentrations of 25 μM or above resulted

in a complete inhibition of Jurkat cell proliferative activity. Since Jurkat cells express multiple Kv channel proteins, this result suggests that there is no redundancy among these channels and that Jurkat cells are absolutely dependent on Kv1.3 activity for proliferation. The results of the experiments with the Kv channel knockdown cell lines further support this conclusion. [Fig. 22 B] Reduction in the level of Kv1.3 expression (an 80 % reduction in transcript as estimated by qPCR-Fig. 19 B) resulted in a major reduction in proliferative activity without complete growth inhibition. This effect was entirely specific for Kv1.3, comparable reductions in the level of expression of Kv1.1, Kv1.2 and Kv1.5 had no effect on the proliferative activity of the Jurkat cells. These observations support the contention that Kv1.3, as distinct from other Kv channels, plays a critical role in supporting Jurkat cell proliferation.

The fact that the Kv1.3 knockdown cells retain a reduced level of proliferative activity suggest that, if the reduced proliferative activity is due to residual Kv1.3 (due to incomplete knockdown) then further addition of either HR-crotamine or CP-339818 should result in a complete inhibition of proliferative activity. [Fig. 22 C and Fig. 22 D] In the control cells (scrambled vector transfected), HR-crotamine caused a well defned dose dependent decrease in proliferative activity with an EC_{50} of approximately 0.2 μM. [Fig. 22 C] In the Kv1.3 channel knockdown cells, the basal rate of proliferation is reduced to about 40% of the control value but addition of HR-crotamine causes a clear dose-dependent decrease in proliferation to 20% or less of the control value. The IC_{50} for the inhibitory activity of HR-crotamine in Kv1.3 channel knockdown cells (400 nM) is comparable to its IC_{50} in control cells (200nM) suggesting that both inhibitory activities

target the same HR-crotamine receptor, CP-339818 also reduced the residual proliferative activity in Kv1.3 specific targeted shRNA transfected Jurkat cells. In both control and Kv1.3 knockdown cells, the highest concentrations of CP-339818 actually reduce the cell number below baseline, suggesting some cytotoxic activity with very high levels of the compound. Whether this cytotoxic activity is related to the Kv1.3 inhibitory activity of the chemical compound or is due to some low affinity "off-target" effect from very high concentrations of the drug is not known.

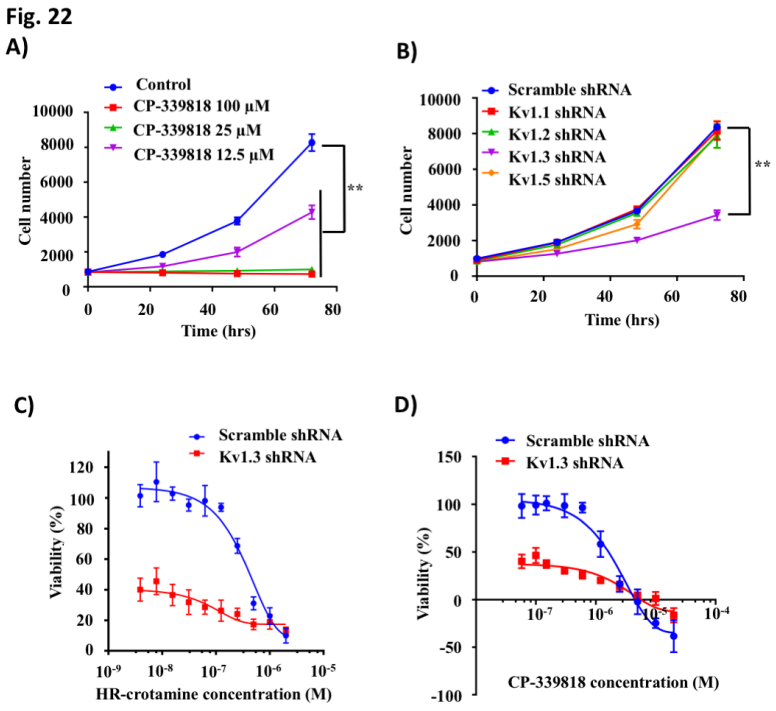

Fig. 22. Effect of Inhibition and knockdown of Kv channels on the proliferative activity and their sensitivity to HR-crotamine of Jurkat cells
A) *Effect of Kv inhibitor CP-339818 on the proliferative activity of Jurkat cells*. The activity of the Kv1.3 channel in Jurkat cells was suppressed using graded concentrations (100 µM, 25 µM, 12.5 µM) of CP-339818 (for experimental methods see Chapter III Methods h. Cell Viability with Kv Channel Knockdown Cells) The proliferative activity

(Fig. 22. Continued)
of the treated cells is compared to the PBS control. Each data point represents mean+/- standard deviation for 4 replicate determinations. B) *Effect of Kv channel knockdown on the proliferative activity of Jurkat cells*. The expression of Kv channels in Jurkat cells was suppressed using an inducible lentiviral expression system containing shRNAs for Kv1.1, Kv1.2, Kv1.3 and Kv1.5 (for experimental methods see Chapter II Methods h. Knockdown of Kv channel in HR-crotamine sensitive cell lines and Fig 19. B and Chapter III Methods h. Cell Viability with Kv Channel Knockdown Cells) The proliferative activity of the knockdown cell lines is compared to the control line (Jurkat cells transfected with the scrambled shRNA construct) cell lines. Each data point represents mean+/- standard deviation for 4 replicate determinations. C) *Effect of HR-crotamine on the proliferative activity of Kv1.3 channel knockdown Jurkat cells* Jurkat cells transfected with the Kv1.3 knockdown construct (Kv1.3 shRNA) or control cells (scrambled shRNA) were treated with graded concentrations of HR-crotamine for 72 hours. Cell proliferation was measured by cell counting as described in Chapter III Methods h. Cell Viability with Kv Channel Knockdown Cells, each data point represents mean+/-standard deviation for 4 replicate determinations. D) *Effect of* CP-339818 *on the proliferative activity of Kv1.3 knockdown Jurkat cells* Jurkat cells transfected with the Kv1.3 knockdown construct (Kv1.3 shRNA) or control cells (scrambled shRNA) were treated with graded concentrations of CP-33918 for 72 hr. Cell proliferation was measured by cell counting as described in Chapter III Methods h. Cell Viability with Kv Channel Knockdown Cells. Each data point represents mean+/- standard deviation for 4 replicate determinations.

Effect of HR-crotamine on calcium signaling in Jurkat cells and lymphocytes

There are published reports that Kv1.3 channels may play an important role in the regulation of membrane potential and calcium influx in non-excitable cells such as lymphocytes(Fung-Leung et al., 2017; Newell & Schlichter, 2005). It is thought that through the combined activity of Kv1.3 channel and $K_{Ca}3.1$ channel, membrane potential can be preserved when the CRAC/ORAI channels open to allow for transmembrane calcium influx. It is thought that transient calcium influx during cell cycle progression plays a critical role in regulating cell proliferation (Hogan, Lewis, & Rao, 2010). To test this in our Jurkat cells, we examined the effect of graded concentrations of SKF-96365, a STIM1 inhibitor that blocks the activity of Store-operated Ca^{2+} entry (SOCE). The

results obtained [Fig. 23 A] showed clearly that inhibition of calcium influx in Jurkat cells has a profound inhibitory effect on cell proliferation. The next step in testing our hypothesis on the mechanisms that mediate the effects of HR-crotamine on cell proliferation was to determine whether exposure to HR-crotamine modifies calcium influx into cells, as reflected in the activation of a calcium-dependent reporter system. We have used a Jurkat cell line containing a stably integrated NFAT-inducible Lucia reporter construct (Jurkat-Lucia™ NFAT cells). In this construct, the Lucia gene, which encodes a secreted coelenterazine-utilizing luciferase, is fused to six copies of the NFAT consensus transcriptional response element. Calcium influx-induced translocation of NFAT can be quantitatively measured by the increased expression of the Lucia reporter transcript product and the increase in Lucia luciferase enzymatic activity. The results of this experiment showed that HR-crotamine produced a clear dose-dependent reduction in luciferase activity reflecting an almost complete inhibition of calcium signaling at the highest concentration tested. [Fig. 23 B] The activity of HR-crotamine was paralleled by CP-339818 and SKF-96365 demonstrating that HR-crotamine's inhibitory activity was comparable to an established Kv1.3 inhibitor and a drug that blocked transmembrane calcium influx in these cells. [Fig. 23 C and Fig. 23 D] We also tested whether knockdown of any of the other Kv channels in Jurkat cells had a similar effect on transmembrane calcium influx and cell signaling. [Fig. 23 E and Fig. 23 F] The results obtained from these studies showed that Kv1.3 was the only Kv channel in Jurkat cells whose knockdown resulted in a decrease (>80%) in trans-membrane signaling and intracellular Ca^{2+} activity. Addition of either HR-crotamine or CP-339818 resulted in a

small but consistent further reduction in trans-membrane calcium influx and signaling. [Fig. 23 C and Fig. 23 D] The results of these studies show clearly that HR-crotamine functions as an indirect inhibitor of calcium influx through the SOCE calcium entry system.

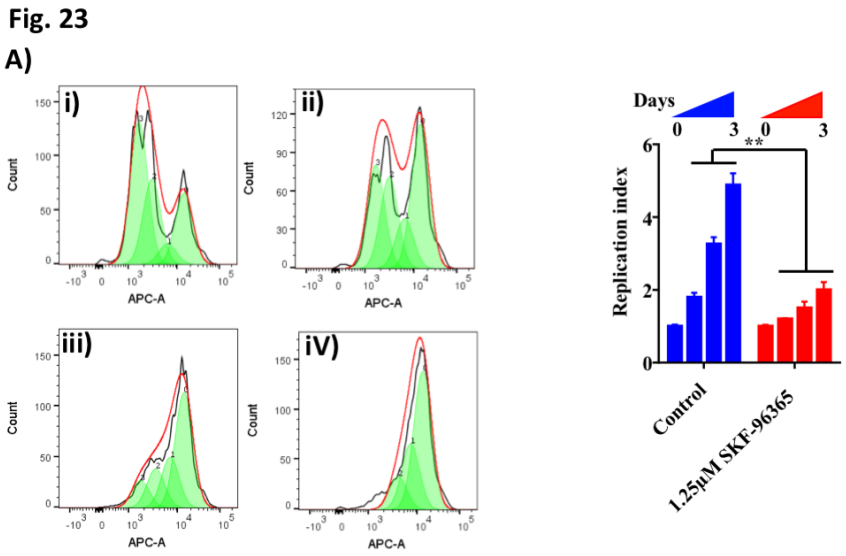

Fig. 23. HR-crotamine's effect on intracellular calcium activity
A) *Analysis of effect on cell cycle kinetics of* SKF-96365 *in Jurkat cells.* Jurkat cells were loaded with CellTracer (far red) dye at T_0 and then were treated with graded concentrations of SKF-96365, a STIM1 inhibitor that blocks the activity of Store-operated Ca^{2+} entry (SOCE) for 72 hr followed by flow cytometric analysis. (for details see Methods c. Cell Cycle Analysis) The green peaks for each cell generation was calculated by Flowjo analysis and the generation numbers were marked on the top of peak. The mathematically smoothed model for the distribution of fluorescent cells was represented by the red line. In the Figure i) Negative Control (buffer only); ii) SKF-96365 0.6 μM; iii) SKF-96365 1.25 μM; iv) SKF-96365 10 μM. Panel on Right displays the replication index (number of cell cycles) for cells treated with PBS buffer (control), or SKF-96365 1.25 μM at T_0, T_{24}, T_{48} and T_{72} hr. Significant decreases in replication index ($P<0.05$) for HR-crotamine treated cells indicated by **.

(Fig. 23. Continued)

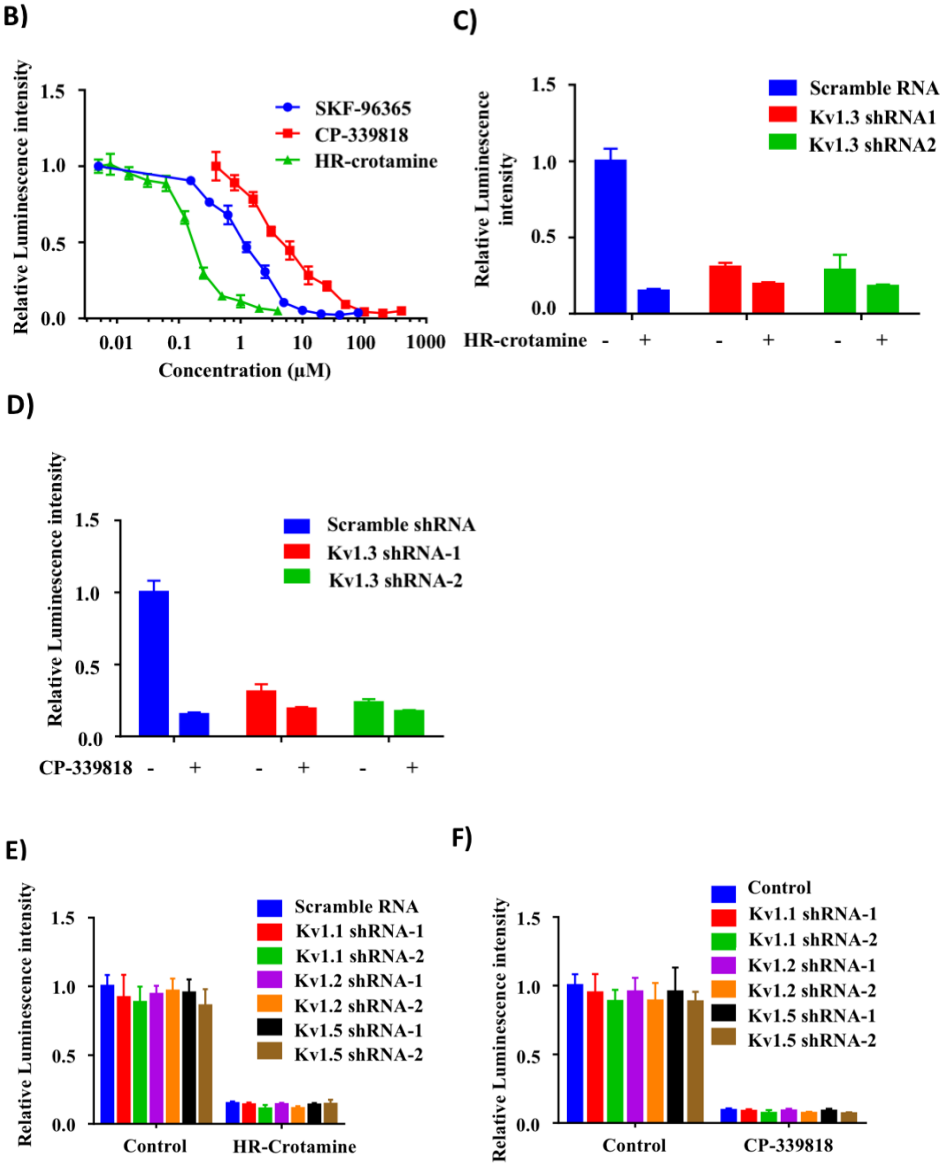

B) Effect of HR-crotamine *on the activity of an intracellular calcium reporter system in Jurkat-Lucia NFAT cells* Jurkat-Lucia NFAT cells were treated with graded concentrations of HR-crotamine (10 nM-2 µM), SKF-96365 (a positive control for inhibition of calcium influx and CP-339818 (a positive control for Kv1.3 inhibition) for 1 hr on ice (under conditions described in Methods i. Intracellular calcium activity analysis). Calcium influx and activation of the NFAT/NF-kB pathways were achieved by addition of 30 ng/ml phorbol myristate acetate and 1.5 µM ionomycin followed by incubation for 12 hr subsequent analysis of luciferase activity in cell lysates. C) *Effect of HR-crotamine on the activity of an intracellular calcium reporter system in Kv1.3 knockdown Jurkat-Lucia NFAT cells* Control Jurkat-Lucia NFAT cells (transfected with scrambled shRNAs) and 2 lines of Kv1.3 channel knockdown cells (each transfected

(Fig. 23. Continued)
with an inducible lentivirus shRNA vector containing two different Kv1.3 inhibitory shRNAs) were treated with 0.5 μM HR-crotamine or buffer control and calcium activity was measured by activation of the luciferase reported gene as described Methods i. Intracellular calcium activity analysis and the legend to Fig. 23 B. Values represent the mean+/-standard deviation of duplicate determinations. D) *Effect of CP-339818 on the activity of an intracellular calcium reporter system in Kv1.3 knockdown Jurkat-Lucia NFAT cells.* Control Jurkat-Lucia NFAT cells (transfected with scrambled shRNAs) and 2 lines of Kv1.3 knockdown cells (each transfected with an inducible lentivirus shRNA vector containing two different Kv1.3 inhibitory shRNAs) were treated with 20 μM CP-339818 or buffer control; and calcium activity was measured by activation of the luciferase reported gene as described Methods i. Intracellular calcium activity analysis and the legend to Fig. 23 B. Values represent the mean+/-standard deviation of 4 replicate determinations E) *Effect of HR-crotamine on the activity of an intracellular calcium reporter system in a series of Kv knockdown Jurkat-Lucia NFAT cells* Control Jurkat-Lucia NFAT cells (transfected with scrambled shRNAs) and 2 lines of Kv knockdown cells (each transfected with an inducible lentivirus shRNA vector containing two different inhibitory shRNAs for Kv1.1, Kv1.2 or Kv1.5) were treated with buffer (Control) or 0.5 μM HR-crotamine and calcium activity was measured by activation of the luciferase reported gene as described Methods i. Intracellular calcium activity analysis and the legend to Fig. 23. B) Values represent the mean+/-standard deviation of 4 replicate determinations F) *Effect of CP-339818 on the activity of an intracellular calcium reporter system in a series of Kv knockdown Jurkat-Lucia NFAT cells* Control Jurkat-Lucia NFAT cells (transfected with scrambled shRNAs) and 2 lines of knockdown cells (each transfected with an inducible lentivirus shRNA vector containing two different inhibitory shRNAs for Kv1.1, Kv1.2 or Kv1.5) were treated with buffer (Control) or 20 μM CP-339818 and calcium activity was measured by activation of the luciferase reported gene as described Methods i. Intracellular calcium activity analysis and the legend to Fig. 23 B. Values represent the mean+/-standard deviation of 4 replicate determinations

Calcium influx into T- and B-cells is linked both to cell activation and the induction of cell proliferation. To assess the effect of HR-crotamine on the lymphocyte activation we have measured the impact of exposure to HR-crotamine on the induction of IL-2 secretion. IL-2 secretion is a well-established marker for T-cell activation (Bartelt, Cruz-Orcutt, Collins, & Houtman, 2009). For these studies, we have extended the test system to include not only T-cell leukemia cells such as Jurkat cells but also

CD4+ positive peripheral blood T-cells. In both Jurkat and CD4+ T-cells increasing concentrations of HR-crotamine resulted in a major inhibition of both T-cell and Jurkat cell activation as measured by IL-2 secretion. [Fig. 24 A] This effect mirrored an equivalent inhibition of activation produced by exposure of the cells to CP-339818, a specific inhibitor of Kv1.3 activity. [Fig. 24 B] An interesting implication of these studies is that the inhibition of calcium influx and activation in these two cell types reflects the fact that although they share expression of Kv1.3 on their membranes they differ in the channels that support calcium entry into the cells. Jurkat cell express CRAC/ORAI1 calcium channel and the CD4+ T-cells express CaV1/ORAI1 calcium channel. The fact that HR-crotamine inhibits calcium activation in both cell types supports the idea that the inhibitory effect of the myotoxin on calcium influx is indeed an indirect effect reflecting the inhibition of Kv1.3 channel activity rather than any direct effect on the calcium entry pathways.

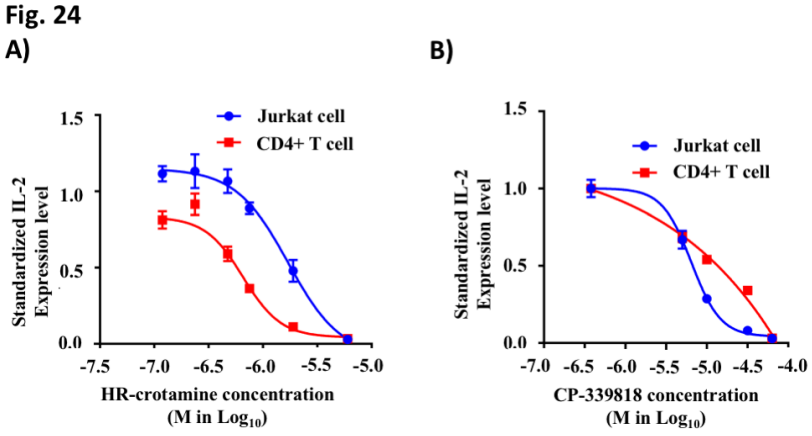

Fig. 24. Effects of HR-crotamine and CP-339818 on IL-2 secretion by Jurkat and CD4+T cells
A) *Effect of HR-crotamine on IL-2 secretion* Jurkat cells and peripheral blood CD4+ T cells (PBTC) were seeded in 96-well plates at $5X10^4$ cell/well in the presence of A)

(Fig. 24. Continued)
graded concentrations of HR-crotamine (0-12μM). or B) CP-339818 (5-50μM). Phytohemagglutinin (PHA) and phorbol ester were added to the cells for 24 hr to activate IL-2 expression and secretion as measured by a human ELISA kit (procedures described in detail in Methods j. IL-2 ELISA Assay) Values represent the mean+/- standard deviation of 4 replicate determinations

Discussion

The results from our study indicate that while HR-crotamine binds to multiple Kv channels including Kv1.1, Kv1.2 and Kv1.3, its functional activity as an inhibitor of the proliferative activity of T-cell leukemia cells is linked specifically to the inhibition of Kv1.3 activity. The results we have obtained point to a model in which the inhibition of Kv1.3 activity leads indirectly to an inhibition of transmembrane calcium flux and a resulting inhibition of calcium-dependent cell signaling. It is ultimately this inhibition of cell signaling that results in an inhibition of cell proliferation and lymphocyte activation. Furthermore, the interaction appears to occur on the outer surface of the cell on the extracellular port for K^+ ion flux since the binding of HR-crotamine to the Jurkat cells is inhibited by the binding of CP-339818 to the cells (Nguyen et al., 1996; Schmitz et al., 2005). Once HR-crotamine is bound to the cell surface Kv1.3 channel, it disables potassium ion out-flow through the channel. Because the conductance of the Kv1.3 channel is reduced by crotamine (Steve Peigneur et al., 2012), the resulting decrease in membrane polarization interferes with calcium and calcium signaling mediated cell activation is halted. As a consequence, the IL-2 secretion was inhibited(Feske, Wulff, & Skolnik, 2015; Hogan et al., 2010). Since cell cycle specific calcium influx also plays a critical role in cell proliferation, the cell growth is inhibited by the blockade of the Kv1.3

channel (Munaron, Antoniotti, & Lovisolo, 2004). We believe that the selective and differential effects of myotoxins on different normal and malignant cell types are likely due to differences in the expression of cell surface Kv1.3 and potentially to differences in which the activity of Kv1.3 plays a critical role in regulating calcium influx in different types of cell. Under our experimental conditions, the functional effect of Kv1.3 blockade by HR-crotamine is very specifically linked to anti-proliferative activity. We detected absolutely no evidence for the inducting of apoptosis or the penetration of the toxin into the body of the cell. Lastly, we note that very specific effect of HR-crotamine in inducing cell cycle arrest at the G1/S boundary matches exactly the temporal pattern of expression of Kv1.3 in lymphocytes. It is thought that the transient induction of Kv1.3 late in G1 leads to a transient spike in calcium influx that promotes the passage of the cell past the G1/S checkpoint. By inhibiting this transient calcium spike, it is very likely that HR-crotamine inhibits progress of the cell through the cycle and ultimately inhibits overall cell proliferation.

There are reports that the Kv1.3 channel is not only expressed on the surface cells but also on the mitochondrial membrane. It has been suggested that malfunction of the mitochondrial Kv1.3 channel may trigger NOS-mediated cell apoptosis in the malignant cells (Leanza et al., 2017). Presumably penetration of the cell membrane must be a necessary prerequisite for any effects of myotoxins on mitochondrial function. In our studies, we have not seen evidence that, under the conditions we have used, cell penetration either occurs or is a necessary step in HR-crotamine's biological activity. Others have suggested that specific HSPG receptors may be required to trigger the cell

membrane penetrating activity of crotamine(Nascimento et al., 2007; Ponnappan & Chugh, 2017). It is possible that the lower levels surface HSPG receptor expression in Jurkat cells compared to other attached cells, such as HeLa cell.(Leanza et al., 2017) may explain why this particular pathway for biological activity was not detected in our studies.

Our study has established a model that demonstrates a pathway starts with the interaction of HR-crotamine with a specific target on the surface of a cell and leads to intracellular mechanisms that affects the proliferation and activation of that cell. These findings can be considered as the foundation for the future research on how one may be able to utilize the selective anti-proliferative effect of HR-crotamine (and crotamine-like proteins) to suppress the growth of certain types of the malignant cells. Ultimately, an understanding of the structure-function relation for HR-crotamine's cell specificity and toxicity has the potential to be extremely helpful in developing the HR-crotamine into a new anti-cancer drug or effective anti-myotoxin antivenom.

Recent studies in our lab have also pointed to another manifestation of the selective activity of HR-crotamine as an inhibitor of biological functions. Working with collaborators, we have discovered that HR-crotamine can disorganize the contraction of the smooth muscle in the lymphatic vessels. Several pieces of evidence suggest that this effect may also reflect inhibition cell surface Kv1.3 activity. Disruption of lymphatic vessel contractility may have important implications not only for the treatment of snake bite but also for the treatment of systematic diseases linked to lymphatic dysfunction.

Our studies have focused on the interactions of HR-crotamine with Kv1.3 channel since this appears to be the most important functional Kv channel in lymphocytes. We recognize that in other cell types, especially excitable cells such as neurons and muscle cells, Kv1.1 and Kv1.2 play a critical role in regulating membrane potentials. HR-crotamine targeting of these receptors is very likely to play an important role in the well documented neurotoxic and myotoxic effects of myotoxins. These include spinal cord paralysis as manifest in hind-limb paralysis in small animals as well as the myofasciculations and rhabdomyolysis that occurs in humans after envenomation with myotoxin contained venoms. (Rizzi et al., 2007)

Further study

According to our understanding, there is still a long way to go to get the full understanding for all of HR-crotamine's targets and their activities. HR-crotamine is a small biotoxin with extremely low immunogenicity. As a consequence, there are no commercial or experimental anti-toxins that can effectively block the toxicity of myotoxins such as HR-crotamine. The model we have developed may prove to be useful in finding new types of molecules that can neutralize the cytotoxicity of HR-crotamine and other myotoxins. Our research can provide a reference point and the foundation for future investigations designed to screen for potential anti-venom molecules. Specifically, the phage display-based screening of single-chain antibody library can be applied to our cell testing model and an *in vivo* test for the effective single chain antibody can be used to validate the result of screening.

Future screens for potential toxin-binding antibodies will be able to use polyclonal phage libraries that can be used to select for HR-crotamine-binding phages selected after multiple rounds of bio-panning against HR-crotamine. The specificity of phage clones that bind to HR-crotamine will be examined by single-chain variable fragment (scFv) ELISA against a panel of structurally related peptides such as human beta-defensins or myotoxin III from venom of *Bothrops asper*. The DNA sequences of the scFv obtained from ELISA will be cloned into *E. coli* for producing soluble scFv with an affinity tag for purification propose. The activity of individual scFv will be determined with the NFAT luciferase assay, by measuring the ability of each scFv to neutralize HR-crotamine's inhibitory activity without interfering with Jurkat cell viability. For these experiments, the Jurkat-Lucia NFAT cells will be incubated with the scFv to eliminate any scFv that have cytotoxicity. The protocol for the test with non-cytotoxic scFv will be same as the NFAT luciferase assay. Some of the most effective scFv will be selected to confirm their ability to suppress HR-crotamine's inhibitory effect on IL-2 secretion in Jurkat cells.

Once we successfully identified the antitoxin with the confirmed toxicity-neutralization activity, the principle behind our screening strategy will have been proven to be successful. Based on the experiences that we acquired through our investigation, similar approaches can be applied in the future to the study of other toxins in the myotoxin family and other small molecule toxins with low immunogenicity.

REFERENCES

"Adult nonfiction: Pure sciences." Booklist **90**(19/20): 1746-1746.

Azam, P., A. Sankaranarayanan, D. Homerick, S. Griffey and H. Wulff (2007). "Targeting effector memory T cells with the small molecule Kv1.3 blocker PAP-1 suppresses allergic contact dermatitis." J Invest Dermatol **127**(6): 1419-1429.

Bayer-Garner, I. B., R. D. Sanderson, M. V. Dhodapkar, R. B. Owens and C. S. Wilson (2001). "Syndecan-1 (CD138) immunoreactivity in bone marrow biopsies of multiple myeloma: shed syndecan-1 accumulates in fibrotic regions." Mod Pathol **14**(10): 1052-1058.

Berg, O. G., M. H. Gelb, M. D. Tsai and M. K. Jain (2001). "Interfacial enzymology: the secreted phospholipase A(2)-paradigm." Chem Rev **101**(9): 2613-2654.

Bielanska, J., J. Hernandez-Losa, T. Moline, R. Somoza, S. Ramon y Cajal, E. Condom, J. C. Ferreres and A. Felipe (2012). "Differential expression of Kv1.3 and Kv1.5 voltage-dependent K+ channels in human skeletal muscle sarcomas." Cancer Invest **30**(3): 203-208.

Bielanska, J., J. Hernandez-Losa, M. Perez-Verdaguer, T. Moline, R. Somoza, Y. C. S. Ramon, E. Condom, J. C. Ferreres and A. Felipe (2009). "Voltage-dependent potassium channels Kv1.3 and Kv1.5 in human cancer." Curr Cancer Drug Targets **9**(8): 904-914.

Bornemann, D. J., S. Park, S. Phin and R. Warrior (2008). "A translational block to HSPG synthesis permits BMP signaling in the early Drosophila embryo." Development **135**(6): 1039-1047.

Bottrall, J. L., F. Madaras, C. D. Biven, M. G. Venning and P. J. Mirtschin (2010). "Proteolytic activity of Elapid and Viperid Snake venoms and its implication to digestion." J Venom Res **1**: 18-28.

Bridges, E. and A. L. Harris (2015). "Vascular-promoting therapy reduced tumor growth and progression by improving chemotherapy efficacy." Cancer Cell **27**(1): 7-9.

Burke, J. E. and E. A. Dennis (2009). "Phospholipase A2 structure/function, mechanism, and signaling." J Lipid Res **50 Suppl**: S237-242.

Chen, P. C., M. A. Hayashi, E. B. Oliveira and R. L. Karpel (2012). "DNA-interactive properties of crotamine, a cell-penetrating polypeptide and a potential drug carrier." PLoS One **7**(11): e48913.

Chittajallu, R., Y. Chen, H. Wang, X. Yuan, C. A. Ghiani, T. Heckman, C. J. McBain and V. Gallo (2002). "Regulation of Kv1 subunit expression in oligodendrocyte progenitor cells and their role in G1/S phase progression of the cell cycle." Proc Natl Acad Sci U S A **99**(4): 2350-2355.

Cui, D., A. Li, S. Zhang, C. Pang, J. Yang, J. Guo, F. Ma, J. Wang and N. Ren (2012). "Microbial community analysis of three municipal wastewater treatment plants in winter and spring using culture-dependent and culture-independent methods." World J Microbiol Biotechnol **28**(6): 2341-2353.

Dalla Valle, L., F. Benato, S. Maistro, S. Quinzani and L. Alibardi (2012). "Bioinformatic and molecular characterization of beta-defensins-like peptides isolated from the green lizard Anolis carolinensis." Dev Comp Immunol **36**(1): 222-229.

Decher, N., T. Gonzalez, A. K. Streit, F. B. Sachse, V. Renigunta, M. Soom, S. H. Heinemann, J. Daut and M. C. Sanguinetti (2008). "Structural determinants of Kvbeta1.3-induced channel inactivation: a hairpin modulated by PIP2." EMBO J **27**(23): 3164-3174.

Derksen, P. W., R. M. Keehnen, L. M. Evers, M. H. van Oers, M. Spaargaren and S. T. Pals (2002). "Cell surface proteoglycan syndecan-1 mediates hepatocyte growth factor binding and promotes Met signaling in multiple myeloma." Blood **99**(4): 1405-1410.

Diaz-Garcia, C. M., C. Sanchez-Soto and M. Hiriart (2010). "Toxins that modulate ionic channels as tools for exploring insulin secretion." Cell Mol Neurobiol **30**(8): 1275-1281.

Doyle, D. A., J. Morais Cabral, R. A. Pfuetzner, A. Kuo, J. M. Gulbis, S. L. Cohen, B. T. Chait and R. MacKinnon (1998). "The structure of the potassium channel: molecular basis of K+ conduction and selectivity." Science **280**(5360): 69-77.

Favre, I., E. Moczydlowski and L. Schild (1996). "On the structural basis for ionic selectivity among Na+, K+, and Ca2+ in the voltage-gated sodium channel." Biophys J **71**(6): 3110-3125.

Fernandes, C. M., F. Pereira Teixeira Cde, A. C. Leite, J. M. Gutierrez and F. A. Rocha (2007). "The snake venom metalloproteinase BaP1 induces joint hypernociception through TNF-alpha and PGE2-dependent mechanisms." Br J Pharmacol **151**(8): 1254-1261.

Gamper, N., S. Fillon, S. M. Huber, Y. Feng, T. Kobayashi, P. Cohen and F. Lang (2002). "IGF-1 up-regulates K+ channels via PI3-kinase, PDK1 and SGK1." Pflugers Arch **443**(4): 625-634.

Gardiner, J. and J. Marc (2013). "Phospholipases may play multiple roles in anisotropic plant cell growth." Protoplasma **250**(1): 391-395.

Gasanov, S. E., R. K. Dagda and E. D. Rael (2014). "Snake Venom Cytotoxins, Phospholipase As, and Zn-dependent Metalloproteinases: Mechanisms of Action and Pharmacological Relevance." J Clin Toxicol **4**(1): 1000181.

Gomis-Ruth, F. X., L. F. Kress and W. Bode (1993). "First structure of a snake venom metalloproteinase: a prototype for matrix metalloproteinases/collagenases." EMBO J **12**(11): 4151-4157.

Goodman, L. S., A. Gilman, L. L. Brunton, J. S. Lazo and K. L. Parker (2006). Goodman & Gilman's the pharmacological basis of therapeutics. New York, McGraw-Hill.

Greenbaum, E., N. Galeva and M. Jorgensen (2003). "Venom variation and chemoreception of the viperid Agkistrodon contortrix: evidence for adaptation?" J Chem Ecol **29**(8): 1741-1755.

Griffin, P. R. and S. D. Aird (1990). "A new small myotoxin from the venom of the prairie rattlesnake (Crotalus viridis viridis)." FEBS Lett **274**(1-2): 43-47.

Gutierrez, J. M. and A. Rucavado (2000). "Snake venom metalloproteinases: their role in the pathogenesis of local tissue damage." Biochimie **82**(9-10): 841-850.

Hayashi, M. A., F. D. Nascimento, A. Kerkis, V. Oliveira, E. B. Oliveira, A. Pereira, G. Radis-Baptista, H. B. Nader, T. Yamane, I. Kerkis and I. L. Tersariol (2008). "Cytotoxic effects of crotamine are mediated through lysosomal membrane permeabilization." Toxicon **52**(3): 508-517.

Hayashi, M. A., E. B. Oliveira, I. Kerkis and R. L. Karpel (2012). "Crotamine: a novel cell-penetrating polypeptide nanocarrier with potential anti-cancer and biotechnological applications." Methods Mol Biol **906**: 337-352.

Hayashida, K., P. D. Stahl and P. W. Park (2008). "Syndecan-1 ectodomain shedding is regulated by the small GTPase Rab5." J Biol Chem **283**(51): 35435-35444.

Heffernan, B. J., B. Thomason, A. Herring-Palmer, L. Shaughnessy, R. McDonald, N. Fisher, G. B. Huffnagle and P. Hanna (2006). "Bacillus anthracis phospholipases C facilitate macrophage-associated growth and contribute to virulence in a murine model of inhalation anthrax." Infect Immun **74**(7): 3756-3764.

Heginbotham, L., Z. Lu, T. Abramson and R. MacKinnon (1994). "Mutations in the K+ channel signature sequence." Biophys J **66**(4): 1061-1067.

Hernandez-Oliveira e Silva, S., S. Rostelato-Ferreira, T. A. Rocha-e-Silva, P. Randazzo-Moura, C. A. Dal-Belo, E. F. Sanchez, C. R. Borja-Oliveira and L. Rodrigues-Simioni (2013). "Beneficial effect of crotamine in the treatment of myasthenic rats." Muscle Nerve **47**(4): 591-593.

Jaakkola, P. and M. Jalkanen (1999). "Transcriptional regulation of Syndecan-1 expression by growth factors." Prog Nucleic Acid Res Mol Biol **63**: 109-138.

Jackson, T. N., K. Sunagar, E. A. Undheim, I. Koludarov, A. H. Chan, K. Sanders, S. A. Ali, I. Hendrikx, N. Dunstan and B. G. Fry (2013). "Venom down under: dynamic evolution of Australian elapid snake toxins." Toxins (Basel) **5**(12): 2621-2655.

Kerkis, A., I. Kerkis, G. Radis-Baptista, E. B. Oliveira, A. M. Vianna-Morgante, L. V. Pereira and T. Yamane (2004). "Crotamine is a novel cell-penetrating protein from the venom of rattlesnake Crotalus durissus terrificus." FASEB J **18**(12): 1407-1409.

Kerkis, I., S. Silva Fde, A. Pereira, A. Kerkis and G. Radis-Baptista (2010). "Biological versatility of crotamine--a cationic peptide from the venom of a South American rattlesnake." Expert Opin Investig Drugs **19**(12): 1515-1525.

Kini, R. M. (2005). "Structure-function relationships and mechanism of anticoagulant phospholipase A2 enzymes from snake venoms." Toxicon **45**(8): 1147-1161.

Kordis, D. and F. Gubensek (2000). "Adaptive evolution of animal toxin multigene families." Gene **261**(1): 43-52.

Leppa, S., M. Mali, H. M. Miettinen and M. Jalkanen (1992). "Syndecan expression regulates cell morphology and growth of mouse mammary epithelial tumor cells." Proc Natl Acad Sci U S A **89**(3): 932-936.

Luna-Ramirez, K., M. A. Sani, J. Silva-Sanchez, J. M. Jimenez-Vargas, F. Reyna-Flores, K. D. Winkel, C. E. Wright, L. D. Possani and F. Separovic (2013). "Membrane interactions and biological activity of antimicrobial peptides from Australian scorpion." Biochim Biophys Acta.

Mamede, C. C., M. R. de Queiroz, K. C. Fonseca, N. C. de Morais, S. A. Filho, M. E. Beletti, L. Stanziola and F. de Oliveira (2013). "Histological and ultrastructural analyses of muscle damage induced by a myotoxin isolated from Bothrops alternatus snake venom." Protein Pept Lett **20**(2): 192-199.

Mandal, S. M., L. Migliolo, S. Das, M. Mandal, O. L. Franco and T. K. Hazra (2012). "Identification and characterization of a bactericidal and proapoptotic peptide from Cycas revoluta seeds with DNA binding properties." J Cell Biochem **113**(1): 184-193.

Markland, F. S., Jr. and S. Swenson (2013). "Snake venom metalloproteinases." Toxicon **62**: 3-18.

Marzioni, D., T. Lorenzi, R. Mazzucchelli, L. Capparuccia, M. Morroni, R. Fiorini, C. Bracalenti, A. Catalano, G. David, M. Castellucci, G. Muzzonigro and R. Montironi (2009). "Expression of basic fibroblast growth factor, its receptors and syndecans in bladder cancer." Int J Immunopathol Pharmacol **22**(3): 627-638.

Matavel, A. C., D. L. Ferreira-Alves, P. S. Beirao and J. S. Cruz (1998). "Tension generation and increase in voltage-activated Na+ current by crotamine." Eur J Pharmacol **348**(2-3): 167-173.

Mouhat, S., N. Andreotti, B. Jouirou and J. M. Sabatier (2008). "Animal toxins acting on voltage-gated potassium channels." Curr Pharm Des **14**(24): 2503-2518.

Mouhat, S., B. Jouirou, A. Mosbah, M. De Waard and J. M. Sabatier (2004). "Diversity of folds in animal toxins acting on ion channels." Biochem J **378**(Pt 3): 717-726.

Moura-da-Silva, A. M., O. H. Ramos, C. Baldo, S. Niland, U. Hansen, J. S. Ventura, S. Furlan, D. Butera, M. S. Della-Casa, I. Tanjoni, P. B. Clissa, I. Fernandes, A. M. Chudzinski-Tavassi and J. A. Eble (2008). "Collagen binding is a key factor for the hemorrhagic activity of snake venom metalloproteinases." Biochimie **90**(3): 484-492.

Nascimento, F. D., M. A. Hayashi, A. Kerkis, V. Oliveira, E. B. Oliveira, G. Radis-Baptista, H. B. Nader, T. Yamane, I. L. Tersariol and I. Kerkis (2007). "Crotamine mediates gene delivery into cells through the binding to heparan sulfate proteoglycans." J Biol Chem **282**(29): 21349-21360.

Nascimento, F. D., L. Sancey, A. Pereira, C. Rome, V. Oliveira, E. B. Oliveira, H. B. Nader, T. Yamane, I. Kerkis, I. L. Tersariol, J. L. Coll and M. A. Hayashi (2012).

"The natural cell-penetrating peptide crotamine targets tumor tissue in vivo and triggers a lethal calcium-dependent pathway in cultured cells." Mol Pharm **9**(2): 211-221.

Nicastro, G., L. Franzoni, C. de Chiara, A. C. Mancin, J. R. Giglio and A. Spisni (2003). "Solution structure of crotamine, a Na+ channel affecting toxin from Crotalus durissus terrificus venom." Eur J Biochem **270**(9): 1969-1979.

Oguiura, N., M. Boni-Mitake, R. Affonso and G. Zhang (2011). "In vitro antibacterial and hemolytic activities of crotamine, a small basic myotoxin from rattlesnake Crotalus durissus." J Antibiot (Tokyo) **64**(4): 327-331.

Oguiura, N., M. Boni-Mitake and G. Radis-Baptista (2005). "New view on crotamine, a small basic polypeptide myotoxin from South American rattlesnake venom." Toxicon **46**(4): 363-370.

Orlova, E. V., M. Papakosta, F. P. Booy, M. van Heel and J. O. Dolly (2003). "Voltage-gated K+ channel from mammalian brain: 3D structure at 18A of the complete (alpha)4(beta)4 complex." J Mol Biol **326**(4): 1005-1012.

Ouadid-Ahidouch, H. and A. Ahidouch (2008). "K+ channel expression in human breast cancer cells: involvement in cell cycle regulation and carcinogenesis." J Membr Biol **221**(1): 1-6.

Ouadid-Ahidouch, H., F. Chaussade, M. Roudbaraki, C. Slomianny, E. Dewailly, P. Delcourt and N. Prevarskaya (2000). "KV1.1 K(+) channels identification in human breast carcinoma cells: involvement in cell proliferation." Biochem Biophys Res Commun **278**(2): 272-277.

Ouadid-Ahidouch, H., M. Roudbaraki, A. Ahidouch, P. Delcourt and N. Prevarskaya (2004). "Cell-cycle-dependent expression of the large Ca2+-activated K+ channels in breast cancer cells." Biochem Biophys Res Commun **316**(1): 244-251.

Ownby, C. L., J. M. Gutierrez, T. R. Colberg and G. V. Odell (1982). "Quantitation of myonecrosis induced by myotoxin a from prairie rattlesnake (Crotalus viridis viridis) venom." Toxicon **20**(5): 877-885.

Pardo, L. A. (2004). "Voltage-gated potassium channels in cell proliferation." Physiology (Bethesda) **19**: 285-292.

Peigneur, S., D. J. Orts, A. R. Prieto da Silva, N. Oguiura, M. Boni-Mitake, E. B. de Oliveira, A. J. Zaharenko, J. C. de Freitas and J. Tytgat (2012). "Crotamine pharmacology revisited: novel insights based on the inhibition of KV channels." Mol Pharmacol **82**(1): 90-96.

Pereira, A., A. Kerkis, M. A. Hayashi, A. S. Pereira, F. S. Silva, E. B. Oliveira, A. R. Prieto da Silva, T. Yamane, G. Radis-Baptista and I. Kerkis (2011). "Crotamine toxicity and efficacy in mouse models of melanoma." Expert Opin Investig Drugs **20**(9): 1189-1200.

Pongs, O., T. Leicher, M. Berger, J. Roeper, R. Bahring, D. Wray, K. P. Giese, A. J. Silva and J. F. Storm (1999). "Functional and molecular aspects of voltage-gated K+ channel beta subunits." Ann N Y Acad Sci **868**: 344-355.

Radis-Baptista, G. and I. Kerkis (2011). "Crotamine, a small basic polypeptide myotoxin from rattlesnake venom with cell-penetrating properties." Curr Pharm Des **17**(38): 4351-4361.

Ridley, R. C., H. Xiao, H. Hata, J. Woodliff, J. Epstein and R. D. Sanderson (1993). "Expression of syndecan regulates human myeloma plasma cell adhesion to type I collagen." Blood **81**(3): 767-774.

Rodrigues, M., A. Santos, B. G. de la Torre, G. Radis-Baptista, D. Andreu and N. C. Santos (2012). "Molecular characterization of the interaction of crotamine-derived nucleolar targeting peptides with lipid membranes." Biochim Biophys Acta **1818**(11): 2707-2717.

Rokyta, D. R., A. R. Lemmon, M. J. Margres and K. Aronow (2012). "The venom-gland transcriptome of the eastern diamondback rattlesnake (Crotalus adamanteus)." BMC Genomics **13**: 312.

Rosso, J. P., J. R. Schwarz, M. Diaz-Bustamante, B. Ceard, J. M. Gutierrez, M. Kneussel, O. Pongs, F. Bosmans and P. E. Bougis (2015). "MmTX1 and MmTX2 from

coral snake venom potently modulate GABAA receptor activity." Proc Natl Acad Sci U S A **112**(8): E891-900.

Rucavado, A., G. Borkow, M. Ovadia and J. M. Gutierrez (1995). "Immunological studies on BaH1 and BaP1, two hemorrhagic metalloproteinases from the venom of the snake Bothrops asper." Toxicon **33**(8): 1103-1106.

Rucavado, A., T. Escalante and J. M. Gutierrez (2004). "Effect of the metalloproteinase inhibitor batimastat in the systemic toxicity induced by Bothrops asper snake venom: understanding the role of metalloproteinases in envenomation." Toxicon **43**(4): 417-424.

Samejima, Y., Y. Aoki and D. Mebs (1991). "Amino acid sequence of a myotoxin from venom of the eastern diamondback rattlesnake (Crotalus adamanteus)." Toxicon **29**(4-5): 461-468.

Sanchez, E. E., R. Gonzalez, S. Lucena, S. Garcia, H. J. Finol, M. Suntravat, M. E. Giron, I. Fernandez and A. Rodriguez-Acosta (2018). "Crotamine-like from Southern Pacific rattlesnake (Crotalus oreganus helleri) Venom acts on human leukemia (K-562) cell lines and produces ultrastructural changes on mice adrenal gland." Ultrastruct Pathol **42**(2): 116-123.

Saviola, A. J., D. Pla, L. Sanz, T. A. Castoe, J. J. Calvete and S. P. Mackessy (2015). "Comparative venomics of the Prairie Rattlesnake (Crotalus viridis viridis) from Colorado: Identification of a novel pattern of ontogenetic changes in venom composition and assessment of the immunoreactivity of the commercial antivenom CroFab(R)." J Proteomics **121**: 28-43.

Schilling, E. A., A. E. Kamholz and P. Yager (2002). "Cell lysis and protein extraction in a microfluidic device with detection by a fluorogenic enzyme assay." Anal Chem **74**(8): 1798-1804.

Shahidi Bonjar, L. (2014). "Design of a new therapy to treat snake envenomation." Drug Des Devel Ther **8**: 819-825.

Sieber, M., B. Bosch, W. Hanke and V. M. Fernandes de Lima (2014). "Membrane-modifying properties of crotamine, a small peptide-toxin from Crotalus durissus terrificus venom." Biochim Biophys Acta **1840**(3): 945-950.

Sugiarto, H. and P. L. Yu (2004). "Avian antimicrobial peptides: the defense role of beta-defensins." Biochem Biophys Res Commun **323**(3): 721-727.

Swartz, K. J. and R. MacKinnon (1997). "Mapping the receptor site for hanatoxin, a gating modifier of voltage-dependent K+ channels." Neuron **18**(4): 675-682.

Takeda, S., H. Takeya and S. Iwanaga (2012). "Snake venom metalloproteinases: structure, function and relevance to the mammalian ADAM/ADAMTS family proteins." Biochim Biophys Acta **1824**(1): 164-176.

Torres, Y. P., F. J. Morera, I. Carvacho and R. Latorre (2007). "A marriage of convenience: beta-subunits and voltage-dependent K+ channels." J Biol Chem **282**(34): 24485-24489.

Toyama, M. H., E. M. Carneiro, S. Marangoni, R. L. Barbosa, G. Corso and A. C. Boschero (2000). "Biochemical characterization of two crotamine isoforms isolated by a single step RP-HPLC from Crotalus durissus terrificus (South American rattlesnake) venom and their action on insulin secretion by pancreatic islets." Biochim Biophys Acta **1474**(1): 56-60.

van Dijk, A., E. J. Veldhuizen and H. P. Haagsman (2008). "Avian defensins." Vet Immunol Immunopathol **124**(1-2): 1-18.

Volk, R., J. J. Schwartz, J. Li, R. D. Rosenberg and M. Simons (1999). "The role of syndecan cytoplasmic domain in basic fibroblast growth factor-dependent signal transduction." J Biol Chem **274**(34): 24417-24424.

Ward, R. J., L. Chioato, A. H. de Oliveira, R. Ruller and J. M. Sa (2002). "Active-site mutagenesis of a Lys49-phospholipase A2: biological and membrane-disrupting activities in the absence of catalysis." Biochem J **362**(Pt 1): 89-96.

Weisman, R. S., S. S. Lizarralde and V. Thompson (1996). "Snake and spider antivenin: risks and benefits of therapy." J Fla Med Assoc **83**(3): 192-195.

Welch, J., K. Svensson, P. Kucharzewska and M. Belting (2011). "Heparan sulfate proteoglycan-mediated polyamine uptake." Methods Mol Biol **720**: 327-338.

White, S. H., W. C. Wimley and M. E. Selsted (1995). "Structure, function, and membrane integration of defensins." Curr Opin Struct Biol **5**(4): 521-527.

Whittington, C. M., A. T. Papenfuss, P. Bansal, A. M. Torres, E. S. Wong, J. E. Deakin, T. Graves, A. Alsop, K. Schatzkamer, C. Kremitzki, C. P. Ponting, P. Temple-Smith, W. C. Warren, P. W. Kuchel and K. Belov (2008). "Defensins and the convergent evolution of platypus and reptile venom genes." Genome Res **18**(6): 986-994.

Wonderlin, W. F. and J. S. Strobl (1996). "Potassium channels, proliferation and G1 progression." J Membr Biol **154**(2): 91-107.

Yount, N. Y., D. Kupferwasser, A. Spisni, S. M. Dutz, Z. H. Ramjan, S. Sharma, A. J. Waring and M. R. Yeaman (2009). "Selective reciprocity in antimicrobial activity versus cytotoxicity of hBD-2 and crotamine." Proc Natl Acad Sci U S A **106**(35): 14972-14977.

Zhang, H. L., R. Han, Z. X. Chen, B. W. Chen, Z. L. Gu, P. F. Reid, L. N. Raymond and Z. H. Qin (2006). "Opiate and acetylcholine-independent analgesic actions of crotoxin isolated from crotalus durissus terrificus venom." Toxicon **48**(2): 175-182.

Zhou, Z. H., T. Unlap, L. Li and H. P. Ma (2002). "Incomplete inactivation of voltage-dependent K+ channels in human B lymphoma cells." J Membr Biol **188**(2): 97-105.

Campelo, I. S., Canel, N. G., Bevacqua, R. J., Melo, L. M., Radis-Baptista, G., Freitas, V. J., & Salamone, D. F. (2016). Crotamine, a cell-penetrating peptide, is able to translocate parthenogenetic and in vitro fertilized bovine embryos but does not improve exogenous DNA expression. *J Assist Reprod Genet, 33*(10), 1405-1413. doi:10.1007/s10815-016-0772-7

Campelo, I. S., Pereira, A. F., Alcantara-Neto, A. S., Canel, N. G., Souza-Fabjan, J. M., Teixeira, D. I., . . . Freitas, V. J. (2016). Effect of crotamine, a cell-penetrating peptide, on blastocyst production and gene expression of in vitro fertilized bovine embryos. *Zygote, 24*(1), 48-57. doi:10.1017/S0967199414000707

Dal Mas, C., Moreira, J. T., Pinto, S., Monte, G. G., Nering, M. B., Oliveira, E. B., . . . Hayashi, M. A. (2016). Anthelmintic effects of a cationic toxin from a South American rattlesnake venom. *Toxicon, 116*, 49-55. doi:10.1016/j.toxicon.2015.11.021

Hayashi, M. A., Nascimento, F. D., Kerkis, A., Oliveira, V., Oliveira, E. B., Pereira, A., . . . Tersariol, I. L. (2008). Cytotoxic effects of crotamine are mediated through lysosomal membrane permeabilization. *Toxicon, 52*(3), 508-517. doi:10.1016/j.toxicon.2008.06.029

Hyun, J. H., Eom, K., Lee, K. H., Bae, J. Y., Bae, Y. C., Kim, M. H., . . . Lee, S. H. (2015). Kv1.2 mediates heterosynaptic modulation of direct cortical synaptic inputs in CA3 pyramidal cells. *J Physiol, 593*(16), 3617-3643. doi:10.1113/JP270372

Jimenez-Perez, L., Cidad, P., Alvarez-Miguel, I., Santos-Hipolito, A., Torres-Merino, R., Alonso, E., . . . Perez-Garcia, M. T. (2016). Molecular Determinants of Kv1.3 Potassium Channels-induced Proliferation. *J Biol Chem, 291*(7), 3569-3580. doi:10.1074/jbc.M115.678995

Militsopoulou, M., Lamari, F., & Karamanos, N. K. (2003). Capillary electrophoresis: a tool for studying interactions of glycans/proteoglycans with growth factors. *J Pharm Biomed Anal, 32*(4-5), 823-828.

Nascimento, F. D., Hayashi, M. A., Kerkis, A., Oliveira, V., Oliveira, E. B., Radis-Baptista, G., . . . Kerkis, I. (2007). Crotamine mediates gene delivery into cells through the binding to heparan sulfate proteoglycans. *J Biol Chem, 282*(29), 21349-21360. doi:10.1074/jbc.M604876200

Peigneur, S., Orts, D. J., Prieto da Silva, A. R., Oguiura, N., Boni-Mitake, M., de Oliveira, E. B., . . . Tytgat, J. (2012). Crotamine pharmacology revisited: novel insights based on the inhibition of KV channels. *Mol Pharmacol, 82*(1), 90-96. doi:10.1124/mol.112.078188

Perez-Garcia, M. T., Cidad, P., & Lopez-Lopez, J. R. (2018). The secret life of ion channels: Kv1.3 potassium channels and proliferation. *Am J Physiol Cell Physiol, 314*(1), C27-C42. doi:10.1152/ajpcell.00136.2017

Rizzi, C. T., Carvalho-de-Souza, J. L., Schiavon, E., Cassola, A. C., Wanke, E., & Troncone, L. R. (2007). Crotamine inhibits preferentially fast-twitching muscles but is inactive on sodium channels. *Toxicon, 50*(4), 553-562. doi:10.1016/j.toxicon.2007.04.026

Vu, T. T., Jeong, B., Yu, J., Koo, B. K., Jo, S. H., Robinson, R. C., & Choe, H. (2014). Soluble prokaryotic expression and purification of crotamine using an N-terminal maltose-binding protein tag. *Toxicon, 92*, 157-165. doi:10.1016/j.toxicon.2014.10.017

Wulff, H., Castle, N. A., & Pardo, L. A. (2009). Voltage-gated potassium channels as therapeutic targets. *Nat Rev Drug Discov, 8*(12), 982-1001. doi:10.1038/nrd2983

Yazama, F., Esaki, M., & Sawada, H. (1997). Immunocytochemistry of extracellular matrix components in the rat seminiferous tubule: electron microscopic localization with improved methodology. *Anat Rec, 248*(1), 51-62.

Yount, N. Y., Kupferwasser, D., Spisni, A., Dutz, S. M., Ramjan, Z. H., Sharma, S., . . . Yeaman, M. R. (2009). Selective reciprocity in antimicrobial activity versus cytotoxicity of hBD-2 and crotamine. *Proc Natl Acad Sci U S A, 106*(35), 14972-14977. doi:10.1073/pnas.0904465106

Yuan, X. L., Zhao, Y. P., Huang, J., Liu, J. C., Mao, W. Q., Yin, J., . . . He, X. H. (2018). A Kv1.3 channel-specific blocker alleviates neurological impairment through inhibiting T-cell activation in experimental autoimmune encephalomyelitis. *CNS Neurosci Ther*. doi:10.1111/cns.12848

Adult nonfiction: Pure sciences. *Booklist, 90*(19/20), 1746-1746.

Bartelt, R. R., Cruz-Orcutt, N., Collins, M., & Houtman, J. C. (2009). Comparison of T cell receptor-induced proximal signaling and downstream functions in

immortalized and primary T cells. *PLoS One, 4*(5), e5430. doi:10.1371/journal.pone.0005430

Bielanska, J., Hernandez-Losa, J., Moline, T., Somoza, R., Ramon y Cajal, S., Condom, E., . . . Felipe, A. (2012). Differential expression of Kv1.3 and Kv1.5 voltage-dependent K+ channels in human skeletal muscle sarcomas. *Cancer Invest, 30*(3), 203-208. doi:10.3109/07357907.2012.654872

Bielanska, J., Hernandez-Losa, J., Perez-Verdaguer, M., Moline, T., Somoza, R., Ramon, Y. C. S., . . . Felipe, A. (2009). Voltage-dependent potassium channels Kv1.3 and Kv1.5 in human cancer. *Curr Cancer Drug Targets, 9*(8), 904-914.

Bottrall, J. L., Madaras, F., Biven, C. D., Venning, M. G., & Mirtschin, P. J. (2010). Proteolytic activity of Elapid and Viperid Snake venoms and its implication to digestion. *J Venom Res, 1*, 18-28.

Bradding, P., & Wulff, H. (2009). The K+ channels K(Ca)3.1 and K(v)1.3 as novel targets for asthma therapy. *Br J Pharmacol, 157*(8), 1330-1339. doi:10.1111/j.1476-5381.2009.00362.x

Bridges, E., & Harris, A. L. (2015). Vascular-promoting therapy reduced tumor growth and progression by improving chemotherapy efficacy. *Cancer Cell, 27*(1), 7-9. doi:10.1016/j.ccell.2014.12.009

Campelo, I. S., Canel, N. G., Bevacqua, R. J., Melo, L. M., Radis-Baptista, G., Freitas, V. J., & Salamone, D. F. (2016). Crotamine, a cell-penetrating peptide, is able to translocate parthenogenetic and in vitro fertilized bovine embryos but does not improve exogenous DNA expression. *J Assist Reprod Genet, 33*(10), 1405-1413. doi:10.1007/s10815-016-0772-7

Checchetto, V., Formentin, E., Carraretto, L., Segalla, A., Giacometti, G. M., Szabo, I., & Bergantino, E. (2013). Functional characterization and determination of the physiological role of a calcium-dependent potassium channel from cyanobacteria. *Plant Physiol, 162*(2), 953-964. doi:10.1104/pp.113.215129

Chen, P. C., Hayashi, M. A., Oliveira, E. B., & Karpel, R. L. (2012). DNA-interactive properties of crotamine, a cell-penetrating polypeptide and a potential drug carrier. *PLoS One, 7*(11), e48913. doi:10.1371/journal.pone.0048913

Chiang, E. Y., Li, T., Jeet, S., Peng, I., Zhang, J., Lee, W. P., . . . Grogan, J. L. (2017). Potassium channels Kv1.3 and KCa3.1 cooperatively and compensatorily regulate antigen-specific memory T cell functions. *Nat Commun, 8*, 14644. doi:10.1038/ncomms14644

Chittajallu, R., Chen, Y., Wang, H., Yuan, X., Ghiani, C. A., Heckman, T., . . . Gallo, V. (2002). Regulation of Kv1 subunit expression in oligodendrocyte progenitor cells and their role in G1/S phase progression of the cell cycle. *Proc Natl Acad Sci U S A, 99*(4), 2350-2355. doi:10.1073/pnas.042698399

Cirrone, G. A. P., Cuttone, G., Raffaele, L., Salamone, V., Avitabile, T., Privitera, G., . . . Valastro, L. M. (2017). Corrigendum: Clinical and Research Activities at the CATANA Facility of INFN-LNS: From the Conventional Hadrontherapy to the Laser-Driven Approach. *Front Oncol, 7*, 247. doi:10.3389/fonc.2017.00247

Comes, N., Bielanska, J., Vallejo-Gracia, A., Serrano-Albarras, A., Marruecos, L., Gomez, D., . . . Felipe, A. (2013). The voltage-dependent K(+) channels Kv1.3 and Kv1.5 in human cancer. *Front Physiol, 4*, 283. doi:10.3389/fphys.2013.00283

Cui, D., Li, A., Zhang, S., Pang, C., Yang, J., Guo, J., . . . Ren, N. (2012). Microbial community analysis of three municipal wastewater treatment plants in winter and spring using culture-dependent and culture-independent methods. *World J Microbiol Biotechnol, 28*(6), 2341-2353. doi:10.1007/s11274-012-1041-2

Curran, M. E., Landes, G. M., & Keating, M. T. (1992). Molecular cloning, characterization, and genomic localization of a human potassium channel gene. *Genomics, 12*(4), 729-737.

Dalla Valle, L., Benato, F., Maistro, S., Quinzani, S., & Alibardi, L. (2012). Bioinformatic and molecular characterization of beta-defensins-like peptides isolated from the green lizard Anolis carolinensis. *Dev Comp Immunol, 36*(1), 222-229. doi:10.1016/j.dci.2011.05.004

Doyle, D. A., Morais Cabral, J., Pfuetzner, R. A., Kuo, A., Gulbis, J. M., Cohen, S. L., . . . MacKinnon, R. (1998). The structure of the potassium channel: molecular basis of K+ conduction and selectivity. *Science, 280*(5360), 69-77.

Favre, I., Moczydlowski, E., & Schild, L. (1996). On the structural basis for ionic selectivity among Na+, K+, and Ca2+ in the voltage-gated sodium channel. *Biophys J, 71*(6), 3110-3125. doi:10.1016/S0006-3495(96)79505-X

Fernandes, C. M., Pereira Teixeira Cde, F., Leite, A. C., Gutierrez, J. M., & Rocha, F. A. (2007). The snake venom metalloproteinase BaP1 induces joint hypernociception through TNF-alpha and PGE2-dependent mechanisms. *Br J Pharmacol, 151*(8), 1254-1261. doi:10.1038/sj.bjp.0707351

Feske, S., Wulff, H., & Skolnik, E. Y. (2015). Ion channels in innate and adaptive immunity. *Annu Rev Immunol, 33*, 291-353. doi:10.1146/annurev-immunol-032414-112212

Fung-Leung, W. P., Edwards, W., Liu, Y., Ngo, K., Angsana, J., Castro, G., . . . Wickenden, A. D. (2017). T Cell Subset and Stimulation Strength-Dependent Modulation of T Cell Activation by Kv1.3 Blockers. *PLoS One, 12*(1), e0170102. doi:10.1371/journal.pone.0170102

Gamper, N., Fillon, S., Huber, S. M., Feng, Y., Kobayashi, T., Cohen, P., & Lang, F. (2002). IGF-1 up-regulates K+ channels via PI3-kinase, PDK1 and SGK1. *Pflugers Arch, 443*(4), 625-634. doi:10.1007/s00424-001-0741-5

Garcia-Calvo, M., Leonard, R. J., Novick, J., Stevens, S. P., Schmalhofer, W., Kaczorowski, G. J., & Garcia, M. L. (1993). Purification, characterization, and biosynthesis of margatoxin, a component of Centruroides margaritatus venom that selectively inhibits voltage-dependent potassium channels. *J Biol Chem, 268*(25), 18866-18874.

Goodman, L. S., Gilman, A., Brunton, L. L., Lazo, J. S., & Parker, K. L. (2006). *Goodman & Gilman's the pharmacological basis of therapeutics* (11th ed.). New York: McGraw-Hill.

Greenbaum, E., Galeva, N., & Jorgensen, M. (2003). Venom variation and chemoreception of the viperid Agkistrodon contortrix: evidence for adaptation? *J Chem Ecol, 29*(8), 1741-1755.

Griffin, P. R., & Aird, S. D. (1990). A new small myotoxin from the venom of the prairie rattlesnake (Crotalus viridis viridis). *FEBS Lett, 274*(1-2), 43-47.

Gutierrez, J. M., & Rucavado, A. (2000). Snake venom metalloproteinases: their role in the pathogenesis of local tissue damage. *Biochimie, 82*(9-10), 841-850.

Gutman, G. A., Chandy, K. G., Grissmer, S., Lazdunski, M., McKinnon, D., Pardo, L. A., . . . Wang, X. (2005). International Union of Pharmacology. LIII. Nomenclature and molecular relationships of voltage-gated potassium channels. *Pharmacol Rev, 57*(4), 473-508. doi:10.1124/pr.57.4.10

Han, S., Yi, H., Yin, S. J., Chen, Z. Y., Liu, H., Cao, Z. J., . . . Li, W. X. (2008). Structural basis of a potent peptide inhibitor designed for Kv1.3 channel, a therapeutic target of autoimmune disease. *J Biol Chem, 283*(27), 19058-19065. doi:10.1074/jbc.M802054200

Hayashi, M. A., Nascimento, F. D., Kerkis, A., Oliveira, V., Oliveira, E. B., Pereira, A., . . . Tersariol, I. L. (2008). Cytotoxic effects of crotamine are mediated through lysosomal membrane permeabilization. *Toxicon, 52*(3), 508-517. doi:10.1016/j.toxicon.2008.06.029

Hayashi, M. A., Oliveira, E. B., Kerkis, I., & Karpel, R. L. (2012). Crotamine: a novel cell-penetrating polypeptide nanocarrier with potential anti-cancer and biotechnological applications. *Methods Mol Biol, 906*, 337-352. doi:10.1007/978-1-61779-953-2_28

Heffernan, B. J., Thomason, B., Herring-Palmer, A., Shaughnessy, L., McDonald, R., Fisher, N., . . . Hanna, P. (2006). Bacillus anthracis phospholipases C facilitate macrophage-associated growth and contribute to virulence in a murine model of inhalation anthrax. *Infect Immun, 74*(7), 3756-3764. doi:10.1128/IAI.00307-06

Hernandez-Oliveira e Silva, S., Rostelato-Ferreira, S., Rocha-e-Silva, T. A., Randazzo-Moura, P., Dal-Belo, C. A., Sanchez, E. F., . . . Rodrigues-Simioni, L. (2013). Beneficial effect of crotamine in the treatment of myasthenic rats. *Muscle Nerve, 47*(4), 591-593. doi:10.1002/mus.23714

Hille, B. (2001). *Ion channels of excitable membranes* (3rd ed.). Sunderland, Mass.: Sinauer.

Hogan, P. G., Lewis, R. S., & Rao, A. (2010). Molecular basis of calcium signaling in lymphocytes: STIM and ORAI. *Annu Rev Immunol, 28*, 491-533. doi:10.1146/annurev.immunol.021908.132550

Hu, L., Gocke, A. R., Knapp, E., Rosenzweig, J. M., Grishkan, I. V., Baxi, E. G., . . . Calabresi, P. A. (2012). Functional blockade of the voltage-gated potassium channel Kv1.3 mediates reversion of T effector to central memory lymphocytes through SMAD3/p21cip1 signaling. *J Biol Chem, 287*(2), 1261-1268. doi:10.1074/jbc.M111.296798

Hyun, J. H., Eom, K., Lee, K. H., Bae, J. Y., Bae, Y. C., Kim, M. H., . . . Lee, S. H. (2015). Kv1.2 mediates heterosynaptic modulation of direct cortical synaptic inputs in CA3 pyramidal cells. *J Physiol, 593*(16), 3617-3643. doi:10.1113/JP270372

Jackson, T. N., Sunagar, K., Undheim, E. A., Koludarov, I., Chan, A. H., Sanders, K., . . . Fry, B. G. (2013). Venom down under: dynamic evolution of Australian elapid snake toxins. *Toxins (Basel), 5*(12), 2621-2655. doi:10.3390/toxins5122621

Jimenez-Perez, L., Cidad, P., Alvarez-Miguel, I., Santos-Hipolito, A., Torres-Merino, R., Alonso, E., . . . Perez-Garcia, M. T. (2016). Molecular Determinants of Kv1.3 Potassium Channels-induced Proliferation. *J Biol Chem, 291*(7), 3569-3580. doi:10.1074/jbc.M115.678995

Kerkis, A., Kerkis, I., Radis-Baptista, G., Oliveira, E. B., Vianna-Morgante, A. M., Pereira, L. V., & Yamane, T. (2004). Crotamine is a novel cell-penetrating protein from the venom of rattlesnake Crotalus durissus terrificus. *FASEB J, 18*(12), 1407-1409. doi:10.1096/fj.03-1459fje

Kerkis, I., Silva Fde, S., Pereira, A., Kerkis, A., & Radis-Baptista, G. (2010). Biological versatility of crotamine--a cationic peptide from the venom of a South American rattlesnake. *Expert Opin Investig Drugs, 19*(12), 1515-1525. doi:10.1517/13543784.2010.534457

Kordis, D., & Gubensek, F. (2000). Adaptive evolution of animal toxin multigene families. *Gene, 261*(1), 43-52.

Leanza, L., Romio, M., Becker, K. A., Azzolini, M., Trentin, L., Manago, A., . . . Szabo, I. (2017). Direct Pharmacological Targeting of a Mitochondrial Ion Channel Selectively Kills Tumor Cells In Vivo. *Cancer Cell, 31*(4), 516-531 e510. doi:10.1016/j.ccell.2017.03.003

Littleton, J. T., & Ganetzky, B. (2000). Ion channels and synaptic organization: analysis of the Drosophila genome. *Neuron, 26*(1), 35-43.

Luna-Ramirez, K., Sani, M. A., Silva-Sanchez, J., Jimenez-Vargas, J. M., Reyna-Flores, F., Winkel, K. D., . . . Separovic, F. (2013). Membrane interactions and biological activity of antimicrobial peptides from Australian scorpion. *Biochim Biophys Acta*. doi:10.1016/j.bbamem.2013.10.022

Mamede, C. C., de Queiroz, M. R., Fonseca, K. C., de Morais, N. C., Filho, S. A., Beletti, M. E., . . . de Oliveira, F. (2013). Histological and ultrastructural analyses of muscle damage induced by a myotoxin isolated from Bothrops alternatus snake venom. *Protein Pept Lett, 20*(2), 192-199.

Mandal, S. M., Migliolo, L., Das, S., Mandal, M., Franco, O. L., & Hazra, T. K. (2012). Identification and characterization of a bactericidal and proapoptotic peptide from Cycas revoluta seeds with DNA binding properties. *J Cell Biochem, 113*(1), 184-193. doi:10.1002/jcb.23343

Markland, F. S., Jr., & Swenson, S. (2013). Snake venom metalloproteinases. *Toxicon, 62*, 3-18. doi:10.1016/j.toxicon.2012.09.004

Matavel, A. C., Ferreira-Alves, D. L., Beirao, P. S., & Cruz, J. S. (1998). Tension generation and increase in voltage-activated Na+ current by crotamine. *Eur J Pharmacol, 348*(2-3), 167-173.

Mouhat, S., Andreotti, N., Jouirou, B., & Sabatier, J. M. (2008). Animal toxins acting on voltage-gated potassium channels. *Curr Pharm Des, 14*(24), 2503-2518.

Mouhat, S., Jouirou, B., Mosbah, A., De Waard, M., & Sabatier, J. M. (2004). Diversity of folds in animal toxins acting on ion channels. *Biochem J, 378*(Pt 3), 717-726. doi:10.1042/BJ20031860

Moura-da-Silva, A. M., Ramos, O. H., Baldo, C., Niland, S., Hansen, U., Ventura, J. S., . . . Eble, J. A. (2008). Collagen binding is a key factor for the hemorrhagic activity of snake venom metalloproteinases. *Biochimie, 90*(3), 484-492. doi:10.1016/j.biochi.2007.11.009

Munaron, L., Antoniotti, S., & Lovisolo, D. (2004). Intracellular calcium signals and control of cell proliferation: how many mechanisms? *J Cell Mol Med, 8*(2), 161-168.

Nascimento, F. D., Hayashi, M. A., Kerkis, A., Oliveira, V., Oliveira, E. B., Radis-Baptista, G., . . . Kerkis, I. (2007). Crotamine mediates gene delivery into cells through the binding to heparan sulfate proteoglycans. *J Biol Chem, 282*(29), 21349-21360. doi:10.1074/jbc.M604876200

Nascimento, F. D., Sancey, L., Pereira, A., Rome, C., Oliveira, V., Oliveira, E. B., . . . Hayashi, M. A. (2012). The natural cell-penetrating peptide crotamine targets tumor tissue in vivo and triggers a lethal calcium-dependent pathway in cultured cells. *Mol Pharm, 9*(2), 211-221. doi:10.1021/mp2000605

Newell, E. W., & Schlichter, L. C. (2005). Integration of K+ and Cl- currents regulate steady-state and dynamic membrane potentials in cultured rat microglia. *J Physiol, 567*(Pt 3), 869-890. doi:10.1113/jphysiol.2005.092056

Nguyen, A., Kath, J. C., Hanson, D. C., Biggers, M. S., Canniff, P. C., Donovan, C. B., . . . Chandy, K. G. (1996). Novel nonpeptide agents potently block the C-type

inactivated conformation of Kv1.3 and suppress T cell activation. *Mol Pharmacol, 50*(6), 1672-1679.

Nicastro, G., Franzoni, L., de Chiara, C., Mancin, A. C., Giglio, J. R., & Spisni, A. (2003). Solution structure of crotamine, a Na+ channel affecting toxin from Crotalus durissus terrificus venom. *Eur J Biochem, 270*(9), 1969-1979.

Oguiura, N., Boni-Mitake, M., Affonso, R., & Zhang, G. (2011). In vitro antibacterial and hemolytic activities of crotamine, a small basic myotoxin from rattlesnake Crotalus durissus. *J Antibiot (Tokyo), 64*(4), 327-331. doi:10.1038/ja.2011.10

Oguiura, N., Boni-Mitake, M., & Radis-Baptista, G. (2005). New view on crotamine, a small basic polypeptide myotoxin from South American rattlesnake venom. *Toxicon, 46*(4), 363-370. doi:10.1016/j.toxicon.2005.06.009

Orlova, E. V., Papakosta, M., Booy, F. P., van Heel, M., & Dolly, J. O. (2003). Voltage-gated K+ channel from mammalian brain: 3D structure at 18A of the complete (alpha)4(beta)4 complex. *J Mol Biol, 326*(4), 1005-1012.

Ouadid-Ahidouch, H., & Ahidouch, A. (2008). K+ channel expression in human breast cancer cells: involvement in cell cycle regulation and carcinogenesis. *J Membr Biol, 221*(1), 1-6. doi:10.1007/s00232-007-9080-6

Ouadid-Ahidouch, H., Chaussade, F., Roudbaraki, M., Slomianny, C., Dewailly, E., Delcourt, P., & Prevarskaya, N. (2000). KV1.1 K(+) channels identification in human breast carcinoma cells: involvement in cell proliferation. *Biochem Biophys Res Commun, 278*(2), 272-277. doi:10.1006/bbrc.2000.3790

Ouadid-Ahidouch, H., Roudbaraki, M., Ahidouch, A., Delcourt, P., & Prevarskaya, N. (2004). Cell-cycle-dependent expression of the large Ca2+-activated K+ channels in breast cancer cells. *Biochem Biophys Res Commun, 316*(1), 244-251. doi:10.1016/j.bbrc.2004.02.041

Ownby, C. L., Gutierrez, J. M., Colberg, T. R., & Odell, G. V. (1982). Quantitation of myonecrosis induced by myotoxin a from prairie rattlesnake (Crotalus viridis viridis) venom. *Toxicon, 20*(5), 877-885.

Pardo, L. A. (2004). Voltage-gated potassium channels in cell proliferation. *Physiology (Bethesda), 19*, 285-292. doi:10.1152/physiol.00011.2004

Peigneur, S., Orts, D. J., Prieto da Silva, A. R., Oguiura, N., Boni-Mitake, M., de Oliveira, E. B., . . . Tytgat, J. (2012). Crotamine pharmacology revisited: novel insights based on the inhibition of KV channels. *Mol Pharmacol, 82*(1), 90-96. doi:10.1124/mol.112.078188

Peigneur, S., Orts, D. J. B., Silva, A. R. P. d., Oguiura, N., Boni-Mitake, M., Oliveira, E. B. d., . . . Tytgat, J. (2012). Crotamine Pharmacology Revisited: Novel Insights Based on the Inhibition of KV Channels. *Mol Pharmacol, 82*(1), 90-96. doi:10.1124/mol.107.037101

Pereira, A., Kerkis, A., Hayashi, M. A., Pereira, A. S., Silva, F. S., Oliveira, E. B., . . . Kerkis, I. (2011). Crotamine toxicity and efficacy in mouse models of melanoma. *Expert Opin Investig Drugs, 20*(9), 1189-1200. doi:10.1517/13543784.2011.602064

Perez-Garcia, M. T., Cidad, P., & Lopez-Lopez, J. R. (2018). The secret life of ion channels: Kv1.3 potassium channels and proliferation. *Am J Physiol Cell Physiol, 314*(1), C27-C42. doi:10.1152/ajpcell.00136.2017

Pongs, O., Leicher, T., Berger, M., Roeper, J., Bahring, R., Wray, D., . . . Storm, J. F. (1999). Functional and molecular aspects of voltage-gated K+ channel beta subunits. *Ann N Y Acad Sci, 868*, 344-355.

Ponnappan, N., & Chugh, A. (2017). Cell-penetrating and cargo-delivery ability of a spider toxin-derived peptide in mammalian cells. *Eur J Pharm Biopharm, 114*, 145-153. doi:10.1016/j.ejpb.2017.01.012

Radis-Baptista, G., & Kerkis, I. (2011). Crotamine, a small basic polypeptide myotoxin from rattlesnake venom with cell-penetrating properties. *Curr Pharm Des, 17*(38), 4351-4361.

Rang, H. P. (2006). The receptor concept: pharmacology's big idea. *Br J Pharmacol, 147 Suppl 1*, S9-16. doi:10.1038/sj.bjp.0706457

Rizzi, C. T., Carvalho-de-Souza, J. L., Schiavon, E., Cassola, A. C., Wanke, E., & Troncone, L. R. (2007). Crotamine inhibits preferentially fast-twitching muscles but is inactive on sodium channels. *Toxicon, 50*(4), 553-562. doi:10.1016/j.toxicon.2007.04.026

Rodrigues, M., Santos, A., de la Torre, B. G., Radis-Baptista, G., Andreu, D., & Santos, N. C. (2012). Molecular characterization of the interaction of crotamine-derived nucleolar targeting peptides with lipid membranes. *Biochim Biophys Acta, 1818*(11), 2707-2717. doi:10.1016/j.bbamem.2012.06.014

Rokyta, D. R., Lemmon, A. R., Margres, M. J., & Aronow, K. (2012). The venom-gland transcriptome of the eastern diamondback rattlesnake (Crotalus adamanteus). *BMC Genomics, 13*, 312. doi:10.1186/1471-2164-13-312

Rucavado, A., Borkow, G., Ovadia, M., & Gutierrez, J. M. (1995). Immunological studies on BaH1 and BaP1, two hemorrhagic metalloproteinases from the venom of the snake Bothrops asper. *Toxicon, 33*(8), 1103-1106.

Rucavado, A., Escalante, T., & Gutierrez, J. M. (2004). Effect of the metalloproteinase inhibitor batimastat in the systemic toxicity induced by Bothrops asper snake venom: understanding the role of metalloproteinases in envenomation. *Toxicon, 43*(4), 417-424. doi:10.1016/j.toxicon.2004.01.016

Samejima, Y., Aoki, Y., & Mebs, D. (1991). Amino acid sequence of a myotoxin from venom of the eastern diamondback rattlesnake (Crotalus adamanteus). *Toxicon, 29*(4-5), 461-468.

Sanchez, E. E., Gonzalez, R., Lucena, S., Garcia, S., Finol, H. J., Suntravat, M., . . . Rodriguez-Acosta, A. (2018). Crotamine-like from Southern Pacific rattlesnake (Crotalus oreganus helleri) Venom acts on human leukemia (K-562) cell lines and produces ultrastructural changes on mice adrenal gland. *Ultrastruct Pathol, 42*(2), 116-123. doi:10.1080/01913123.2017.1422827

Saviola, A. J., Pla, D., Sanz, L., Castoe, T. A., Calvete, J. J., & Mackessy, S. P. (2015). Comparative venomics of the Prairie Rattlesnake (Crotalus viridis viridis) from Colorado: Identification of a novel pattern of ontogenetic changes in venom composition and assessment of the immunoreactivity of the commercial antivenom CroFab(R). *J Proteomics, 121*, 28-43. doi:10.1016/j.jprot.2015.03.015

Schilling, E. A., Kamholz, A. E., & Yager, P. (2002). Cell lysis and protein extraction in a microfluidic device with detection by a fluorogenic enzyme assay. *Anal Chem, 74*(8), 1798-1804.

Schmitz, A., Sankaranarayanan, A., Azam, P., Schmidt-Lassen, K., Homerick, D., Hansel, W., & Wulff, H. (2005). Design of PAP-1, a selective small molecule Kv1.3 blocker, for the suppression of effector memory T cells in autoimmune diseases. *Mol Pharmacol, 68*(5), 1254-1270. doi:10.1124/mol.105.015669

Shahidi Bonjar, L. (2014). Design of a new therapy to treat snake envenomation. *Drug Des Devel Ther, 8*, 819-825. doi:10.2147/DDDT.S65395

Sieber, M., Bosch, B., Hanke, W., & Fernandes de Lima, V. M. (2014). Membrane-modifying properties of crotamine, a small peptide-toxin from Crotalus durissus terrificus venom. *Biochim Biophys Acta, 1840*(3), 945-950. doi:10.1016/j.bbagen.2013.10.031

Soares, A. M., Andriao-Escarso, S. H., Angulo, Y., Lomonte, B., Gutierrez, J. M., Marangoni, S., . . . Giglio, J. R. (2000). Structural and functional characterization of myotoxin I, a Lys49 phospholipase A(2) homologue from Bothrops moojeni (Caissaca) snake venom. *Arch Biochem Biophys, 373*(1), 7-15. doi:10.1006/abbi.1999.1492

Swartz, K. J., & MacKinnon, R. (1997). Mapping the receptor site for hanatoxin, a gating modifier of voltage-dependent K+ channels. *Neuron, 18*(4), 675-682.

Takeda, S., Takeya, H., & Iwanaga, S. (2012). Snake venom metalloproteinases: structure, function and relevance to the mammalian ADAM/ADAMTS family proteins. *Biochim Biophys Acta, 1824*(1), 164-176. doi:10.1016/j.bbapap.2011.04.009

Toyama, M. H., Carneiro, E. M., Marangoni, S., Barbosa, R. L., Corso, G., & Boschero, A. C. (2000). Biochemical characterization of two crotamine isoforms isolated by a single step RP-HPLC from Crotalus durissus terrificus (South American rattlesnake) venom and their action on insulin secretion by pancreatic islets. *Biochim Biophys Acta, 1474*(1), 56-60.

van Dijk, A., Veldhuizen, E. J., & Haagsman, H. P. (2008). Avian defensins. *Vet Immunol Immunopathol, 124*(1-2), 1-18. doi:10.1016/j.vetimm.2007.12.006

Volk, R., Schwartz, J. J., Li, J., Rosenberg, R. D., & Simons, M. (1999). The role of syndecan cytoplasmic domain in basic fibroblast growth factor-dependent signal transduction. *J Biol Chem, 274*(34), 24417-24424.

Ward, R. J., Chioato, L., de Oliveira, A. H., Ruller, R., & Sa, J. M. (2002). Active-site mutagenesis of a Lys49-phospholipase A2: biological and membrane-disrupting activities in the absence of catalysis. *Biochem J, 362*(Pt 1), 89-96.

Weisman, R. S., Lizarralde, S. S., & Thompson, V. (1996). Snake and spider antivenin: risks and benefits of therapy. *J Fla Med Assoc, 83*(3), 192-195.

Welch, J., Svensson, K., Kucharzewska, P., & Belting, M. (2011). Heparan sulfate proteoglycan-mediated polyamine uptake. *Methods Mol Biol, 720*, 327-338. doi:10.1007/978-1-61779-034-8_20

White, S. H., Wimley, W. C., & Selsted, M. E. (1995). Structure, function, and membrane integration of defensins. *Curr Opin Struct Biol, 5*(4), 521-527.

Whittington, C. M., Papenfuss, A. T., Bansal, P., Torres, A. M., Wong, E. S., Deakin, J. E., . . . Belov, K. (2008). Defensins and the convergent evolution of platypus and reptile venom genes. *Genome Res, 18*(6), 986-994. doi:10.1101/gr.7149808

Wonderlin, W. F., & Strobl, J. S. (1996). Potassium channels, proliferation and G1 progression. *J Membr Biol, 154*(2), 91-107.

Wulff, H., Castle, N. A., & Pardo, L. A. (2009). Voltage-gated potassium channels as therapeutic targets. *Nat Rev Drug Discov, 8*(12), 982-1001. doi:10.1038/nrd2983

Yount, N. Y., Kupferwasser, D., Spisni, A., Dutz, S. M., Ramjan, Z. H., Sharma, S., . . . Yeaman, M. R. (2009). Selective reciprocity in antimicrobial activity versus cytotoxicity of hBD-2 and crotamine. *Proc Natl Acad Sci U S A, 106*(35), 14972-14977. doi:10.1073/pnas.0904465106

Yuan, X. L., Zhao, Y. P., Huang, J., Liu, J. C., Mao, W. Q., Yin, J., . . . He, X. H. (2018). A Kv1.3 channel-specific blocker alleviates neurological impairment through inhibiting T-cell activation in experimental autoimmune encephalomyelitis. *CNS Neurosci Ther*. doi:10.1111/cns.12848

Zhang, H. L., Han, R., Chen, Z. X., Chen, B. W., Gu, Z. L., Reid, P. F., . . . Qin, Z. H. (2006). Opiate and acetylcholine-independent analgesic actions of crotoxin isolated from crotalus durissus terrificus venom. *Toxicon, 48*(2), 175-182. doi:10.1016/j.toxicon.2006.04.008

Zhou, Z. H., Unlap, T., Li, L., & Ma, H. P. (2002). Incomplete inactivation of voltage-dependent K+ channels in human B lymphoma cells. *J Membr Biol, 188*(2), 97-105. doi:10.1007/s00232-001-0176-0

APPENDIX A

CELL SURFACE KV1.3 CHANNEL STAINING

In Chapter I, we measured the level of Kv1.3 transcripts in HR-crotamine sensitive and insensitive cells, to confirm that the level of transcript was correlated with the amount of protein expressed on the surface of cells, we measured cell surface Kv1.3 staining in both Jurkat and C2C12 cells using a FITC conjugated anti-Kv1.3 channel antibody coupled with flow cytometric analysis [Fig. AP1]. The rightward of the FITC curve in cells treated with the FITC conjugated anti-Kv1.3 channel antibody compared to controls in both C2C12 and Jurkat cells confirms the presence of cell surface Kv1.3 on both cell types. The much larger shift for Jurkat cells, compared to C2C12 cells confirms that there is a larger amount of Kv1.3 expressed on the surface of Jurkat compared to C2C12 cells, an observation that also correlates with their relative sensitivity to HR-crotamine's cytotoxic activity.

Fig. AP1.

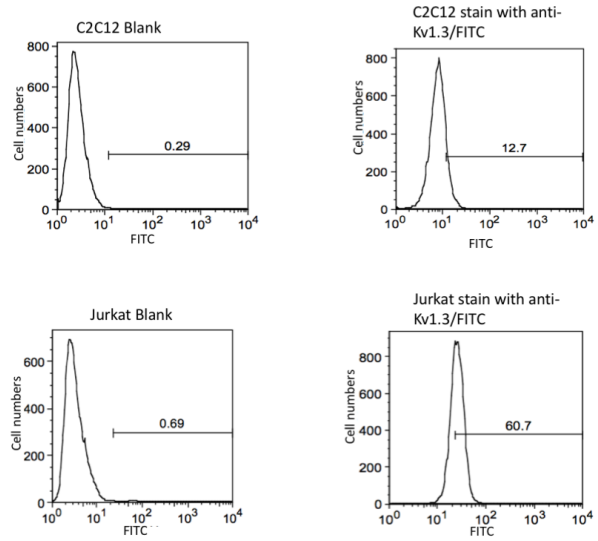

Fig. AP1. Cell surface Kv1.3 channel staining.
Jurkat and C2C12 cells were stained with FITC-conjugated anti-Kv1.3 antibody and analyzed by flow cytometry on FITC channel. Blank represents the FITC signal of cell without FITC-conjugated anti-Kv1.3 antibody to show the base line of FITC reading. The gate bar showing the percentage of the FITC positive cell population.

APPENDIX B

OVEREXPRESSION OF THE TAGGED KV CHANNELS

In Chapter I, we have demonstrated the successful overexpression of Kv channels in the HeLa cells by Western blot. Meantime, each of the Kv channel expression vectors were transfected into HeLa cells and the expression of the channel proteins was confirmed by the detection of the mCherry fusion protein by fluorescence microscopy [Fig. AP2].

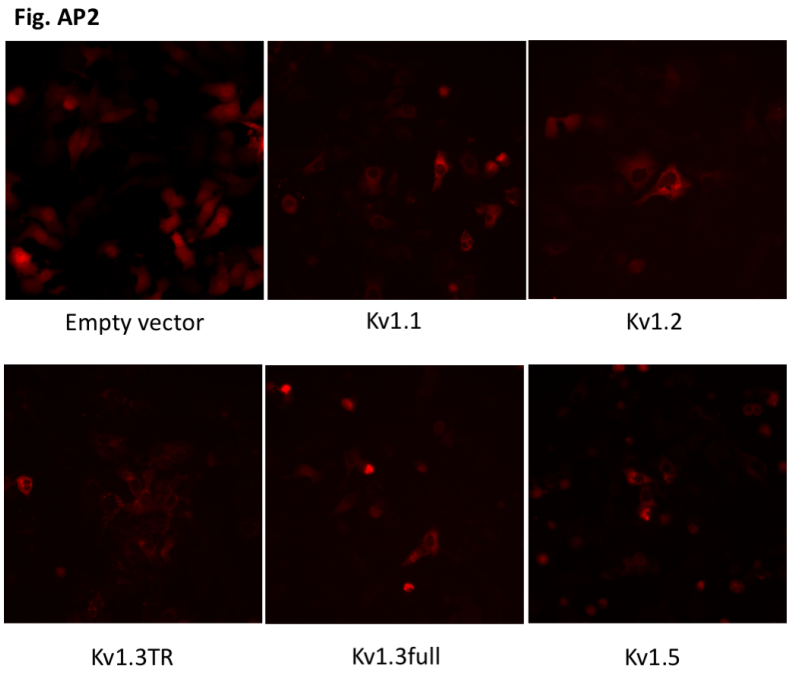

Fig. AP2. Overexpression of the Kv channels in HeLa cells
Expression of Kv channel-mCherry fusion proteins in transfected HeLa cells. Kv channel expression vectors were transfected into HeLa cells with Lipofectamine 3000 using the vendor-recommended protocol. After 48 hr, cells were imaged using a DeltaVision fluorescent microscope. In the images, the red fluorescence is due to the fluorescence of the mCherry tag in the overexpressed Kv channel fusion proteins.

APPENDIX C

PULL DOWN CONDITION EXPLORATION

Pull down analysis is widely considered as a method that can directly prove the protein-protein interaction. According to the preliminary analysis, the Dynabeads M-280 without immobilized HR-crotamine does not indicate the Kv channel protein binding or indicate background level protein binding. This indicates the low background and the high reliability of the results from our test groups. The binding and washing condition were also tested to optimize the protocol with the maximum contrast between the signal and the non-specific background. In the preliminary test, we aimed to achieve the condition to produce the best contrast in the Western blot and SDS-PAGE. Different binding buffer/ wash buffer combination (with detergent present or absent) was tested. The protein samples were extracted from the cytoplasm membrane of HeLa cell overexpressed Kv channels and an equal amount of the protein was loaded to the pull-down system. Based on the result from Western blot, the protein has better binding result in PBS buffer compare with TBS buffer. This result may cause by the difference of the *pH* between these two buffers. The detergent can reduce the binding, but the background for the control without wash by detergent buffer also has attracted our attention. The high salt wash buffer, containing 150 mM NaCl, can reduce the electronic binding as well, so the bands indicate the binding is not only electronic charge depend. Refer to these observations, the binding and wash condition was determined. [Fig. AP3]

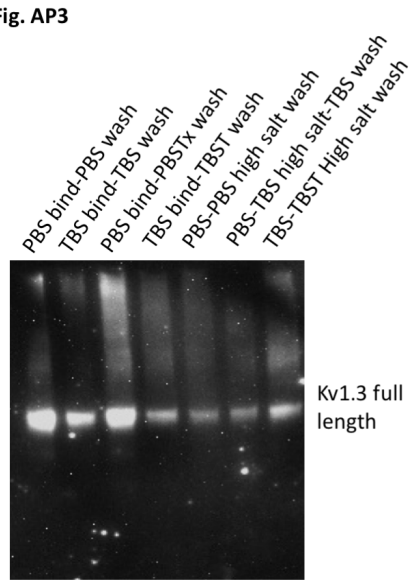

Fig. AP3. Pull down condition exploration
The Jurkat cell was transfected with Kv channel overexpression vector (pCIG3 vector). The cell membrane protein was prepared by the Membrane Prep kit. In the pull-down analysis, the protein was trapped by streptavidin immobilized biotin-HR-crotamine and the sample was applied to the Western blot following the conventional protocol. The rabbit anti-Flag antibody was used in 1:1000 dilution. Multiple binding and washing condition were tested for the maximum contrast between the specific band and non-specific background